

**CHEMINFORMATICS-BASED SCREENING FOR  $\alpha$ -AMYLASE  
AND  $\alpha$ -GLUCOSIDASE INHIBITORS FROM NATURAL  
PRODUCTS ACTIVITY AND SPECIES SOURCE DATABASE  
FOR MANAGEMENT OF POSTPRANDIAL HYPERGLYCEMIA**


**WILBERFORCE KOECH NDARAWIT**

**A THESIS SUBMITTED IN PARTIAL FULFILMENT OF THE  
REQUIREMENTS FOR THE AWARD OF THE DEGREE OF  
MASTER OF SCIENCE IN CHEMISTRY OF THE UNIVERSITY  
OF EMBU**

**AUGUST, 2025**

## DECLARATION

This thesis is my original work and has not been presented elsewhere for a degree or any other award.

Signature...  ..... Date... 5/8/2025 .....

Wilberforce K. Ndarawit

B523/1463/2021

Department of Physical Sciences

University of Embu

This thesis has been submitted for examination with our approval as the supervisors.

Signature...  ..... Date... 05.08.2025 .....

Dr. Mark Kimani

Department of Physical Sciences

University of Embu

Signature...  ..... Date... 5<sup>th</sup>, August, 2025...

Dr. Charles Ochieng

Department of Chemistry

Maseno University

Signature...  ..... Date... 5<sup>th</sup>, August, 2025...

Dr. David Angwenyi

Department of Mathematics

Masinde Muliro University of Science and Technology

## ACKNOWLEDGEMENT

In the pursuit of knowledge, I am deeply indebted to the Almighty God for granting me the strength, wisdom, and perseverance to embark on this academic journey. To the esteemed University of Embu, under the leadership of the Vice Chancellor, Prof. Daniel Mugendi, I extend my heartfelt appreciation for providing conducive environment where intellectual curiosity flourishes. I am profoundly grateful to my supervisors, Dr. Mark N. Kimani, Dr. Charles Otieno and Dr. David Angwenyi whose unwavering support, invaluable insights, and constructive criticism have been pivotal in the development of this work. Their mentorship has been a beacon of light, guiding me through the intricate maze of research. Their expertise and encouragement have been instrumental in shaping the direction of my research. A special acknowledgment goes to Dr. Cleydson B. R. Santos and Prof. Jordi Neves Cruz of the Laboratory of Modeling and Computational Chemistry, Federal University of Amapá, Brazil. Their kindness in providing the necessary software's for computational studies and running MD simulations has been instrumental in advancing the scientific exploration of my research. I am indebted to the Physical Science Department at the University of Embu, led by Dr. Nyamato Simba, for providing a conducive environment for academic growth and research excellence. To my colleagues, especially Kibet Shadrack, your camaraderie, support, and shared passion for knowledge have made this journey not only intellectually stimulating but also deeply fulfilling. To my beloved Mercy Chepchirchir, your unwavering love, patience, and encouragement have been my source of strength throughout this endeavor. I express profound gratitude to all my family members, whose unwavering support, encouragement, and belief in my abilities have been a constant source of strength. Your sacrifices to support me during this journey have been immeasurable, and I am deeply grateful. Finally, I offer a special tribute to my late Mother, whose boundless love, sacrifices, and unwavering belief in my abilities continue to inspire me every day. Though you are no longer with us, your spirit lives on in every achievement, and this thesis is dedicated to your memory.

## TABLE OF CONTENTS

<b>DECLARATION</b> .....	ii
<b>ACKNOWLEDGEMENT</b> .....	iii
<b>LIST OF FIGURES</b> .....	vii
<b>LIST OF TABLES</b> .....	ix
<b>LIST OF ABBREVIATIONS AND ACRONYMS</b> .....	x
<b>LIST OF APPENDICES</b> .....	xi
<b>ABSTRACT</b> .....	xii
<b>CHAPTER ONE</b> .....	1
<b>INTRODUCTION</b> .....	1
1.1 Background information.....	1
1.2 Statement of the problem.....	4
1.3 Objectives.....	5
1.3.1 General objective.....	5
1.3.2 Specific objective.....	5
1.4 Research questions.....	5
1.5 Justification.....	6
1.6 Significance of the research.....	6
<b>CHAPTER TWO</b> .....	8
<b>LITERATURE REVIEW</b> .....	8
2.1 Diabetes Mellitus.....	8
2.2 Carbohydrates digesting enzymes.....	8
2.2.1 $\alpha$ -amylase.....	9
2.2.2 $\alpha$ -glucosidase.....	10
2.3 Treatment of hyperglycemia.....	11
2.4 Conventional antidiabetic drugs.....	11
2.5 Natural compounds as potential anti-hyperglycemic.....	12
2.6 Chemical databases in modern research.....	17
2.7 Computer-Aided Drug Design (CADD).....	19
2.7.1 Structure-based and ligand-based virtual screening.....	20
2.7.1.1 Ligand-based approach.....	20
2.7.1.2 Structure-based virtual screening.....	20
2.7.2 Molecular Docking.....	20

2.7.2.1 Search algorithm .....	21
2.7.2.2 Scoring function.....	21
2.7.3 ADMET and drug-like studies .....	21
<b>CHAPTER THREE .....</b>	<b>24</b>
<b>MATERIALS AND METHODOLOGY.....</b>	<b>24</b>
3.1 Retrieval and preparation of ligands for docking.....	24
3.1.1 Drug-likeness and <i>In-silico</i> pharmacokinetics screening .....	24
3.1.2 Toxicity based screening .....	25
3.2 Retrieval and preparation of receptor ( $\alpha$ -amylase and $\alpha$ -glucosidase).....	25
3.3 Molecular docking.....	26
3.3.1 Summary flow .....	27
3.3.2 Docking validation .....	27
3.4 Molecular dynamics simulation .....	27
3.4.1 Summary workflow .....	28
3.5 Energy minimization calculations.....	28
<b>CHAPTER FOUR.....</b>	<b>29</b>
<b>RESULTS AND DISCUSSION .....</b>	<b>29</b>
4.1 Virtual screening .....	29
4.1.1 Drug-likeness and <i>in-silico</i> pharmacokinetics screening .....	30
4.1.2 Toxicity based screening .....	33
4.1.3 Molecular docking studies.....	35
4.1.3.1 Binding interaction analysis of $\alpha$ -amylase (3BAJ) .....	36
4.1.3.2 Binding interaction analysis of $\alpha$ -glucosidase (2QMJ).....	37
4.1.3.3 Molecular docking studies of the selected dual inhibitors and the Acarbose with $\alpha$ -amylase and $\alpha$ -glucosidase .....	39
4.1.3.4 Binding interaction analysis of the selected two dual inhibitors .....	40
4.2 Pharmacokinetics properties of NPC204580 and NPC137813 .....	47
4.3 Synthetic Accessibility (SA) .....	49
4.4 Molecular Dynamic Simulations.....	50
4.4.1 Ligand Root Mean Square Deviation (RMSD) .....	50
4.4.2 Root-Means-Square Fluctuation (RMSF) .....	52
4.4.3 Molecular mechanism/ Generalized Born surface area (MM/GBSA) .....	55
<b>CHAPTER 5 .....</b>	<b>56</b>

<b>SUMMARY, CONCLUSION AND RECOMMENDATION</b> .....	56
5.1 Summary of the study .....	56
5.2 Conclusion.....	56
5.3 Recommendation.....	57
5.4 Suggestions for further studies .....	57
<b>REFERENCES</b> .....	58
<b>APPENDICES</b> .....	71

## LIST OF FIGURES

<b>Figure 1:</b> Crystallographic structure of $\alpha$ -amylase co-crystalized with Acarbose (green), (Viewed with PyMOL) .....	9
<b>Figure 2:</b> Crystallographic structure of $\alpha$ -glucosidase co-crystalized with Acarbose (cyan) (Viewed with PyMOL) .....	10
<b>Figure 3:</b> Examples of currently marketed antidiabetic drugs that work through inhibition of the hydrolytic enzymes. (Drawn with ChemDraw professional 16.0).....	12
<b>Figure 4:</b> Stages involved in CADD development adopted from (Maia et al., 2020) .	19
<b>Figure 5:</b> ADMET and drug-like flagship.....	22
<b>Figure 6:</b> Superposed structures of co-crystalized and best docked acarbose in $\alpha$ -amylase (3BAJ) and $\alpha$ -glucosidase (2QMJ). The most favorable docking poses of 3BAJ and 2QMJ is represented in blue and the crystallographic pose shown in green. ....	27
<b>Figure 7:</b> Schematic flow chart of structure-based virtual screening of the 30,926 Natural Products Activity and Species Source Database (NPASS) compounds. ....	29
<b>Figure 8:</b> Properties distribution of the remaining molecules (2228) (a) Molecular Weight, (b) Hydrogen bond acceptors (c) Hydrogen bond donors (d) number of rotatable bonds. ....	32
<b>Figure 9:</b> Properties distribution of the remaining molecules (2228) (e) Number of heavy atoms, (f) Topological polar surface area, (g) summation of hydrogen bond acceptors and donor, (h) The partition coefficient between n-octanol and water (Log Po/w). ....	33
<b>Figure 10:</b> Graphs of toxicological properties of the 2228 screened molecules: (a) stack bar graphs showing toxicity end point determined using the pkCSM, (b) Stacked bar graphs showing toxicity end point determined using Data Warrior. ....	35
<b>Figure 11:</b> Active-site of the Human pancreatic $\alpha$ -amylase with co-crystalized molecule Acarbose (cyan) .....	36
<b>Figure 12:</b> Active-site of the Human pancreatic $\alpha$ -glucosidase with co-crystalized molecule Acarbose (cyan).....	38
<b>Figure 13:</b> Docking scores and RMSD bar graphs for selected ligands in both (a) $\alpha$ -amylase and (b) $\alpha$ -glucosidase receptors. ....	39
<b>Figure 14:</b> Top ten poses of NPC204580, NPC137813, and Acarbose on the x-axis plotted against the binding affinity (S-score) for $\alpha$ -amylase (a) and $\alpha$ -glucosidase (b).	

The greater the negative value of S-score, the stronger the predicted binding affinity.  
.....40

**Figure 15:** 2D structures of the proposed molecules NPC204580 and NPC137813  
(Drawn with ChemDraw professional 16.0).....43

**Figure 16:** 2D interaction of the selected two ligands; NPC204580 and NPC137813  
Acarbose with the receptors 3BAJ and 2QMJ .....45

**Figure 17:** 3D docking conformation of the selected ligands; NPC204580 and  
NPC137813 and Acarbose in the binding site of  $\alpha$ -amylase (3BAJ) and  $\alpha$ -glucosidase  
(2QMJ). The molecular surface is colored green for the lipophilic regions and purple  
for the hydrophilic region of the receptor. ....46

**Figure 18:** BOILED-Egg plot for proposed molecules Molecule\_1 (NPC204580) and  
Molecule\_2 (NPC137813). ....48

**Figure 19:** The Bioavailability Radar of the proposed ligands. ....49

**Figure 20:** Graphical representation of the protein backbone RMSD (black) and ligand  
RMSD of the proposed molecules (a) NPC204580\_3BAJ, (b) NPC137813\_3BAJ, (c)  
NPC204580\_2QMJ and (d) NPC137813\_2QMJ.....52

**Figure 21:** Graphical representation of the RMSF trajectories of individual amino acids  
of both the 3BAJ (a) and 2QMJ (b) receptors, in associated with the proposed ligands  
(a) 3BAJ (NPC204580-black, NPC137813-red) and (b) 2QMJ (NPC204580-blue,  
NPC137813-yellow). ....54

## LIST OF TABLES

<b>Table 1:</b> Examples of isolated natural products with reported postprandial hyperglycemic inhibitory activity .....	14
<b>Table 2:</b> Docking score, RMSD values, and the interactions of selected dual inhibitors ligands and acarbose with the receptors 3BAJ and 2QMJ residues revealed during structure visualization. ....	44
<b>Table 3:</b> Pharmacological features of the proposed compounds.....	50
<b>Table 4:</b> Binding free energy (GBSA) of NPC137813 and NPC204580 in the two receptors.....	55

## **LIST OF ABBREVIATIONS AND ACRONYMS**

ADMET	Absorption, Distribution, Metabolism, Excretion, and Toxicity
AI	Artificial Intelligence
ARDS	Acute Respiratory Distress Syndrome
BBB	Blood Brain Barrier
bRO5	beyond Lipinski Rule of 5
CADD	Computer-Aided Drug Design
DM	Diabetes Mellitus
IDDM	Insulin-Dependent Diabetes Mellitus
GBSA	Generalized Born surface area
HNE	Human Neutrophil Elastase
HIA	Human Intestinal Absorption
MD	Molecular Dynamics
ML	Machine Learning
NCBI	National Center for Biotechnology Information
NPASS	Natural Products Activity and Species database
NIDDM	Non-insulin Dependent Diabetes Mellitus
PDB	Protein Data Bank
QSAR	Quantitative Structure-Activity Relationship
ROS	Reactive Oxygen Species
RMSD	Root Mean Square Deviation
RMSF	Root Mean Square Fluctuation
SBVS	Structure-Based Virtual Screening
SAR	Structure-Activity Relationship
T <sub>1</sub> DM	Type 1 Diabetes Mellitus
T <sub>2</sub> DM	Type 2 Diabetes Mellitus
TCM	Traditional Chinese Medicine
VS	Virtual Screening
WHO	World Health Organization

## **LIST OF APPENDICES**

**APPENDIX 1:** Docking score and the interactions of selected compounds and acarbose with the  $\alpha$ -amylase receptor (3BAJ) residues discovered during structure visualization

**APPENDIX 2:** Docking score and the interactions of selected top four compounds and acarbose with the  $\alpha$ -glucosidase receptor upon visualization.

**APPENDIX 3:** Top ten docked poses of the selected molecules; NPC137813, NPC204580, and the reference molecules Acarbose in 3BAJ and 2QMJ receptors.

**APPENDIX 4:** Articles published

## ABSTRACT

Postprandial hyperglycemia, typical manifestation of Type 2 Diabetes Mellitus (T<sub>2</sub>DM), is associated with notable global mortality over the past years. One way of preventing this condition's advancement is by delaying glucose absorption rate through inhibition of  $\alpha$ -amylase and  $\alpha$ -glucosidase enzymatic activities. Conventional methods of drug discovery have led to isolation of molecules with a variety of biological activities against diverse illnesses. For instance, the Natural Products Activity and Species database (NPASS) comprise of 30,926 unique active natural compounds from 25,041 sources, primarily from organisms. Most of these compounds are used in Traditional Chinese Medicine (TCM) and other traditional medicine, but there is no detailed information regarding their use to control T<sub>2</sub>DM. Additionally, current antidiabetic drugs such as Acarbose, Miglitol, Voglibose and 1-deoxynojirimicin (DNJ) have been associated with unpleasant side effects, hence necessitating the need for finding a more efficacious and safer antidiabetic drug. Therefore, the current study utilized computer-aided drug design (CADD), as a quick and affordable method to find a substitute drug template from NPASS database that can be used to control postprandial hyperglycemia by modulating the activity of  $\alpha$ -amylase and  $\alpha$ -glucosidase enzymes. The Natural Products Activity and Species source database (30,926 compounds) was screened *in silico*, with a focus on evaluating drug-likeness, toxicity profiles and ability to bind on a target protein. Two molecules NPC204580 (Chrotacumine C) and NPC137813 (1-O-(2-Methoxy-4-Acetylphenyl)-6-O-(E-Cinnamoyl)- $\beta$ -D-Glucopyranoside) were identified as potential dual inhibitors for  $\alpha$ -amylase and  $\alpha$ -glucosidase. Their docking scores was -14.46 kcal/mol and -12.58 kcal/mol for  $\alpha$ -amylase, and -8.42 kcal/mol and -8.76 kcal/mol for  $\alpha$ -glucosidase, respectively. Moreover, 100 nanoseconds (ns) molecular dynamic simulations revealed that the two molecules were stable on the receptor's active sites based on analysis metrics such as root mean square deviation (RMSD), root mean square fluctuations (RMSF) and free binding energy calculation as per the Generalized Born surface area (MM/GBSA). Additionally, the molecules demonstrated acceptable pharmacokinetic and toxicological profiles as substances that can be easily delivered to the intended site of action. Therefore, the two compounds are thus promising therapeutic agents for T<sub>2</sub>DM that merit further investigation (*in-vitro* and *in-vivo*) due to their excellent binding energies, encouraging pharmacokinetics and toxicity profiles, as well as the stability demonstrated in simulation studies.

# CHAPTER ONE

## INTRODUCTION

### 1.1 Background information

Diabetes, a challenging metabolic illness, is projected by WHO to be the seventh leading cause of death globally by 2030 (Balakumar et al., 2016). Diabetes Mellitus prevails in most countries globally and is now a major concern. According to a report by the International Diabetes Federation (IDF), 536 million people worldwide suffer from diabetes mellitus, a global health concern that is predicted to double over the next 25 years (Saeedi et al., 2019). Globally, 10% of the global population (536.6 million persons) were estimated to have diabetes in 2021, with projections suggesting it will increase to 12.2 % (783.2 million people) by 2030 and 883 million by 2045 (Wen et al., 2024).

Diabetes Mellitus is classified into two primary forms T<sub>1</sub>DM (Insulin-dependent diabetes mellitus (IDDM)) and T<sub>2</sub>DM, (non-insulin-dependent diabetes mellitus (NIDDM)). Type-2 Diabetes Mellitus, is the most dominant in both developed and developing countries as the traditional meals are being replaced with processed foods that are high in calories (Fareed et al., 2017). The prevalence of overweight (obesity) and the rising sedentary lifestyle are significant contributors to the development of T<sub>2</sub>DM (Kishimoto & Ohashi, 2021). Managing Type-2 Diabetes Mellitus involves reducing sugar intake or using pharmaceutical drugs that can lower blood glucose levels, although eliminating sugar from the diet entirely is impractical, hence making it difficult to control sugar intake from food products. Postprandial hyperglycemia is the major manifestation of T<sub>2</sub>DM characterized by unusually higher sugar levels, resulting in serious health issues such as diabetic neuropathy and cardiovascular diseases (World Health Organization, 2016).

Digestive enzymes  $\alpha$ -amylase and  $\alpha$ -glucosidase are essential for the digestion of carbohydrates, aiding in breaking down starch and glycogen to simpler monosaccharides (Kandra, 2003).  $\alpha$ -amylase is a calcium metalloenzyme that catalyzes the cleavage of  $\alpha$ -D-(1-4) glycosidic bonds in starch and oligosaccharides (Lordan et al., 2013). Whereas  $\alpha$ -glucosidase, an enzyme found in the brush-border surface membrane of intestinal cells breaks down complex carbohydrates and oligosaccharides

into absorbable monosaccharides such as glucose (Lordan et al., 2013). Therefore, regulation of postprandial hyperglycemia heavily relies on the activities of these two enzymes, as inhibiting these hydrolytic enzymes reduces available glucose for absorption from the ileum into the bloodstream, thereby mitigating postprandial hyperglycemia. Thus, one of the well-established therapeutic strategies for T<sub>2</sub>DM control is to hinder the activity of these hydrolytic enzymes by blocking their active sites hence decreasing polysaccharide substrate availability for glucose release into the gut (Kajaria et al., 2013).

Acarbose and miglitol, common anti-diabetic drugs, work through inhibition of  $\alpha$ -amylase and  $\alpha$ -glucosidase metabolic activity, thereby lowering the amount of glucose ready for assimilation in the alimentary canal and consequently lowering sugar levels in the body (Funke & Melzig, 2006). However, these anti-diabetic drugs have been linked to negative/ unfavorable side effects such as stomach upset, nausea and liver diseases (Fujisawa et al., 2005; Murai et al., 2002; Palanisamy et al., 2018). Therefore necessitating the exploration for alternative management options, particularly from natural sources like medicinal plants and their phytoconstituents (Krupanidhi et al., 2016; Missoun et al., 2018).

Reports (Table 1) suggest promising drug candidates in medicinal plants, encouraging further research for drug templates that can be used for further formulation of drug candidates. Pharmacologically active components of plants, such as vitamins, carotenoids, phenolic, anthocyanins, alkaloids, and triterpenoids can provide an armor against postprandial hyperglycemia. They achieve this by reducing blood sugar in diabetic patients through inhibition  $\alpha$ -amylase and  $\alpha$ -glucosidase hence reducing direct and indirect effects of postprandial hyperglycemia complications (Asmaa et al., 2016). Notable, pharmacological research achievements include the discovery of gelagine, guanidine which was originally isolated from *Galega officinalis* L, and later developed into a group of antidiabetic drugs namely, metformin, phenformin, buformin and proguanil (Bailey & Day, 2004). Antidiabetic drugs like Acarbose, an  $\alpha$ -glucosidase inhibitors from microbial metabolite, and miglitol, a derivative of 1-desoxynojirimycin are known for their effectiveness in treating diabetes (van de Laar et al., 2005).

The discovery of these drug templates and many other antidiabetic compounds were established based on conventional pharmacological procedures. Still there are many compounds that require structure-activity relationship studies (SAR) to establish their potential. However, SAR following experimental models through to clinical trials has been overtaken by events due to cost and the trial-and-error steps involved. It is estimated that the process of drug discovery pipeline spanning from the identification of lead compounds through to clinical trials, can take approximately fourteen years and incur a cost amounting to 800 \$ million (Lavecchia & Giovanni, 2013). Such limitation brings into play the recent computational approach which forecast molecules capable of effectively binding to specific targets such as enzymes and receptor proteins involved in disease metabolic pathways. Therefore, CADD, such as drug-likeness screening, toxicity screening, molecular docking, and molecular dynamic simulations, has been introduced in the design and unearthing of new drugs template/candidates. This is because these approaches allow for better focusing on an experiment which significantly helps to minimize the duration and expenses associated with researching novel therapeutics (Kitchen et al., 2004), hence guiding this study. A structure-based drug design was employed in finding a probable dual inhibitor for  $\alpha$ -amylase and  $\alpha$ -glucosidase receptors following beyond Lipinski rule of 5 (bRO5) comprising of varied MedChem Mnemonic Rules such as Lipinski, Verber, Shultz, and Meanwell rules (Lipinski et al., 2001; Meanwell, 2016; Shultz, 2019; Veber et al., 2002).

In contemporary research, numerous endeavors have focused on uncovering efficient  $\alpha$ -glucosidase and  $\alpha$ -amylase inhibitors, obtained from natural products, these include various classes of bioactive phytochemicals such as flavonoids, alkaloids, terpenoids, etc. Most of these inhibitors have been isolated from plants, and they work by hindering the assimilation of glucose through the inhibition of carbohydrates-hydrolyzing enzymes (Kumar et al., 2011; Li et al., 2022). A huge number of metabolites derived from natural sources especially plants, have been isolated and collated as databases such as ZINC 15, Drug Bank, PubChem, NPASS, and Enamine. Several of these databases furnish detailed structural and associated information including qualitative information, but with limited experimental activities (Zeng et al., 2018).

NPASS database (<http://bidd2.nus.edu.sg/NPASS>) was thus developed to supplement other databases by offering experimental activity data and species sources of 30,926 compounds derived from 25,041 species (Zeng et al., 2018). Apart from these isolated natural products, various organisms (either whole or specific parts) have been utilized as medicinal materials in Traditional Chinese Medicine (TCM) and other traditional healing practices for many years (Zeng et al., 2018; Zhao et al., 2023). In its coverage, NPASS includes qualitative activity of important NP data together with information on mechanisms, chemical properties, and taxonomic profiles (Zeng et al., 2018). Such information makes drug discovery studies on mechanisms and many *in silico* studies easier, as it aids in understanding the molecular mechanism underlying the effects of NPs.

In addition to providing detailed information regarding the chemical properties and toxicological profiles of NPs, the NPASS database categorizes target proteins into different classes such as enzymes, membrane receptors, ion channels, and transporters which form a benchmark for other *in silico* studies (Zhao et al., 2023). Therefore, in these categories of targets, studies on hydrolytic enzymes such as  $\alpha$ -glucosidase and  $\alpha$ -amylase have not been studied. Consequently, *in-silico* virtual screening was conducted on 30,926 compounds from the NPASS database in quest of finding an  $\alpha$ -amylase and  $\alpha$ -glucosidase drug template using chemoinformatic tools.

### **1.2 Statement of the problem.**

Postprandial hyperglycemia has emerged as the seventh foremost cause of death worldwide. The available synthesized drugs such as Acarbose, Voglibose and, Metformin acting through inhibition of hydrolytic enzymes ( $\alpha$ -glucosidase and  $\alpha$ -amylase) have been linked with adverse undesired effects necessitating further investigations to find an alternative drug template. The search for a drug substitute that can effectively be used to manage diabetes-related conditions is hindered by several constraints. These include inconclusive clinical trial results, incomplete drug validation process, unmet safety and efficacy requirements, and the significant expense and time consumption involved in the process. Natural products remain a viable source for research into safe and efficient diabetic medication templates because they provide an alternative reservoir for drug therapeutic search. Recent research has led to the

unearthing and isolation of bioactive phytochemicals from natural sources, such as plants and other organisms. The majority of these compounds have been confirmed to be active against diverse infections. However, there is a paucity of information detailing their activity against T<sub>2</sub>DM.

The NPASS database contains a compilation of such bioactive compounds that have been isolated, analyzed, and found to have a variety of biological activities. Despite extensive information on bioactive compounds and their structure-activity relationships, no potential therapeutic agents for managing Type-2 Diabetes Mellitus have been identified from the NPASS databases. Moreover, there are numerous *in-silico* reports in the NPASS database for bioactive compounds and protein targets, but no reports regarding  $\alpha$ -amylase and  $\alpha$ -glucosidase inhibitions are provided. It is in this regard, a strategic re-evaluation of NPASS database was done to establish the lead-like candidate for postprandial hyperglycemia through virtual screening.

### **1.3 Objectives**

#### **1.3.1 General objective**

To establish  $\alpha$ -amylase and  $\alpha$ -glucosidase inhibitors from Natural Products Activity and Species Source (NPASS) database using *in silico* approach.

#### **1.3.2 Specific objectives**

- 1) To determine for drug-like molecules from NPASS database utilizing structure activity based virtual screening techniques (beyond Lipinski rule of five (bRO5)).
- 2) To determine the molecular interaction and stability of the selected drug-like molecules with  $\alpha$ -glucosidase and  $\alpha$ -amylase enzymes using structure-based molecular docking and simulation techniques.
- 3) To predict the pharmacokinetics and pharmacodynamics properties of the most promising bioactive compounds utilizing *in-silico* approaches.

### **1.4 Research questions**

1. Which are the chemical compounds with drug-like properties and have no adverse toxicity profiles are there in the NPASS database?

2. What are the functional units among the selected natural products with drug-likeness properties enhance the molecular inhibitory interactions with the target protein?
3. Among the top ranked compound with a high affinity for modulation of  $\alpha$ -glucosidase and  $\alpha$ -amylase, what are their pharmacokinetics and pharmacodynamics for the management of T<sub>2</sub>DM?

### **1.5 Justification**

Conventional antihyperglycemics in clinical use have several drawbacks such as insufficient efficacy, high cost, inaccessibility, and undesirable side effects. The limitations of conventional therapies necessitate the search for new, effective compounds as alternative options. The global prevalence of diabetic illnesses necessitates the development of alternative remedies and accurate therapeutic forecasts to address the high morbidity and mortality rates. Hence compelling the need to find novel and safe  $\alpha$ -amylase and  $\alpha$ -glucosidase inhibitors. Numerous efforts have been undertaken to uncover efficient  $\alpha$ -glucosidase and  $\alpha$ -amylase inhibitors, from natural sources through conventional pharmacological procedures, that are expensive and time consuming. The challenges in drug discovery through conventional methods necessitate the use of computer-aided drug design (CADD), a cost-effective method for identifying promising drug candidates and reducing animal models in pharmacological studies. Therefore, this study pointed out the most promising drug candidate from NPASS database without going through conventional methods which are expensive and time-consuming.

### **1.6 Significance of the research**

This research holds significant values for the Kenya's socio-economic and health priorities as outlined in Kenya Vision 2030, the sustainable development goals (SDGs), and the Big Four Agenda. Diabetes, particularly Type 2 Diabetes Mellitus, is a growing health burden in Kenya and globally, contributing to increased morbidity, mortality, and high health care cost. By employing advanced cheminformatics techniques to identify potential inhibitors from existing natural products database, this research supports SDG 3 (Goal Health and Well-being) by fostering the discovery of affordable and effective treatment options that can control the impact of this non-communicable disease. Its

computational approach also reduces research cost and time, making the drug discovery more efficient and scalable, hence supporting vision 2030 social pillar of building a healthy and globally competitive nation while strengthening the country's biomedical research capabilities.

## **CHAPTER TWO**

### **LITERATURE REVIEW**

#### **2.1 Diabetes mellitus**

Diabetes mellitus (DM) has emerged to be one of the highly predominant metabolic illnesses with the growing obesity crisis increasing the risk of cardiovascular diseases and even mortality (Glovaci et al., 2019). The disease is categorized into two domain: insulin-dependent (T<sub>1</sub>DM) and non-insulin dependent (T<sub>2</sub>DM), caused by immune-mediated cell destruction and insulin secretion deficiency or resistance, respectively (Asmat et al., 2016). Type one Diabetes Mellitus usually occurs during early stages of human growth, when the immune system halts the pancreas from producing insulin. The exact reason for this immunological reaction is yet to be fully understood. Therefore, individuals' plasma glucose levels need to be closely monitored regularly because sudden changes can be fatal. Patients suffering from T<sub>1</sub>DM usually need to take insulin on a regular basis in order to control their blood sugar levels.

Type two Diabetes Mellitus is the most predominant compared with T<sub>1</sub>DM, accounting for 90-95% of Diabetes Mellitus diagnoses. It arises as results of defective insulin secretion by pancreatic cells and the peripheral tissue's inability to utilize insulin, therefore resulting in significant abrupt blood glucose levels, known as postprandial hyperglycemia (Goyal et al., 2022). Long-term hyperglycemia causes oxidative stress, which is caused by the reactive oxygen species (ROS) (Yaribeygi et al., 2020). Reactive oxygen species have the potential to induce damage to microvascular tissues, increasing the likelihood of micro and macro-vascular illnesses like hypertension, myocardial infarction, diabetes retinopathy, and dyslipidemia (Yaribeygi et al., 2020). Maintaining stable blood glucose levels can be achieved by delaying its absorption via the inhibition of hydrolytic enzymes responsible for carbohydrates hydrolysis in the alimentary canal.

#### **2.2 Carbohydrates digesting enzymes**

Starch, a key substrate in energy metabolism, is a major ingredient in human diet as a source of glucose. Starch is composed of two major structural elements: amylose and amylopectin, made of  $\alpha$  (1-4)-linked glucosyl units, and  $\alpha$  (1-4) as well as  $\alpha$  (1-6) linkages for amylopectin (Sim et al., 2008). Carbohydrates digestion in human digestive system is completed by four enzymes' i.e., endo-hydrolases which breaks the  $\alpha$ -(1-4)

bonds in polysaccharides like starch into much shorter dextrin chains. Subsequently, the resulting dextrin mixture is further broken down into simpler monosaccharide (glucose) by sucrase-isomaltose and maltase-glucoamylase in the brush border of the ileum (Sim et al., 2008).

### 2.2.1 $\alpha$ -amylase

Human pancreatic  $\alpha$ -amylase Figure 1 is a hydrolase enzyme found in microbes, plants, and animals (Anitha Gopal & Muralikrishna, 2009). “ $\alpha$ -amylase, an enzyme present in saliva and pancreatic secretions, hydrolyzes  $\alpha$ -linked polysaccharides such as starch and glycogen resulting into simpler monosaccharides like glucose and maltose which are then absorbed into the bloodstream” (Chaudhury et al., 2017). Porcine pancreatic  $\alpha$ -amylase, a metalloenzyme with 83% sequence homology to human pancreatic  $\alpha$ -amylase and consisting of 496 amino acid residues, necessitates the presence of at least one  $\text{Ca}^{2+}$  ion per molecule for its catalytic activity and structural stability (Sui et al., 2016). Figure 1 present the crystallographic conformation of the enzyme’s molecular structure, and the active site having the co-crystallized ligand Acarbose (green), and other conformations that give this particular enzyme its catalytic selectivity.

For Educational Use Only

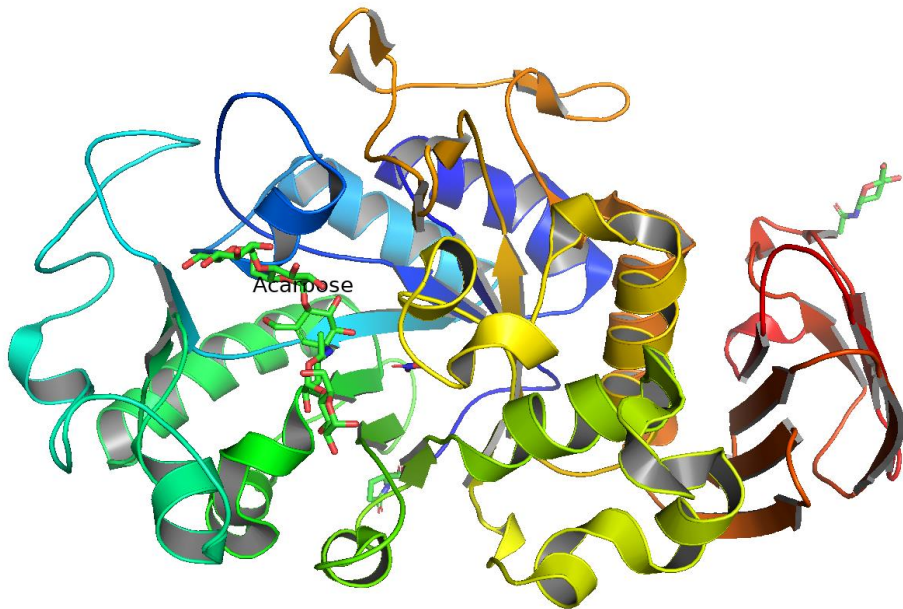


**Figure 1:** Crystallographic structure of  $\alpha$ -amylase co-crystallized with Acarbose (green), (Viewed with PyMOL)

### 2.2.2 $\alpha$ -glucosidase

$\alpha$ -Glucosidase (Figure 2) is a membrane-bound enzyme localized at the epithelium tissues of the small intestines. This enzyme is crucial in carbohydrate digestion, catalyzing the hydrolytic reaction to release  $\alpha$ -glucose from the substrate, as well as transferring reactions and hydration of D-glucal (Tundis et al., 2010). Other than hydrolysis of polysaccharide in both human and animals,  $\alpha$ -glucose also plays a crucial role in other industrial processes such as food processing, brewing, and biofuel production (Tundis et al., 2010). The enzyme generally exhibits a  $(\beta/\alpha)$ 8-barrel conformation, crucial for its catalytic functions. Figure 2 presents crystals structure with its active site that enable enzymatic cleavage having a co-crystallized ligand Acarbose (green). Therefore, inhibition of  $\alpha$ -glucosidase could delay hydrolysis of oligosaccharides in the small intestine making it an effective strategy for managing hyperglycemic conditions.

For Educational Use Only

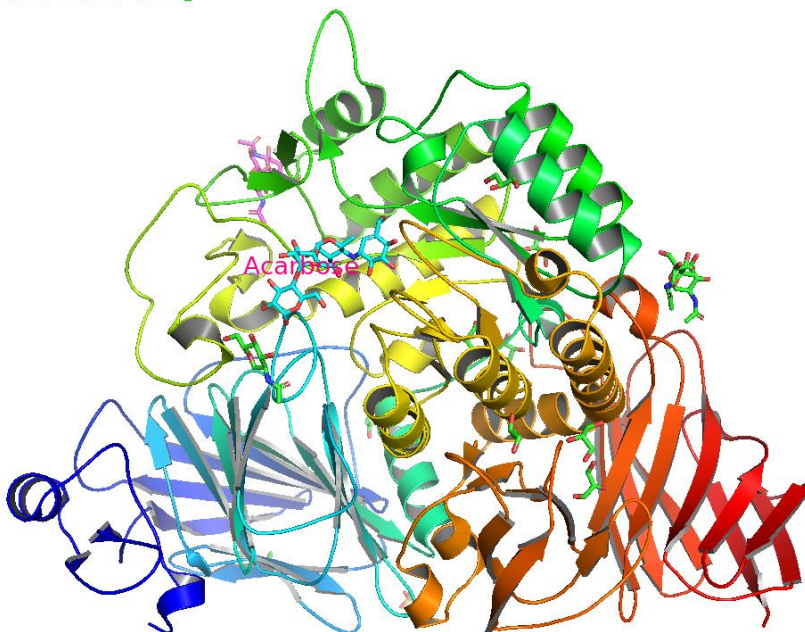


**Figure 2:** Crystallographic structure of  $\alpha$ -glucosidase co-crystallized with Acarbose (cyan) (Viewed with PyMOL)

### **2.3 Treatment of hyperglycemia**

Inhibition of hydrolytic enzymes can reduce post-prandial blood glucose spike after a mixed diet of carbohydrates, hence management of T<sub>2</sub>DM. However, the prolonged use of conventional drugs such as Acarbose, Voglibose and, Metformin as inhibitors has led to various clinical side effects (Fujisawa et al., 2005; Murai et al., 2002; Palanisamy et al., 2018), prompting ongoing research to discover novel therapeutics, particularly from natural sources.

### **2.4 Conventional antidiabetic drugs.**

Currently, available antidiabetic drugs, as shown in Figure 3, form the existing armor against postprandial hyperglycemia. They help to control blood glucose levels by either boosting insulin secretion, enhancing insulin sensitivity, reducing intestinal glucose absorption, and increasing glucose uptake by tissue cells (Dixit & Bharatam, 2013). Drugs that lower blood sugar come in a variety of forms, such as insulin secretagogues (Sulfonylureas and Meglitinides), insulin sensitizers (Biguanides, Metformin, and Thiazolidinediones), and  $\alpha$ -glucosidase inhibitors (Miglitol, Acarbose) (Pankaj Modi, 2007). Exenatide, Liraglutide, and Dipeptidyl peptidase (DPP)-4 inhibitors are examples of new peptide analogs that enhance Glucagon-Like Peptide (GLP-1) blood levels and decrease gastrointestinal emptying (Hui et al., 2005). Most medications used to lower blood sugar may cause adverse effects like extreme hypoglycemia, lactic acidosis, liver cell impairment, cognitive deficiency, digestive pain, and headache (Ganesan et al., 2024). New treatments are increasingly targeting drug designs that reduce plasma glucose concentration and sustain blood glucose homeostasis with minimal adverse effects through the use of herbs, medicinal plants, animals, and microorganisms (Jhong et al., 2015).

The three common antidiabetic drugs that help to regulate plasma sugar levels by inhibiting carbohydrates digestion and consequently absorption include Acarbose, Voglibose, and Miglitol (Nakano et al., 2009). Acarbose is the first hydrolytic enzyme inhibitor commonly used for management of T<sub>2</sub>DM by inhibiting carbohydrate digestion and absorption (Nakano et al., 2009). Miglitol, a derivative of 1-deoxynojirimycin, is a potent inhibitor of Sucrase, Glucoamylase, and Isomaltase activities, thereby reducing blood glucose levels (Chaudhury et al., 2017). Voglibose,

a bacterial compound, is known to inhibit the hydrolytic activities of  $\alpha$ -glucosidase on sucrose, Isomaltase, and Maltase (Fujisawa et al., 2005). Conventional drugs can treat diabetic patients by improving insulin sensitivity and increasing or decreasing glucose levels, but total recovery is not yet possible. Conventional drugs are not always satisfactory in maintaining blood glucose levels, necessitating the urgent need for new products for diabetic treatment.

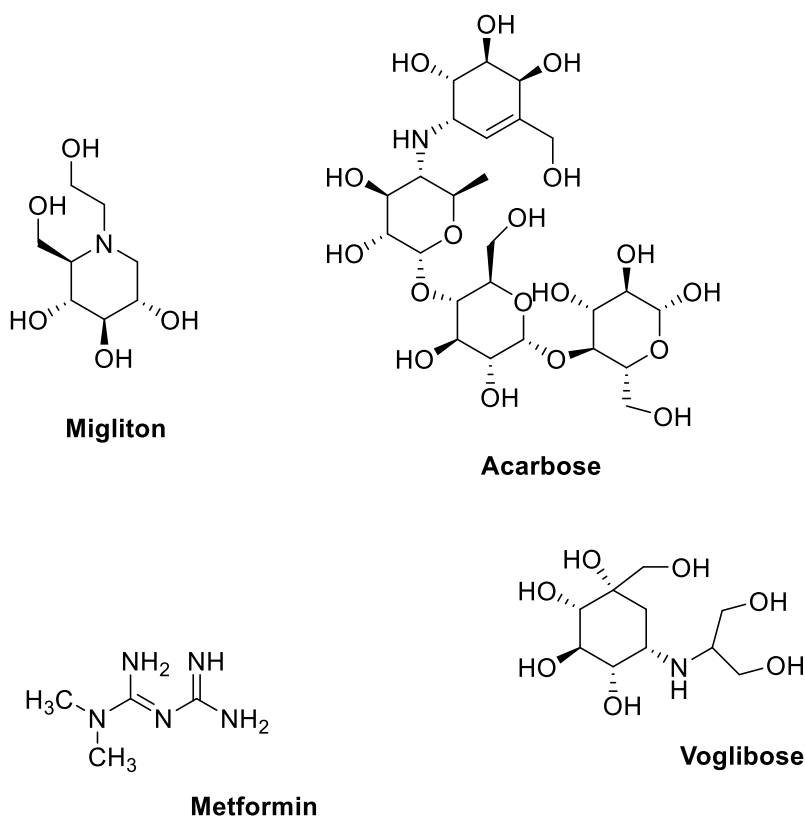


**Figure 3:** Examples of currently marketed antidiabetic drugs that work through inhibition of the hydrolytic enzymes. (Drawn with ChemDraw professional 16.0)

### 2.5 Natural compounds as potential anti-hyperglycemic

Medicinal plants and herbs have shown promising pharmacological activities in folk medicine, with hydrolytic enzymes ( $\alpha$ -glucosidase and  $\alpha$ -amylase) inhibitors having been developed and used as lead compounds for diabetes mellitus control (Dutra et al., 2016; Prasathkumar et al., 2021). Researchers are exploring natural compounds for effective oral hyperglycemic agents with minimal side effects, with several plants being empirically used worldwide (Tundis et al., 2010). Therefore,  $\alpha$ -glucosidase and  $\alpha$ -amylase inhibitors from natural products offer an attractive approach for the

management of T<sub>2</sub>DM. Table 1 highlight the different classes of some molecules that have been isolated and reported as potential hyperglycemic agents following significant inhibitory activities against hydrolytic enzymes, such as  $\alpha$ -amylase and  $\alpha$ -glucosidase in *in-vitro* studies.

**Table 1:** Examples of isolated natural products with reported postprandial hyperglycemic inhibitory activity

	<b>Compound Name</b>	<b>Class</b>	<b>Inhibitory activity</b>	<b>Plant species</b>	<b>Reference</b>
1	Skimmianine, norchelerythrine, 6-acetonyldihydrochelerythrine and 6-hydroxy-N-methyl decarine	Alakloids	47.72, 49.36,48.91 ( $\mu\text{M}$ ) for $\alpha$ -amylase and 47.63,47.27, 49.20 ( $\mu\text{M}$ ) for $\alpha$ -glucosidase	<i>Zanthoxylum chalybeum</i>	(Ochieng et al., 2020)
2	7 $\beta$ ,6 $\beta$ -dihydroxyroyleanone	Abietane diterpenoids	274.9 $\mu\text{g/mL}$	<i>Plectranthus madagascariensis</i>	(Kubínová et al., 2014)
3	7 $\beta$ -acetoxo-6 $\beta$ -hydroxyroyleanone	Abietane diterpenoids	108.2 $\mu\text{g/mL}$	<i>Plectranthus madagascariensis</i>	(Kubínová et al., 2014)
4	Coleon U quinone	Abietane diterpenoids	142.7 $\mu\text{g/mL}$	<i>Plectranthus madagascariensis</i>	(Kubínová et al., 2014) ,(Wellsow et al., 2006)
5	Ailanthoidol, 2,3-epoxy-6,7-methylenedioxy coniferyl alcohol, sesamine	Lignans	48.34, 54.67 ( $\mu\text{M}$ ) for $\alpha$ -amylase and 47.45,54.77 ( $\mu\text{M}$ ) for $\alpha$ -glucosidase	<i>Zanthoxylum chalybeum</i>	(Ochieng et al., 2020)
6	Pedunculagin, strictinin, sanguiin H-5, lambertianin and, rubusuarin	Tannins	14.8, 56.2, 56.3, 36.9, 54.2 % Enzyme inhibition	<i>Rubus suavissimus</i>	(Tundis et al., 2010)
7	Spicatanol	Diterpenes	89.5 % Enzyme inhibition	<i>Hedychium spicatum</i>	(Prabhakar Reddy et al., 2009)
8	Spicatanol methyl ether	Diterpenes	54.1 % Enzyme inhibition	<i>Hedychium spicatum</i>	(Prabhakar Reddy et al., 2009)

<b>9</b>	Hedychenone	Diterpenes	55.6 % Enzyme inhibition	<i>Hedychium spicatum</i>	(Prabhakar Reddy et al., 2009)
<b>10</b>	D-Galactopyranosyl harpagoside	Terpenoids	2.16 mmol/L	<i>Scrophularia ningpoensis</i>	(Hua et al., 2014)
<b>11</b>	8-O-feruloyl harpagide	Terpenoids	3.02 mmol/L	<i>Scrophularia ningpoensis</i>	(Hua et al., 2014)
<b>12</b>	8-O-(coumaroyl)harpagide	Terpenoids	3.09 mmol/L	<i>Scrophularia ningpoensis</i>	(Hua et al., 2014)
<b>13</b>	Diosgenin, diosgenin, and pennogenin	Steroids	38.9 ± 7.8, 29.4 ± 4.5, 24.7 ± 5.1 µg/mL	<i>Dioscorea polygonoides</i>	(McAnuff et al., 2005)
<b>14</b>	1-deoxymannojirimycin	Alkaloid	600 µM	<i>Adenophora spp</i>	(Ikeda et al., 1999), (Shibano et al., 2008), (Tabopda et al., 2008)
<b>15</b>	1,5-dihydroxy-2-isopropenyldihydrofuran[3,4-c] acridone	Acridones	56 ± 5.4 µmol/L	<i>Oriciopsis glaberrima</i>	(Wansi et al., 2006)
<b>16</b>	bis-5-hydroxy-(10H)-hydronoracromycine	Acridones	34.05 ± 17 µmol/L	<i>Oriciopsis glaberrima</i>	(Wansi et al., 2006)
<b>17</b>	1,3,5-trihydroxyl-4-prenylacridone	Acridones	17 ± 1 µmol/L	<i>Oriciopsis glaberrima</i>	(Wansi et al., 2006)

18	Harmanyl $\beta$ -D-glucopyranoside	Glycoalkaloid	24 $\mu\text{mol/L}$	<i>Buthus martensii</i> Karsch	(Kim, 2013)
19	Chlorogenic acids (CGAs)	Polyphenolic	54 %	<i>Green coffee</i>	(Narita & Inouye, 2015)
20	Torachryson-8-O- $\beta$ -D-glucopyranoside	Anthraquinones	75 %	<i>Rheum emodi</i>	(Suresh Babu et al., 2004)
21	Chrysophanol-8-O- $\beta$ -D-glucopyranoside	Anthraquinones	84 %	<i>Rheum emodi</i>	(Suresh Babu et al., 2004)
22	3-O- $\beta$ -D-glucopyranosyl-1-hydroxy-4,5-dimethoxyxanthone	Xanthone glycosides	> 1000 $\mu\text{mol/L}$	<i>Swertia bimaculate</i>	(Yue et al., 2014)
23	1-O- $\beta$ -D-glucopyranosyl-3,8-dihydroxy-4,5-dimethoxyxanthone	Xanthone glycosides	578 $\pm$ 39 $\mu\text{mol/L}$	<i>Swertia bimaculate</i>	(Yue et al., 2014)
24	3-O- $\beta$ -D-glucopyranosyl-1,8-dihydroxy-5-methoxyxanthone	Xanthone glycosides	> 1000 $\mu\text{mol/L}$	<i>Swertia bimaculate</i>	(Yue et al., 2014)
25	7-O-[ $\alpha$ -L-rhamnopyranosyl-(1 $\rightarrow$ 2)- $\beta$ -D-xylopyranosyl-1,8-dihydroxy-3-methoxyxanthone	Xanthone glycosides	765 $\pm$ 54 $\mu\text{mol/L}$	<i>Swertia bimaculate</i>	(Yue et al., 2014)
26	kaempferol-3-O- $\alpha$ -L-rhamnopyranoside 3",4"-di-E-p-coumaric acid ester	Acylated flavonoids	6.10	<i>Machilus philippinensis</i>	(Lee et al., 2008)
27	3"-E,4"-Z-di-p-coumaric acid ester	Acylated flavonoids	1.00 $\mu\text{mol/L}$	<i>Machilus philippinensis</i>	(Lee et al., 2008)

Polyphenols, including flavonoids, phenolic acids, and galloyl, are the most commonly reported inhibitors of  $\alpha$ -amylase and  $\alpha$ -glucosidase due to their better inhibitory activity (Sun et al., 2016). The binding interactions between polyphenol and amylase are influenced by polar molecular structures, including hydrogen bonding and hydrophobic forces (Lo Piparo et al., 2008). Moreover, electron delocalization between C=C or C=O and aromatic rings in polyphenols could enhance the hydrophobic interactions between the phenolic and the enzymes (Xiao et al., 2013). However, the fine details have not been established in a number of the phytochemicals listed in Table 1, probably due to the large number and variations among the plant metabolites. Moreover, the active mechanisms of the lead compounds obtained remain unclear. Nonetheless, numerous phytochemicals have been isolated, characterized and cataloged in various chemical databases such as PubChem, Enamine, ChemSpider, ChEMBL, Drugbank, and NPASS, among others. These repositories contain an extensive collection of chemical structures along with associated biological activities and properties. Therefore, this underscores the importance of leveraging computational approach, to explore these databases for novel therapeutic candidates against P. Hyperglycemia.

## **2.6 Chemical databases in modern research**

Chemical databases are essential in various scientific disciplines today, such as chemistry, biochemistry, pharmacology, and materials science (Turban et al., 2021; Williams, 2008). These databases contain significant amount of information regarding the molecules, their properties, reactions and biological activities among other properties. Centralizing these data, scientific researchers are able to find comprehensive information for these compounds in one source thus sparing them the trouble of scouring through literature or carrying out repetitive experimental procedures. This speeds up the process of scientific drug discovery and innovation through the provision of information on molecular targets, biological activities, and SARs (Structure-Activity Relationships) of the molecules. Examples of these database include; PubChem, Enamine, ChemSpider, ChEMBL, Drugbank, NPASS.

PubChem maintained by the NCBI is one of the largest and broadest chemical databases of chemical molecules in the world. It contains a plethora of molecules including small molecules, peptides and biological macromolecules (Kim et al., 2023). Therefore, it

becomes an important source of reference for scientists working in different disciplines, such as pharmaceutical industries, and academic institutions. ChemSpider database is managed by the Royal Society of Chemistry. It focuses on organic, inorganic, and organometallic compounds (Ayers, 2012). However, it contains diverse chemical data it acquires from publishers, users and chemical vendors on a global scale. It has an extensive database that hosts a variety of information regarding chemical particles' structure spectrum among other properties. Additionally, its' user-friendly interface allows for easy searching and browsing of chemical compounds, with detailed information provided for each entry. ChEMBL is maintained by the European Bioinformatics Institute (EMBL-EBI). The platform gives extensive information on compounds that have been examined for their interaction with biological targets such as proteins, enzymes as well as nucleic acids (Gaulton et al., 2017). ChEMBL integrates data from scientific literature, patents, and high-throughput screening assays, offering valuable insights into compound potency, selectivity, and pharmacological profile (Gaulton et al., 2017). Even though its main focus is on pharmaceuticals and pharmacology research, ChEMBL is freely accessible hence fostering collaboration and knowledge exchange within the scientific community.

The NPASS database is a unique database dedicated to natural products and their biological activities. It compiles data on natural compounds sourced from plants, microbes, and marine organisms and aggregates their information alongside their biological activities and species sources (Zeng et al., 2018). The version (V1.0) of NPASS database, contains “30,926 distinct natural compounds obtained from 25,041 source organisms, in addition to 446,552 activity records on 5,863 targets” (Zeng et al., 2018). Researchers interested in natural products for drug discovery or biomedical research may benefit from this invaluable reservoir. The sources of information are scientific literature, patents, and databases related to natural products chemistry and pharmacology. NPASS' web interface provides easy access of information to the users, allowing them to explore and analyze compounds derived from natural products. Therefore, leveraging these chemical databases with computational tools for *in-silico* screening presents a viable strategy to uncover novel therapeutic agents with improved

efficacy and safety profiles for managing hyperglycemia and related metabolic disorders.

## 2.7 Computer-Aided Drug Design (CADD)

Drug development and discovery in the fight against diseases is a costly and time-consuming process (Singh et al., 2019). Figure 4 depicts the stages that are involved in the drug discovery procedure, including target identification, target validation, hit identification, lead discovery and optimization, biological testing, and clinical trials (Maia et al., 2020). Computational techniques enhance research productivity, save time and money, and are crucial in drug discovery. Computer-aided drug design emerged in the 1960s and since then, it has expanded and evolved into a crucial component of drug discovery due to advancements in computer hardware and software as well as the growing accessibility of protein structures of pharmaceutically relevant biochemical targets (Zhao et al., 2020). Numerous studies have been conducted to describe specific computational techniques, their purpose and significance, pointing out recent developments and their advantages and disadvantages (Zhao et al., 2020). This methodology is widely utilized in the creation of pharmaceutical drugs, particularly in the analysis of enzyme protein targets. Nguyen (2015), suggests that computational methods can predict and simulate conformational, steric, and physicochemical properties of target proteins, aiding in understanding drug action, inhibition, and structure-activity relationships.

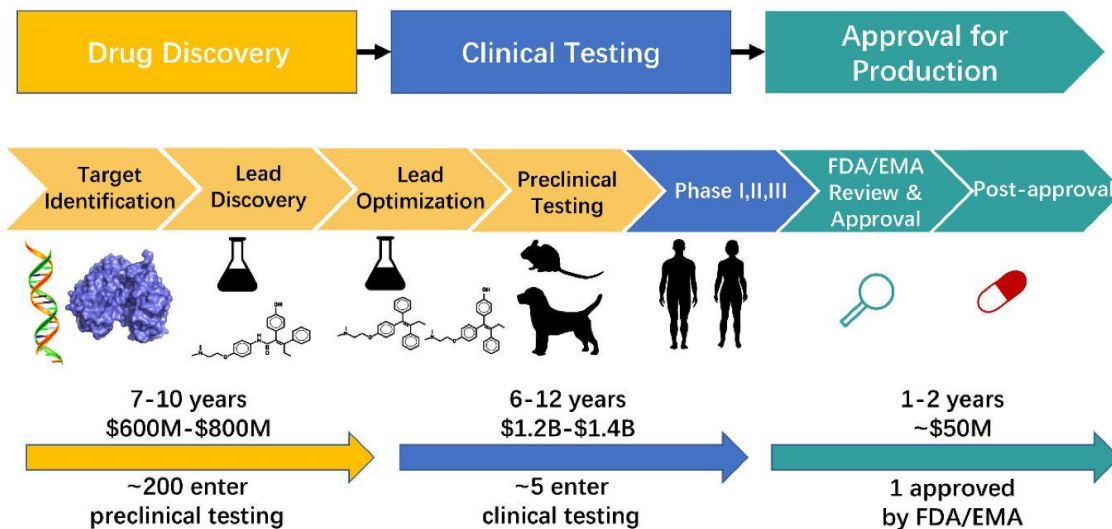


**Figure 4:** Stages involved in development adopted from (Maia et al., 2020)

The ligand-based approaches and the structure-based drug design are the two main groups of computational approaches in CADD.

## **2.7.1 Structure-based and ligand-based virtual screening**

### **2.7.1.1 Ligand-based approach**

This method use identified active compounds and make use of similar descriptors based on molecular features, properties, and biological activity to explain the structural and physicochemical characteristics of ligands (Kirchmair et al., 2011). Ligand-based approaches define a pharmacophore as a set of steric and electronic features necessary to explain molecular interactions with a protein target and activate or inhibit its biological response (Kapetanovic, 2008). This indirect strategy is helpful when there isn't a tentative receptor structure and it's challenging to create a solid model (Tiwari & Singh, 2022). A pharmacophore model describes three-dimensional chemical characteristics using pharmacophoric descriptors like hydrophobic, aromatic, positive, and negative ionizable groups. Similarly, molecular properties, shaped-based models, and QSA relationships are used in ligand-based method. The premise is that ligands with similar physiochemical characteristics are likely to display similar activity spectra.

### **2.7.1.2 Structure-based virtual screening**

Structure-based virtual screening (SBVS) or target-based virtual screening (TBVS) predicts the most effective interaction of ligands to form a complex against a molecular target (Maia et al., 2020). SBVS methods rank ligands based on binding affinity, with promising compounds at the top. Understanding the target protein's 3D structure is crucial for *in silico* interaction prediction (Liu et al., 2019). This method selects and categorizes chemical compounds based on their binding affinity to the receptor active site, identifying ligands with better pharmacological activity and scoring functions confirm this affinity. Molecular docking is used in SBVS techniques due to its low computational cost and effective results, but for accurate virtual screening specific docking protocols such as search algorithm and the score function are required.

## **2.7.2 Molecular docking**

Molecular docking comprises of three interconnected objectives; virtual screening, binding affinity simulation, and pose prediction (Kontoyianni, 2017). The planning and development of novel drugs in pharmaceutical industries, in this era of Artificial

intelligence (AI) heavily relies on molecular docking techniques. An effective docking technique should accurately predict molecular interactions, native ligand posture, rank docked ligands, and discriminate binding from non-binding compounds in large compound libraries. Docking methodology uses search algorithms and energy-scoring functions to generate and evaluate ligand conformation, aiding in drug design by accurately describing receptor ligand interactions and managing system flexibility (Gaitonde et al., 2020).

#### **2.7.2.1 Search algorithm**

Search algorithms are used to efficiently determine ligand conformation and orientation at a receptor's active site, with a good docking protocol providing the most practical results. These algorithms employ systematic, stochastic, or hybrid methods to efficiently generate and evaluate potential binding poses (Ruiz-Tagle et al., 2017). Rigid docking uses translational and rotational degrees of freedom, while flexible docking adds conformational degrees, with three categories: systematic, stochastic, and deterministic” (Ruiz-Tagle et al., 2017). To achieve better results, some software combines more than one of these techniques.

#### **2.7.2.2 Scoring function**

The strength of the interactions between a docked ligand and the receptor or molecular target can be determined using scoring functions in molecular docking software. Huang et al. (2010), highlight the significance of a scoring function in SBVS, as it estimates the binding potential of a target and ligand. The success of docking tools is primarily determined by the scoring functions. Scoring functions in molecular docking studies aid in identifying target and ligand conformations, exploring allosteric sites, forecasting protein-ligand docking scores/binding affinity, and optimizing lead (Gaitonde et al., 2020; Zheng et al., 2022).

#### **2.7.3 ADMET and drug-like studies**

Drug research and development require understanding a compound's pharmacokinetic and pharmacodynamic characteristics, which are determined by ADMET studies (Figure 5) and drug-likeness assessment, which helps in lead identification and optimization during drug discovery (Sucharitha et al., 2022). The structure-activity

relationship (SAR) analysis can also be used to optimize lead compounds based on their chemical structures and biological activities (Martinez-Gonzalez et al., 2019). *In-silico* ADMET and drug-likeness studies employ computational methods such as Artificial Intelligence (AI) and Machine Learning (ML) algorithms in assessing quantitative structure-activity relationship (QSAR) of the molecule hence providing predictive insights into a compound's ADMET profile and drug-likeness (Abdullahi et al., 2020). Advancements in organ-on-a-chip technology offer physiologically relevant platforms for studying ADMET properties and toxicity *in-silico*, enabling lead compound optimization through structure-activity relationship analysis (Siramshetty et al., 2024). AI-powered machine learning algorithms have made it possible to analyze vast datasets and predict ADMET properties and optimize lead compounds, significantly accelerating drug development timelines (Kumar et al., 2021). Additionally, metabolomics and systems pharmacology methods help understand drug metabolism and toxicity, enabling personalized medicine strategies. 3D bioprinting enables complex tissue models for drug interactions and toxicity studies (Kumar et al., 2021).

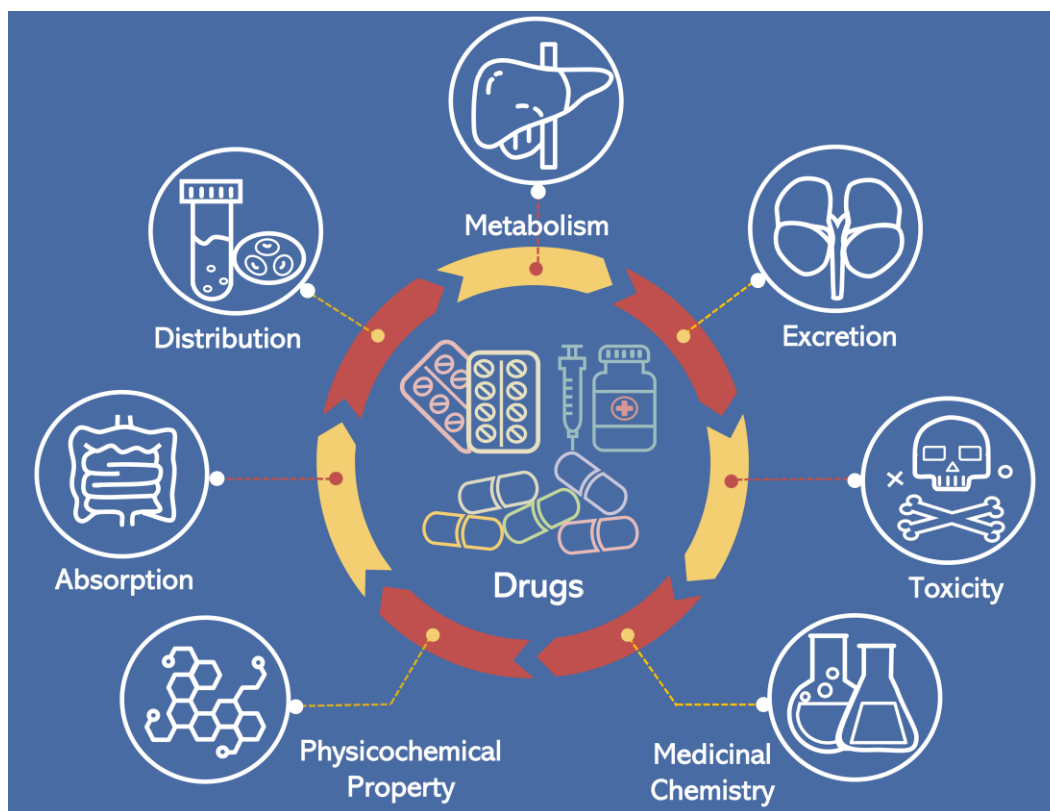


**Figure 5:** ADMET and drug-like flagship (Source: Creative commons)

Therapeutic lead compounds both extracted from natural sources or synthesized often fail in clinical trials due to adversative absorption, distribution, metabolism, and elimination issues, with nearly half failing due to biological efficacy and 40% due to toxicity issues (Brown et al., 2021). For instance, Mibefradil, soruvidine, and phenylpropanolamine hydrochloride were withdrawn from the market due to drug-drug interactions, hepatotoxicity, cardiac toxicity, and potential carcinogenicity (Wang et al., 2017).

Regulatory bodies and pharmaceutical companies recognize the significance of ADME/Tox studies in drug candidate success, now performing these early in the drug discovery process using AI development (Elhag, 2023). Hit molecules' potential for treating type 2 diabetes depends on their adherence to ADME parameters and toxicological endpoints, including carcinogenicity, hepatotoxicity, reproductive effect, skin sensitization, and blood-brain barrier permeation (Veber et al., 2002). Human intestinal absorption and solubility significantly influence the oral bioavailability, cell permeation, metabolism, and intestinal absorption of substances for treating type 2 diabetes (Wang et al., 2017). Therefore, the pharmaceutical industries need to access and evaluate the ADMET parameters virtually in early stages of drug development and identify hit molecules that can be development as novel therapeutics.

## CHAPTER THREE

### MATERIALS AND METHODOLOGY

Virtual screening is a crucial and often applied method in cheminformatics to investigate prospective lead compounds that may modulate protein targets through inhibition or activation. The use of both receptor-based and ligand-based techniques in the VS has been demonstrated to be viable and effective in drug discovery (Vázquez et al., 2020). Therefore, Structure Based Drug-design (SBD) was adopted in this method of screening an NPASS database to find an alternative inhibitor that can be used to control T<sub>2</sub>DM. Step-by-step cutting-edge cheminformatics techniques, including *in-silico* drug-likeness screening, pharmacokinetics, toxicity, molecular docking and, molecular dynamic simulation was employed to screen the curated NPASS database in finding possible dual inhibitors for  $\alpha$ -amylase and  $\alpha$ -glucosidase enzymes.

#### **3.1 Retrieval and preparation of ligands for docking**

A total of 30,926 molecules used in the study, were sourced from the NPASS database ([NPASS Database \(bidd.group\)](#)). Since its initial release in 2017, the NPASS has been one of the most important data source for natural product research community (Zhao et al., 2023). These molecules were accessed on December 20<sup>th</sup>, 2022, and downloaded in SDF format. The 3D molecular structure of acarbose was acquired from PubChem in SDF format. Acarbose was used as a reference molecule owing to it being co-crystallized with both  $\alpha$ -glucosidase (2QMJ) and  $\alpha$ -amylase (3BAJ) proteins. All the molecules in the form of structure Data File (SDF) were then exported into MOE in which 3D representations of respective ligands were generated. The molecules underwent curation by washing to remove duplicate molecules and molecules with errors or inconsistencies in their structure. Additionally, protonation at a temperature of 300 K and a pH of 7 was done so has the necessary hydrogen atoms are added to ensure the molecular structure is accurately represented. Subsequently, the energy of the molecules was minimized using MOE, employing the default parameters for the computation and energy minimization of the molecules (command: compute, molecules, energy minimize).

##### **3.1.1 Drug-likeness and *In-silico* pharmacokinetics screening**

Beyond Lipinski's rule of five (bRO5) was used to characterize and screen the Pharmacokinetics and drug-likeness characteristics of the molecules following

MedChem Mnemonic Rules such as Lipinski, Verber, Shultz, and Meanwell (Lipinski et al., 2001; Meanwell, 2016; Shultz, 2019; Veber et al., 2002). The database was screened using the tenets of bRO5 including, Molecular weight (MW) range from 260 to 500, Topological polar surface area (TPSA) ranges from 75-140 Å<sup>2</sup>, HBA ≤ 10, HBD ≤ 5; number of rotatable bonds (RT) ≤ 10; and hydrophobicity (log P) ≤ 5, Heavy atoms count (HA) < 25, and total HBA + HBD ≤ 12. The MOE was modified to screen non-drug-like molecules using the aforementioned criteria, as generated by the MOE (Compute, descriptors;(MW, HBA, HBD, TPSA, HA, RT and log P), calculate).

### **3.1.2 Toxicity based screening**

The toxicity parameters of the compounds that were retained after performing *in-silico* pharmacokinetics and drug-likeness screening were determined using pkCSM webserver ([pkCSM \(uq.edu.au\)](http://pkCSM.uq.edu.au)) (Pires et al., 2015) and Data Warrior software version 6.1.0 (Sander et al., 2015). The toxicity metrics acquired from the pkCSM comprised AMES toxicity, hERG I & II inhibitor, maximum tolerant dose (human) (MTD), Oral Rat Acute Toxicity LD<sub>50</sub>, Minnow toxicity, and skin sensitization (SS). Whereas Data Warrior was also used to determine compounds that were mutagenic, tumorigenic, reproductive-effective, and irritating molecules. All the toxicity parameters mentioned were assessed for the compounds identified after doing drug-likeness and *in-silico*-pharmacokinetics screening.

### **3.2 Retrieval and preparation of receptor ( $\alpha$ -amylase and $\alpha$ -glucosidase)**

The 3D Crystal Structure of Catalytic  $\alpha$ -Glucosidase (2QMJ) and Human Pancreatic  $\alpha$ -Amylase (3BAJ) in Complex with Acarbose were retrieved from Protein Data Bank (PDB) on May 2, 2023 (Maurus et al., 2008; Sim et al., 2008). Examination of the ligand interaction of the co-crystallized ligand with the receptor was carried out to determine the protein's active site, eliminate any water molecules, and residual ligand, and correct any missing amino acid residues. (Compute, Prepare, Structure preparation, Correct). The protein model's molecular systems were then protonated, ionization states assigned and hydrogen atoms positioned using the MOE at 300 K and pH 7.0. Finally, the models' energy system was minimized to obtain a relaxed receptor for molecular docking (Command: Compute, Energy Minimize, and Tether Atoms), followed by

tethering of atoms to ensure that the receptor structure established by experimentation did not significantly vary with the prepared receptor.

### **3.3 Molecular docking**

Molecular docking is a good computational technique for finding probable chemical entities that might be employed in investigating the binding potency of chemical compounds to a particular target such as enzymes. Molecular docking has evolved over the past 20 years into the model for structure-based screening of numerous internally produced chemical libraries or virtually accessible chemical databases (Bender et al., 2021). Similar to previous studies, the remaining compounds upon drug-likeness, and toxicity screening, underwent screening utilizing molecular docking methodologies, in which they were docked into the active sites of proteins  $\alpha$ -amylase (3BAJ) and  $\alpha$ -glucosidase (2QMJ). Subsequently, a screening was performed based on their respective docking scores. Prior to docking, the receptor active sites for each enzyme model consisting of Trp59, Tyr62, Gln63, Thr163, Arg195, Asp197, Lys200, His201, Glu233, Glu240, and Asp300 for  $\alpha$ -amylase and Thr205, Asp203, Met444, Asp542, Asp443, Asp327, Arg526, and His600 for  $\alpha$ -glucosidase were carefully selected and occupied by dummy atoms of molecules. The MOE-Dock module with the following parameters: placement-Triangle matcher, rescoring-London dg, refinement-rigid receptor was set for docking. The conformations of respective ligand were subjected to docking within a designated binding pocket of respective enzymes; 3BAJ and 2QMJ and each molecule's ideal positioning/orientation within the respective receptor pocket were calculated. The resulting root mean square deviation (RMSD) values and binding affinities of the highest-ranked molecule having the highest binding affinity (the most negative) were used to investigate the binding interactions of the ligands with 2QMJ and 3BAJ proteins. Through conformational sampling, the best binding modes for the identified molecules were determined. The Protein-Ligand Interaction Fingerprints (PLIF), was utilized to visualize binding modes between the receptor's binding pocket and the ligand molecule with the best docking score. The software calculates various types of interactions, such as hydrogen bonds, water-mediated protein-ligand interactions, ionic interactions, surface contacts, metal binding, and aromatic interactions between the ligand and the receptor, all in 2D format.

### 3.3.1 Summary flow

Receptor Prep → Ligand Prep → Grid Generation → Docking Search → Scoring → Pose Selection → Interaction Analysis

### 3.3.2 Docking validation

The molecular docking approach that was utilized in this research was validated using the Acarbose (a co-crystallized ligand and known inhibitor for the two enzymes) before docking was done on the two enzymes with the screened NPASS molecules. The Acarbose was subsequently re-docked to the original site where the co-crystal ligand initially interacted with the corresponding receptor. The experimental conformational (the crystallographic pose) and the postures produced by docking with the reference acarbose were superposed and compared (Figure 6). The conformer with highest binding affinity and having a comparable posture with a co-crystallized ligand from the validation docking for each receptor was selected for each enzyme structure and served as the standard for all succeeding docking simulations with the two proteins.



**Figure 6:** Superposed structures of co-crystallized and best docked acarbose in  $\alpha$ -amylase (3BAJ) and  $\alpha$ -glucosidase (2QMJ). The most favorable docking poses of 3BAJ and 2QMJ is represented in blue and the crystallographic pose shown in green.

### 3.4 Molecular dynamics simulation

Molecular dynamic (MD) simulation of the four complexes were conducted using Amber 16 software package. The ligand's partial atomic charges were calculated using the electrostatic potential (RESP) method implemented in within the Gaussian 09 program at the Hartree-Fock level with the 6-31G\* basis set. The biomolecular systems were placed in an octahedral periodic boundary box, solvated with the TIP3P water model. A 12 Å cutoff was applied between the atoms of the solvated system and the

water box wall. Sodium ions  $\text{Na}^+$  were added to the system to ensure charge neutrality. The ff14SB force fields and the General Amber Force field (GAFF) were employed in parameterizing the biomolecular systems as well as the ligand structures respectively (Wang et al., 2006). Energy minimization protocol was performed for all the systems through six steps with steep-descent and conjugate gradient algorithm. This was performed following a series of 10,000 cycles for each step to minimize the hydrogen atoms, water and ions and completely minimizing the whole system with the progressive decrease of restrains. Next the system was heated from 0 to 300 K over 800ps in three stages and maintained at 300 K by coupling to a Langevin thermostat using collision frequency of  $2 \text{ ps}^{-1}$  and a constant pressure of 1 bar. Equilibration was performed over 2 ns at constant temperature without any restrains. Subsequently, 100 ns of MD simulation was carried out for each complex using the NVT ensemble. Ligand Root mean square deviation (RMSD) and receptor Root-mean-square fluctuation (RMSF) in each complex system were calculated using the MD simulation trajectories.

### 3.4.1 Summary workflow

Structure Prep → Parameterization → Solvation/Ionization → Energy Minimization  
→ Equilibration (NVT/NPT) → Production MD → Trajectory Analysis

### 3.5 Energy minimization calculations

The binding free energy of the ligands in the receptor was determined using mechanics-generalized surface area (MM-GBSA) method (Neves Cruz et al., 2020). 500 snapshots of the last 5ns of the MD trajectories were used in determining the free binding energy according to the following equations:

$$\Delta G_{bind} = \Delta H - T\Delta S \approx \Delta EMM + \Delta G_{solv} - T\Delta S$$

$\Delta G_{bind}$ : free energy of the system resulting from the sum of the mechanistic energy ( $\Delta EMM$ ), the de-solvation free energy ( $\Delta G_{solv}$ ) and the entropy ( $T\Delta S$ ).

Root-mean-square fluctuation (RMSF), ligand RMSD, and molecular mechanism/Generalized Born surface area (MM/GBSA) in each complex system were calculated using the MD simulation trajectories.

## CHAPTER FOUR

### RESULTS AND DISCUSSION

#### 4.1 Virtual screening

A preliminary step in virtual screening involved a curation process, from which 150 molecules out of 30,926 of NPASS molecules were eliminated. The refined 30,776 molecules were subjected to systematic virtual screening as summarized in Figure 7. Virtual screening (VS) is a crucial method often applied procedure in drug development while investigating prospective lead molecules that can inhibit or trigger biomolecular receptors (Vázquez et al., 2020). Typically, the initial stages of any pharmaceutical/drug-based projects involve the identification of biologically active molecules from a vast array of molecules available in different databases. In this context, utilizing computer based virtual screening proves to be a highly effective method for swiftly evaluating compound libraries, significantly reducing the demanding tasks associated with drug development involved in conventional/traditional methods (Cheenpracha et al., 2016; Saddique et al., 2018).

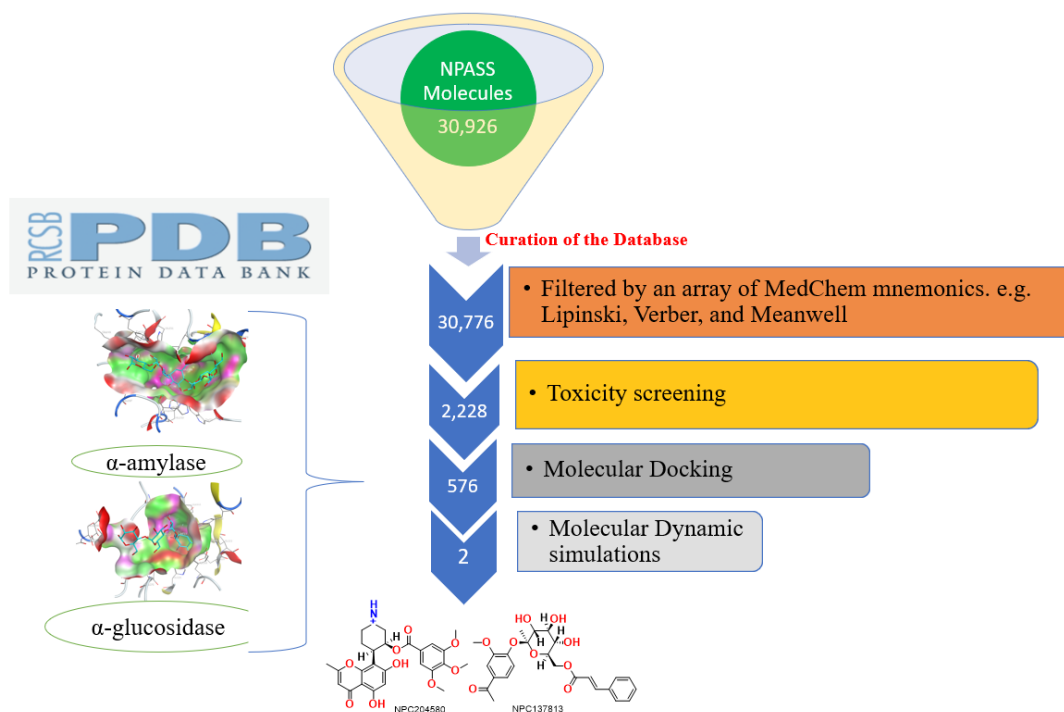


**Figure 7:** Schematic flow chart of structure-based virtual screening of the 30,926 Natural Products Activity and Species Source Database (NPASS) compounds.

#### 4.1.1 Drug-likeness and *in-silico* pharmacokinetics screening

A compound's potential as a therapeutic agent is largely dependent on its molecular physicochemical properties as predisposing conditions for drug-likeness (Narayanaswamy, 2014; Sucharitha et al., 2022). Beyond Lipinski rule of five (bRO5) was utilized in screening 30,926 molecules from the NPASS database based on physicochemical properties to have drug-like molecules with favorable pharmacokinetic properties, emphasizing compounds that meet the requirements with zero violations of bRO5. The curation process of NPASS database eliminated 150 molecules from the initial set of 30,926 molecules, specifically removing duplicate entries and incomplete or incorrect data ensuring a refined selection of relevant quality candidates for further virtual screening. A further curation following the rules delineated by MedChem mnemonics such as Lipinski, Verber and Meanwell resulted in 2,228 molecules; their physicochemical properties are summarized in Figure 8 & 9.

The dataset comprised 2,228 molecules, and their physicochemical property distribution was first analysed to assess drug-likeness and chemical diversity. Key descriptors evaluated included molecular weight (MW), lipophilicity (LogP), topological polar surface area (TPSA), number of hydrogen bond donors (HBD) and acceptors (HBA), and rotatable bonds. All molecules exhibited MW values between 260–500 Da, with LogP values distributed mainly in the range of 1–4, indicating balanced hydrophilicity and lipophilicity. TPSA values clustered below 120 Å<sup>2</sup>, while HBD and HBA counts largely fell within Lipinski's acceptable thresholds ( $\leq 5$  and  $\leq 10$ , respectively). These findings suggest that the majority of molecules are within the physicochemical space favorable for oral bioavailability.

According to Lipinski, a molecule having a molecular weight (MW) falling within the range of 260 to 500 Daltons often exhibits desirable absorption, distribution, metabolism, and excretion (ADME) properties which are essential in ensuring effective drug metabolism (Tibbitts et al., 2015). The partition coefficient between n-octanol and water ( $\text{Log } P_{o/w}$ ) is crucial for evaluation of a compound's lipophilicity, which determines its solubility and ability to pass through biological membranes (Tsopelas et al., 2017). Appropriate Log P for good drug-like molecules should be  $< 5$  to enhance the equilibrium between hydrophilicity and lipophilicity, which is vital for bioavailability

of the molecule (Velmourougane, 2022). The number of heavy atoms (HA) and the number of rotatable bonds play a crucial role in the compound's stability, flexibility and interactions with the biological target (Lipinski, 2004). Molecules that surpassed the metrics of  $HA < 26$  and  $< 10$  rotatable bonds fail to meet the bRO5.

Topological polar surface area (TPSA) is a crucial factor in the selection of drug candidates during virtual screening as it has effects on drug permeability, bioavailability, solubility, and receptor interactions (Bastos et al., 2023; Silva et al., 2021; Tibbitts et al., 2015). Therefore, druglike molecules with TPSA values ranging between  $75 \text{ \AA}^2$  to  $140 \text{ \AA}^2$  were considered to be prospective drug candidates as they could have an optimal surface area (SA) to interact with the target receptor and have no effects on membrane permeability. Hydrogen bond acceptor (HBA) and hydrogen bond donors (HBD) play a crucial role in determining a compound's ability to interact with specific target receptors. The stringent criteria of having a maximum of 10 HBA and a maximum of 5 HBD ensure the optimal chemical interactions that are essential for biological activity (Lipinski et al., 2001). Their presence influences the capacity of a molecule to establish chemical interactions with specific proteins or receptors. Therefore, we further screened the remaining molecules using these characteristics to guarantee the identification of compounds that can form crucial hydrogen bonding interactions, which are necessary for achieving specific and strong binding with biological target.

virtual screening criteria filtered out molecules down to 2,228 and their physicochemical properties are summarized in Figure 8 and 9. Looking into the graphs of the remaining molecules, it is evident that their features are more closely aligned with the criteria bRO5, suggesting their potential as therapeutic candidates. The selected fraction exhibits great potential for further comprehensive analysis to determine their pharmacological and toxicity activities. Therefore, further screening was performed based on toxicity end-points such as AMES toxicity, hERG II inhibitor, Hepatotoxicity, and skin sensitization (SS), tumorigenic, reproductive-effective with the help of pkCSM webserver and Data Warrior software.

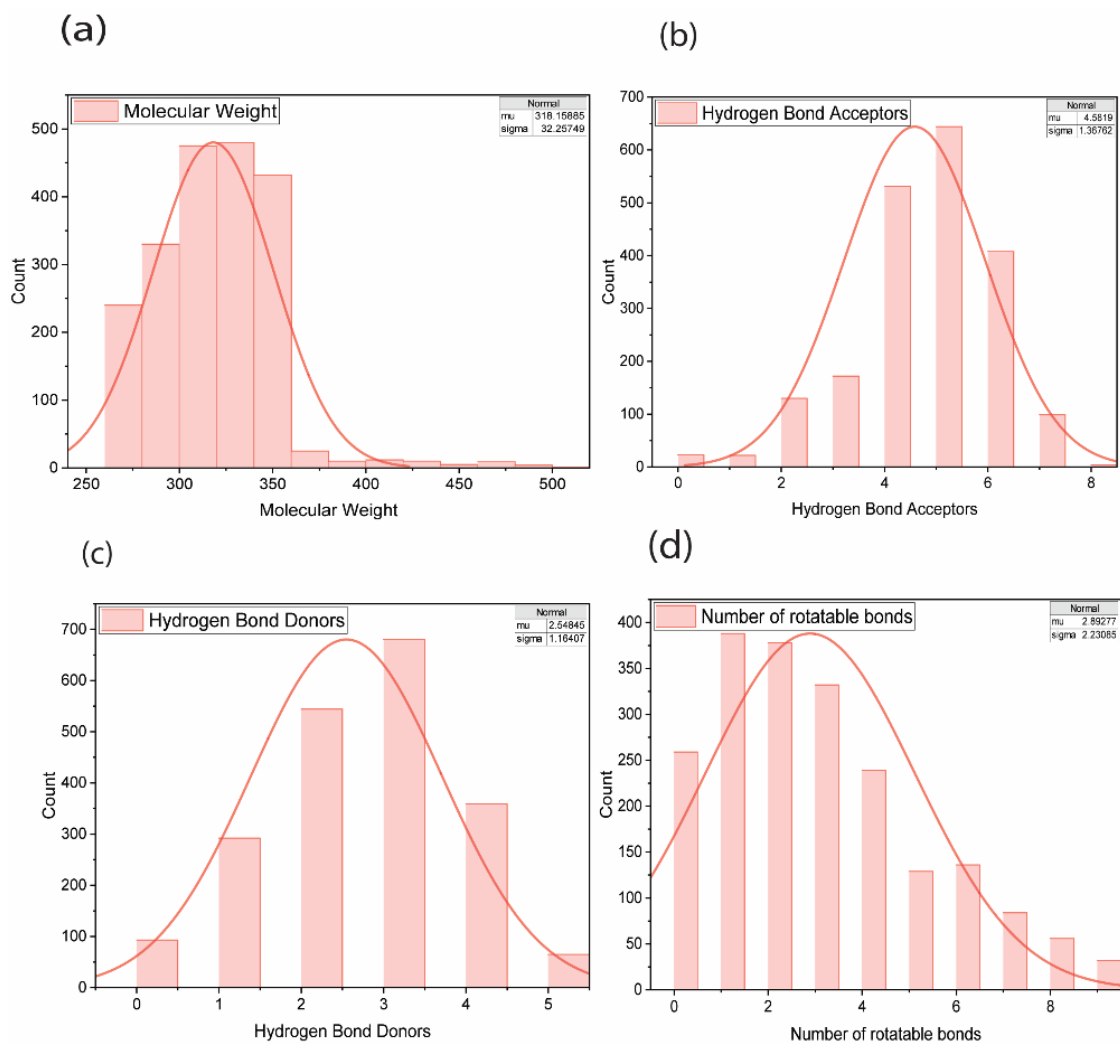


**Figure 8:** Properties distribution of the remaining molecules (2228) (a) Molecular Weight, (b) Hydrogen bond acceptors (c) Hydrogen bond donors (d) number of rotatable bonds.

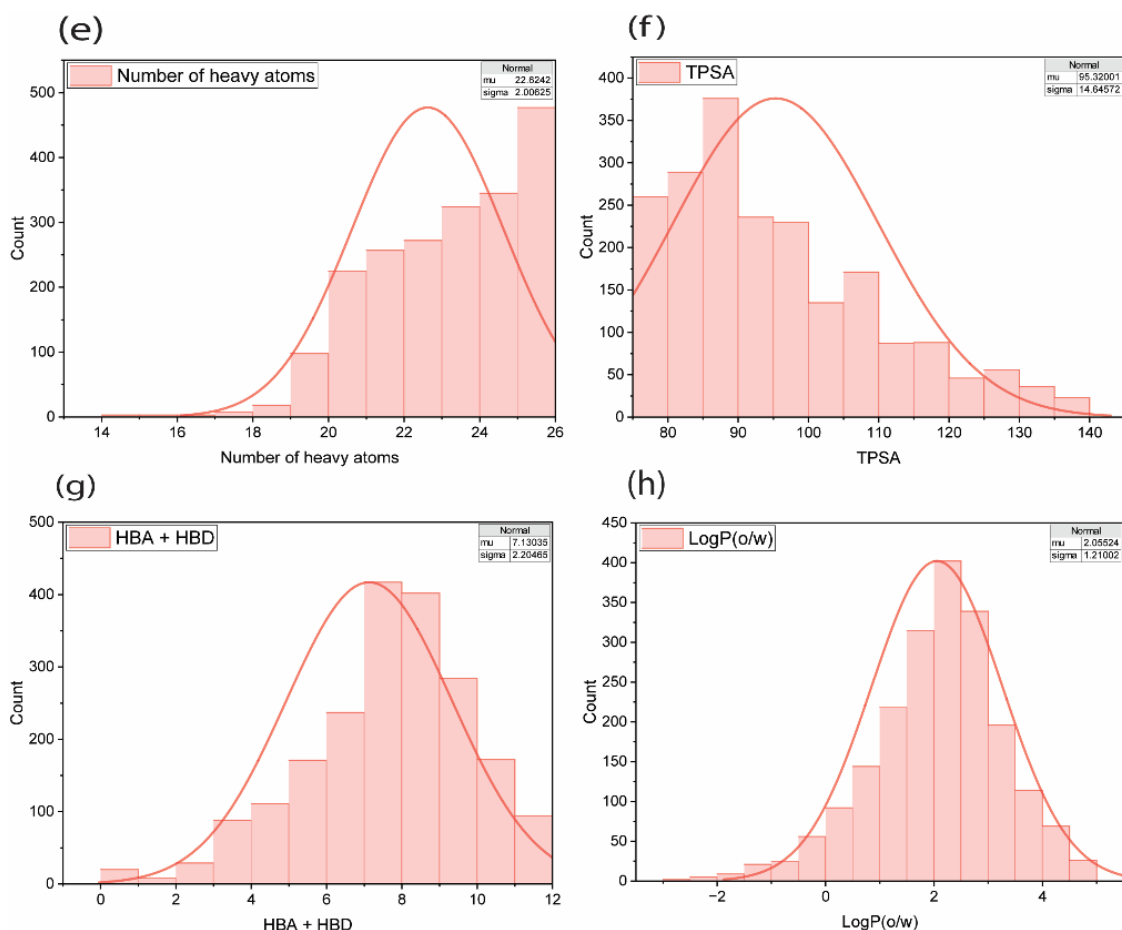


**Figure 9:** Properties distribution of the remaining molecules (2228) (e) Number of heavy atoms, (f) Topological polar surface area, (g) summation of hydrogen bond acceptors and donor, (h) The partition coefficient between n-octanol and water (Log Po/w).

#### 4.1.2 Toxicity based screening

Toxicity-based screening is an essential procedure in the pharmaceutical industries in assessing the safety profiles of molecules (Parasuraman, 2011). The process entails a thorough assessment of substances to determine any potential hazards or adverse effects they may have on human health. In this study pkCSM webserver and Data-warrior were used to evaluate and screen the molecules based on toxicity parameters such as AMES toxicity, hERG Inhibitor, Hepatotoxicity, and Skin Sensitization, tumorigenic, reproductive-effective, and irritating molecules, the toxicity profile of the molecules are given in Figure 10 (a) and (b).

The AMES toxicity parameter is a reliable method for predicting the mutagenicity and carcinogenic potential of chemical substance (Kibet et al., 2024). It primarily identifies compounds that can cause genetic mutations, leading to cancer or in-hereditary genetic disorders (Honma, 2020). Out of the 2228 molecules analyzed using pkCSM, 36.5% exhibited AMES toxicity which concurred with results from Data warrior showing 38.2% of the molecules showed as mutagenic, indicating a high likelihood of causing genetic mutations in an organism. Consequently, these identified compounds were eliminated because of their capacity to induce detrimental impacts on human health.

The primary factor responsible for the emergence of acquired long QT syndrome, which can result in fatal ventricular arrhythmia or other severe cardiac ailments, is the suppression of potassium channels encoded by hERG (human ether-a-go-go-gene) (Itoh et al., 2016). A number of drugs have been withdrawn from the pharmaceutical market due to their potential to inhibit hERG channels. Therefore, in the virtual screening, 20.1% of the molecules that exhibited hERG inhibition were eliminated to mitigate the risk of severe cardiovascular adverse effects linked to the safety profiles of pharmaceutical medications in the developmental stages. Hepatotoxicity screening is essential as it assesses the molecule's potential harm to the liver, a vital organ responsible for detoxification and metabolism of chemical substances and nitrogenous waste in the body (Mohiuddin & Khattar, 2023). The toxicological analysis eliminated up to 17.2% of molecules that exhibited hepatotoxic properties during screening. Therefore, these molecules were eliminated to avoid detrimental impacts on liver functionality, hence guaranteeing the identification of a secure drug candidate.

Similarly, the assessment of the skin sensitization (irritant screening) predicts the capacity of a drug to elicit allergic reactions when it comes into contact with the skin (Pires et al., 2015). Out of the compounds analyzed with pkCSM, 2.6% of the compounds exhibited skin sensitization whereas 26.4% (19.6%-High and 6.8%-Low) of the compounds were found to have the potential to cause general allergic reactions based on Data warrior results. Therefore, these compounds were excluded to mitigate the potential for allergic skin reactions, with a focus on promoting the development of a safer drug.

Tumorigenic screening is a process that seeks to detect substances that have the potential to cause the development or expansion of tumors (Minhas et al., 2017). This assessment is important in order to prevent exposure to possible cancer-causing agents. Reproductive-effect evaluations are crucial for assessing potential adverse effects on fertility, pregnancy, or fetal development, ensuring drug safety (Parasuraman, 2011). Molecules that exhibited any form of toxicity based on tumorigenic and reproductive effectiveness (Figure 10) were eliminated during the screening process. Through this extensive screening, the pool of prospective therapeutic candidates was reduced to 576 compounds that satisfied the safety criteria. These molecules were further subjected to molecular dockings to predict their binding interactions with target proteins, aiding in understanding their mechanism of action and potential as therapeutic agents.

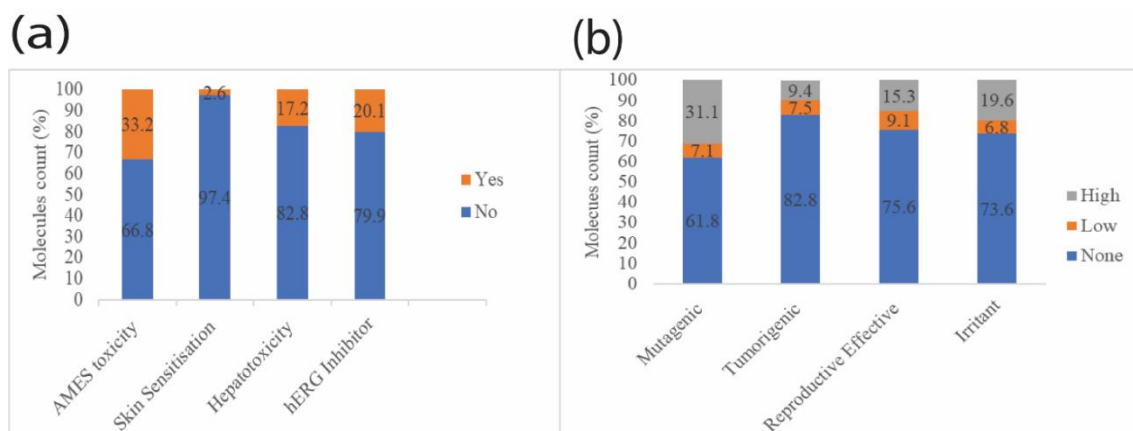


**Figure 10:** Graphs of toxicological properties of the 2228 screened molecules: (a) stack bar graphs showing toxicity end point determined using the pkCSM, (b) Stacked bar graphs showing toxicity end point determined using Data Warrior.

#### 4.1.3 Molecular docking studies

Molecular docking stands out as a powerful computation technique for finding probable chemical entities that can be utilized in investigating the binding potency of chemical molecules to a particular target such as enzymes and nucleic acid (Islam et al., 2022). Over the past two-decade molecular docking has emerged as the standard method for structure based virtual screening of various in-house curated chemical libraries or virtually accessible chemical databases (Bender et al., 2021). Correspondingly, molecular docking technique was employed in exploring detailed molecular docking studies of the five hundred and seventy-six NPASS chemical compounds and the

respective target receptors (2QMJ and 3BAJ). Binding interaction residues, root mean square deviation, and docking score were used to grade compounds in comparison to the reference ligand Acarbose and the results of the top ranked molecules in the two receptors are presented in Figure 13, Appendix 1 and 2.

#### 4.1.3.1 Binding interaction analysis of $\alpha$ -amylase (3BAJ)

Human pancreatic  $\alpha$ -amylase is classified as an endoglycosidase enzyme and is responsible for the metabolism of starch and other glycosyl-polysaccharides with R-1,4-linkages (Maurus et al., 2008). The active site of the Human pancreatic  $\alpha$ -amylase (Figure 11), containing the selected amino acid residues Trp59, Tyr62, Gln63, Thr163, Arg195, Asp197, Lys200, His201, Glu233, Glu240, and Asp300, was docked with the optimized 576 screened molecules from the NPASS database.

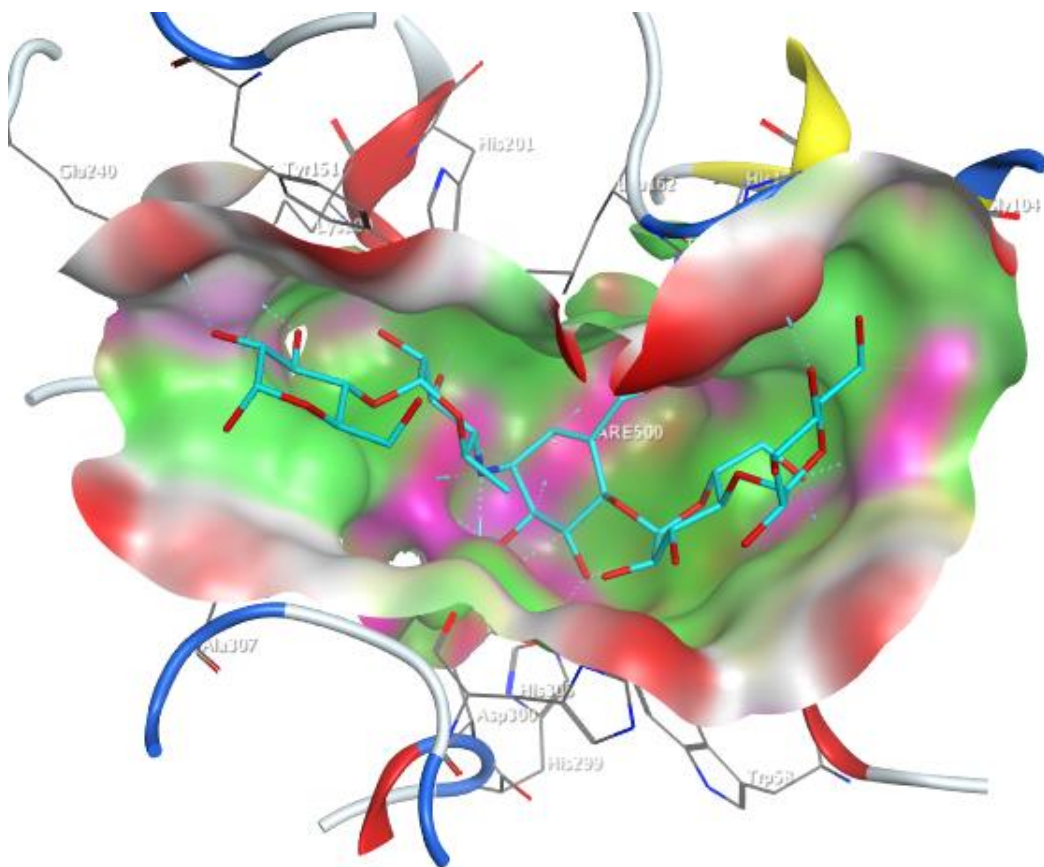


**Figure 11:** Active-site of the Human pancreatic  $\alpha$ -amylase with co-crystallized molecule Acarbose (cyan)

Upon docking the docked molecules were screened based on the docking threshold of -10.0 kcal/mol and  $\leq 2.0$  Å RMSD values, as these were considered the most stable ligand in the pocket of the receptor. Four ligands (NPC204580, NPC137813, NPC76084, and NPC27750) were regarded as the most probable inhibitors of 3BAJ protein among the screened derivatives due to their high binding affinities, and outstanding ligand interactions with the designated amino acid, in addition to low RMSD values. The selected molecules' binding interactions, docking scores, and RMSD values were analyzed and the findings are shown in Appendix 1. It is noted that all the four ligands formed more than three hydrogen bond interactions with the amino acid, as indicated in Appendix 1. However, two of the ligands (NPC204580 and NPC137813) exhibited docking score comparable with Acarbose, whereas NPC76084 and NPC27750 displayed significantly low binding affinities relative to the reference compound Acarbose. Therefore, NPC204580 and NPC137813 were considered for further studies as potential inhibitors based on this rationale. The NPC204580 molecule formed an ionic bond with Asp 197 and a 6-ring pi bond interaction with His 201 residues, alongside three hydrogen bonds with Asp300, Glu233 and Lys200, hence accounting for its high binding affinity of -14.46 kcal/mol docking score. NPC137813 on the other hand formed four hydrogen bonds with Asp 300, Asp 197, His 299, and Arg 195 amino acid residues which also gave it a high binding affinity of -12.58 kcal/mol.

#### **4.1.3.2 Binding interaction analysis of $\alpha$ -glucosidase (2QMJ)**

The selected structures of NPASS molecules were also docked into the determined active site of the human maltase-glucoamylase receptor (PDB ID: 2QMJ) (Figure 12), containing the selected amino acid residues Asp203, Tyr299, Asp327, Ile364, Trp406, Trp441, Asp443, Met444, Arg526, Trp539, Gly541, Asp542, Asp571, Phe575, Arg598, and His600 was also docked with the optimized 576 screened molecules.

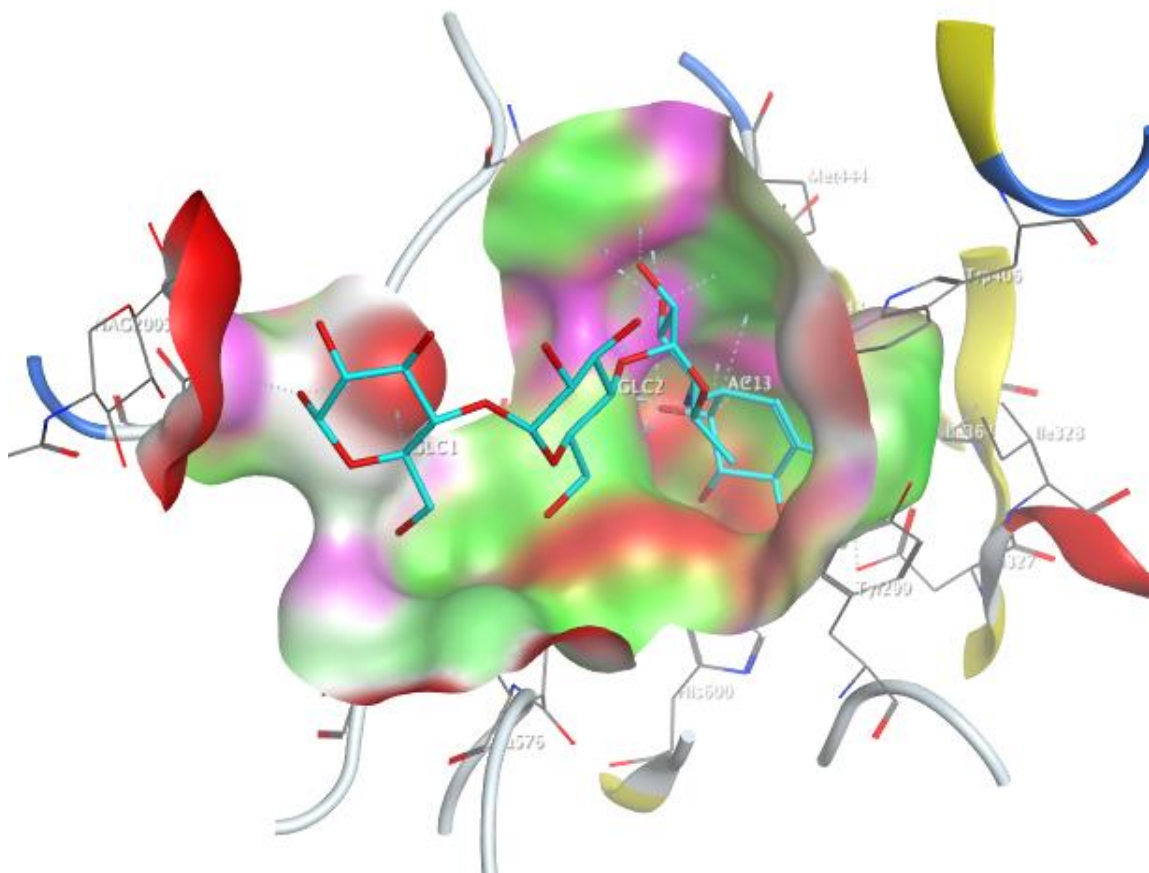


**Figure 12:** Active-site of the Human pancreatic  $\alpha$ -glucosidase with co-crystallized molecule Acarbose (cyan)

The derivatives NPC25750, NPC137813, NPC76084, and NPC204580 of the NPASS database demonstrated docking score ranging from -8.42 kcal/mol to -9.08 kcal/mol, closely aligning with the docking score of the reference compound Acarbose (-8.22 kcal/mol) as shown in Appendix 2. Furthermore, the ligands exhibited exceptional binding affinity towards key amino acid residues of Human pancreatic  $\alpha$ -glucosidase, including; Thr205, Asp203, Met444, Asp542, Asp443, Asp327, Arg526, and His600 (Appendix 2). These interactions significantly contributed to their high binding affinities.

The docking scores and root mean square deviation (RMSD) of the four ligands and the reference compound Acarbose were analyzed and compared in both receptors as illustrated in Figure 13 (13a\_3BAJ and 13b\_2QMJ). The comparison of these parameters highlights the relative binding efficacy and structural alignment of the

ligands with the standard drug acarbose, offering critical insights into their potential inhibitory activity. The results revealed that the selected four ligands had demonstrated significantly comparable docking scores with acarbose in  $\alpha$ -glucosidase. However, NPC76084 and NPC25750 were found to be less effective in inhibiting  $\alpha$ -amylase compared to acarbose, leaving only NPC204580 and NPC137813 as dual inhibitors with a docking scores of -14.46 kcal/mol and -12.58 kcal/mol for  $\alpha$ -amylase, and -8.42 kcal/mol and -8.76 kcal/mol for  $\alpha$ -glucosidase, respectively.

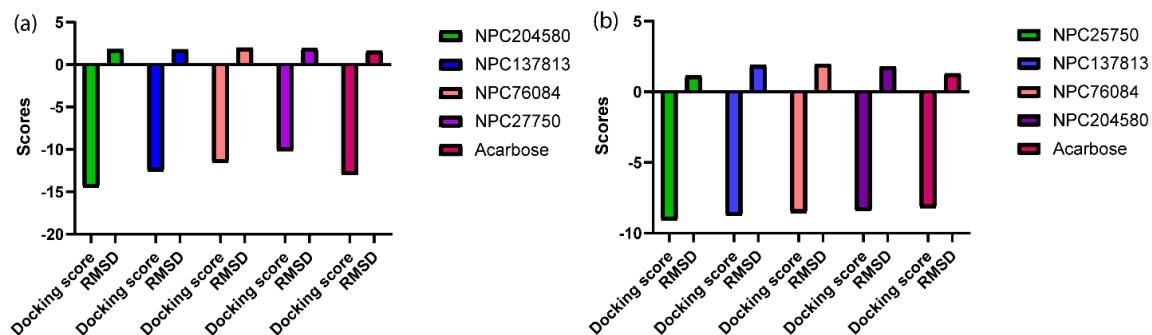


**Figure 13:** Docking scores and RMSD bar graphs for selected ligands in both (a)  $\alpha$ -amylase and (b)  $\alpha$ -glucosidase receptors.

#### 4.1.3.3 Molecular docking studies of the selected dual inhibitors and the Acarbose with $\alpha$ -amylase and $\alpha$ -glucosidase

Molecular docking studies of the selected dual inhibitors and the Acarbose (reference) revealed that all ten poses of the molecules demonstrated comparable docking scores with Acarbose as illustrated in Figure 14 and Appendix 3. The two molecules NPC204580 and NPC137813 with  $\alpha$ -glucosidase revealed that all of their ten poses demonstrated lower docking score (S-score) than the Acarbose (Figure 14b), suggesting that the two molecules possess stronger binding affinity towards the  $\alpha$ -glucosidase, potentially leading to a more effective inhibition of the  $\alpha$ -glucosidase. Additionally, NPC204580 exhibited lower S-score than acarbose with  $\alpha$ -amylase, suggesting a better binding affinity, but the S-score of NPC137813 was higher than that of reference molecules acarbose in all the ten poses with  $\alpha$ -amylase (Figure 14a). However, the difference was comparable. Therefore, both NPC204580 and NPC137813 were considered promising therapeutic candidate against T<sub>2</sub>DM due to their favorable

binding affinities with  $\alpha$ -amylase and  $\alpha$ -glucosidase which are key target for inhibiting carbohydrates digestion and glucose absorption in the gut.

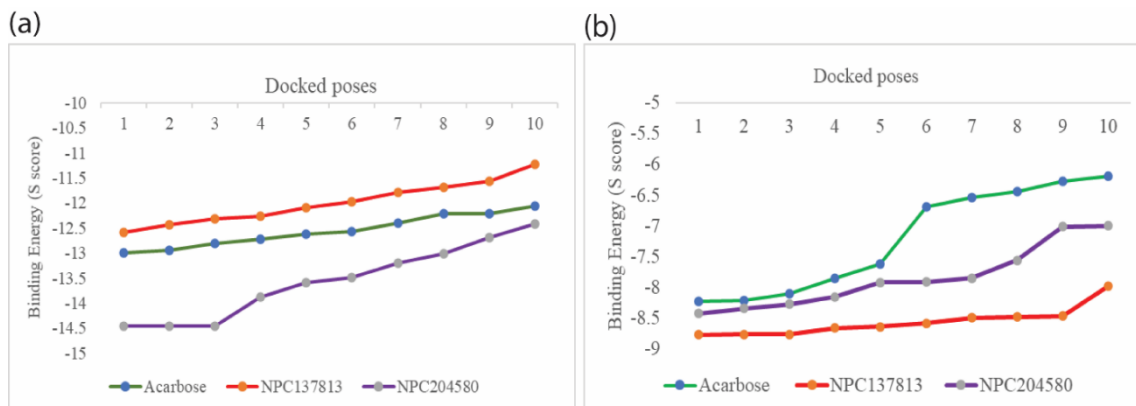


**Figure 14:** Top ten poses of NPC204580, NPC137813, and Acarbose on the x-axis plotted against the binding affinity (S-score) for  $\alpha$ -amylase (a) and  $\alpha$ -glucosidase (b). The greater the negative value of S-score, the stronger the predicted binding affinity.

#### 4.1.3.4 Binding interaction analysis of the selected two dual inhibitors

A detailed examination of binding interactions of the best-docked poses of the two ligands NPC204580, NPC137813 and Acarbose with the receptors  $\alpha$ -amylase (3BAJ) and  $\alpha$ -glucosidase (2QMJ) was conducted. This analysis revealed a significant binding interaction as illustrated in Table 2 along with their docking scores and RMSD values. The estimated binding free energy for NPC204580 and NPC137813 with  $\alpha$ -amylase was -14.46 kcal/mol and -12.58 kcal/mol, respectively while in  $\alpha$ -glucosidase it demonstrated -8.42 kcal/mol and -8.76 kcal/mol, respectively. Additionally, the RMSD values of the two ligands were less than 2 Å in each receptor, suggesting structural stability of the binding predictions.

Further, visualization of the 2D (Figure 16) and 3D (Figure 17) interaction of the two molecules with the two receptors revealed that, NPC204580 molecule formed five interactions at Asp300, Glu233, Lys200, Asp197, and His200 amino acid residues of the  $\alpha$ -amylase, and five interactions at Met444, Asp542, Asp203, Asp542, and Phe575 amino acid residues of  $\alpha$ -glucosidase. The interaction culminated in an RMSD value of 1.8 Å and docking score of -14.46 kcal/mol with  $\alpha$ -amylase. These interactions included two hydrogen bonds with Asp300 and Asp197 residues via the C atom and NH<sup>+</sup> group. Moreover, the ligand exhibited an ionic interaction with Asp197, pi-H interaction with

His201 and H-acceptor interaction with Lys200, establishing a comprehensive binding profile with  $\alpha$ -amylase. Interaction of the same ligand (NPC204580) with  $\alpha$ -glucosidase was also examined and it revealed that -8.42 kcal/mol docking score and 1.79 Å RMSD, was as a result of important interactions between the ligand and the receptor. With 2D studies, two prominent hydrogen bonds at Met444 and Asp542, two ionic interactions with Asp203 and Asp542, and H-pi interactions at Phe575 residues. These interactions of the ligand in both receptors justified the high binding affinity of the ligand and low RMSD values observed in the two enzymes.

The ligand NPC204580 named Chrotacumine C is a naturally occurring chromone alkaloid isolated from leaves and barks of *Dysoxylum acutangulum* where it was established to be active against cancer cell lines (Ismail et al., 2009). Moreover, the compound was discovered to inhibit Human Neutrophil Elastase (HNE), owing to its significant role in acute respiratory distress syndrome (ARDS), and various inflammatory disorders such as atherosclerosis, and dermatitis (Narayanaswamy, 2014). Therefore, the compound Chrotacumine C is noted to be a potential drug candidate that can be structurally optimized further for the management of various pathophysiological conditions such as postprandial hyperglycemia.

The ligand NPC137813 with docking score of -12.58 kcal/mol and 1.79 Å RMSD value with  $\alpha$ -amylase formed four hydrogen bond interactions at Asp 300, Asp 197, His 299, and Arg 195 amino residues of  $\alpha$ -amylase via OH groups. In addition to, it also portrayed an excellent docking score with less than two RMSD values with  $\alpha$ -glucosidase (-8.76 kcal/mol and 1.88 Å, respectively). The ligand formed two hydrogen interactions at Thr 205, and Arg 202 via OH and carbonyl group respectively, alongside Pi-H interaction at Thr204 amino acid residues via a 6-ring molecule. Therefore, the interactions of these ligands with the respective receptor and low RMSD value in both receptors justifies its binding affinity with the respective enzymes;  $\alpha$ -amylase (-12.58 kcal/mol) and  $\alpha$ -glucosidase (-8.76 kcal/mol). The molecule NPC137813 was previously isolated from *Picrorhiza scrophulariiflora* alongside other ten compounds and was established to be good antimalarial compound against *Plasmodium falciparum* (Wang et al., 2013). However, there is a paucity of information detailing the inhibitory activity of this compound against  $\alpha$ -amylase and

$\alpha$ -glucosidase receptors and the study has thus proved its potential which then requires further optimization for management of postprandial hyperglycemia.

In addition to the selected amino acid residues, the two ligands NPC204580 and NPC137813 formed several additional bond interactions with important catalytic amino acids of the receptor as evident in Figure 16, which will play a considerable role in interfering with the physiological normal functioning of these two enzymes.

Acarbose molecule was used as a control in this study, it displayed a binding score of -12.99 kcal/mol and 1.61 Å RMSD value with  $\alpha$ -amylase enzyme and formed hydrogen bond with Gln 63 residue and H-pi interaction with Trp 59 amino acid residue. An RMSD value of 1.29 Å and a binding score of -8.22 kcal/mol were observed with  $\alpha$ -glucosidase. The binding pocket amino acid residues form hydrogen bonds with Asp 203, Asp 542, Asp 327, Met 444, Asp 443, Arg 526, and His 600 in addition to their ionic interaction with the amino acid residue Asp 542. The presence of a greater number of hydroxyl functional groups in the Acarbose structure appears to be the cause of the increased number of hydrogen bonds observed between the ligand and the active site of the receptor (Aminu et al., 2022). The findings from the docking studies indicate that the chosen ligands exhibit robust binding to the active sites of both receptors. These ligands established strong interactions with crucial catalytic amino acid residues, and their binding affinities are favorable, as seen by RMSD values below 2Å.

Looking into the structural and chemical features of the two molecules (Figure 15), it revealed both molecules contain an aromatic ring with methoxy (-OCH<sub>3</sub>) substitution contributing to their electron-donating capacity and hydrophobic features. Moreover, chiral centers in each molecule introduces stereoisomeric complexity, which contributes significantly in binding specificity of the two target enzymes. The chiral piperidine ring in NPC204580 and the sugar-like moiety in NPC137813 enables the two molecules to adopt specific conformations. Additionally, both molecules also contain multiple hydroxy (-OH) and carbonyl (C=O) groups, strategically enhancing their ability to form hydrogen bond with the amino acid residues in the active site of the receptor, hence stabilizing inhibitor binding.

An optimal balance of hydrophilic and lipophilic regions is crucial for orally administered drug candidates targeting enzymes in the gastrointestinal tract (Xu et al., 2020). Both molecules NPC204580 and NPC137813 demonstrated a well balance profile; the hydrophilic carbonyl and hydroxyl groups enhance solubility in the gut aqueous environment, while lipophilic methoxy-substituted aromatic rings enhance overall bioavailability. Therefore, this intricate balance of the profiles suggest that the two molecules could remain sufficiently soluble to exert local inhibitory effects on the target enzymes in the gastrointestinal tract. Consequently, the structural attributes of both molecules – including their aromatic scores, stereoisomeric features, hydroxyl groups, and balanced amphipathic characteristics- collectively indicate potential for effective inhibition of the target enzymes when orally administered. Therefore, the two molecules identified in this study are considered to be able to disrupt a crucial carbohydrate metabolic process and may serve as a starting point for structural optimization in finding more effective inhibitors of carbohydrate metabolism hence managing hyperglycemic conditions.

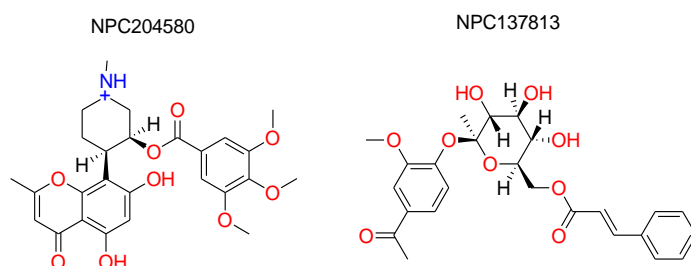
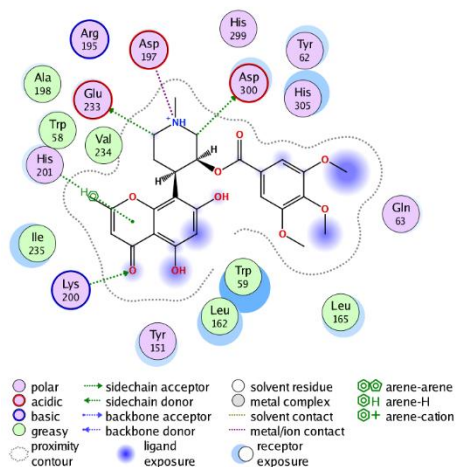


**Figure 15:** 2D structures of the proposed molecules NPC204580 and NPC137813 (Drawn with ChemDraw professional 16.0)

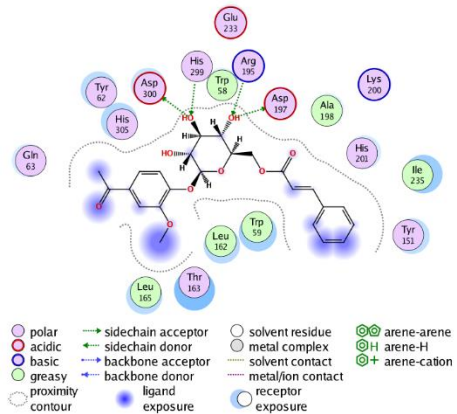
**Table 2:** Docking score, RMSD values, and the interactions of selected dual inhibitors ligands and acarbose with the receptors 3BAJ and 2QMJ residues revealed during structure visualization.

<b><math>\alpha</math>-amylase (ID: 3BAJ)</b>					<b><math>\alpha</math>-glucosidase (ID: 2QMJ)</b>			
Compound	Docking score Kcal/mol	RMSD values (Å)	Binding residues	Interaction	Docking score Kcal/mol	RMSD values (Å)	Binding residues	Interaction
NPC204580	-14.46	1.80	Asp 300 Glu 233 Lys 200 Asp 197 His 201	H-donor H-donor H-acceptor Ionic pi-H	-8.42	1.79	Met 444 Asp 542 Asp 203 Asp 542 Phe 575	H-donor H-donor Ionic Ionic H-pi
NPC137813	-12.58	1.79	Asp 300 Asp 197 His 299 Arg 195	H-donor H-donor H-acceptor H-acceptor	-8.76	1.88	Thr 205 Arg 202 Thr 204	H-acceptor H-acceptor Pi-H
Acarbose	-12.99	1.61	Gln 63 Trp 59	H-donor H-pi	-8.22	1.29	Asp 203 Asp 542 Asp 327 Met444 Asp 443 Arg 526 His 600 Asp 542	H-donor H-donor H-donor H-donor H-acceptor H-acceptor Ionic

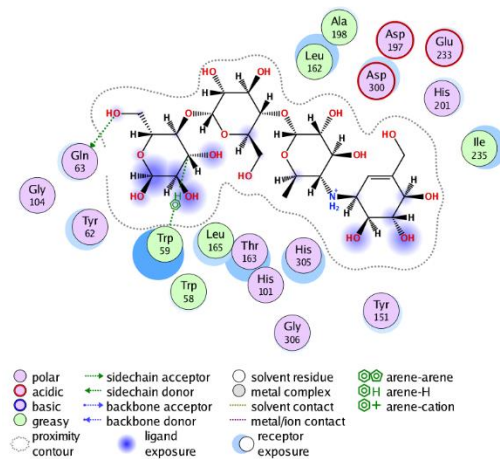
NPC204580 (3BAJ)



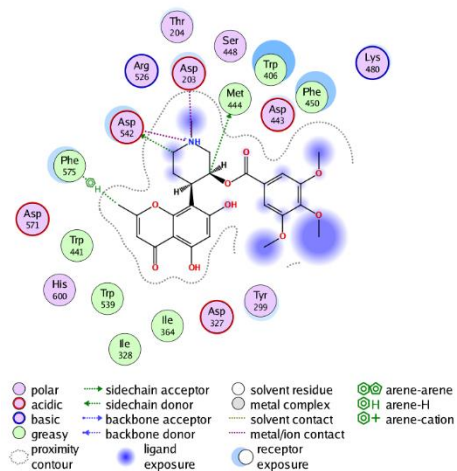
NPC137813 (3BAJ)



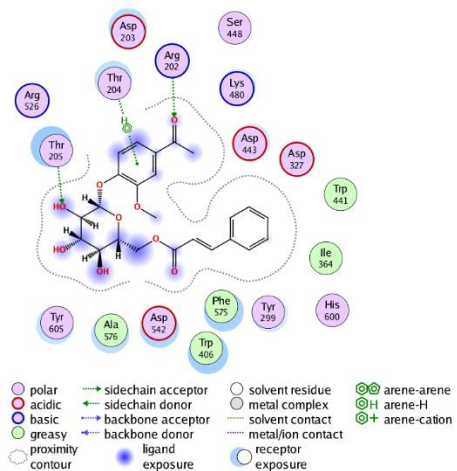
Acarbose (3BAJ)



NPC204580 (2QMJ)



NPC137813 (2QMJ)



Acarbose (2QMJ)

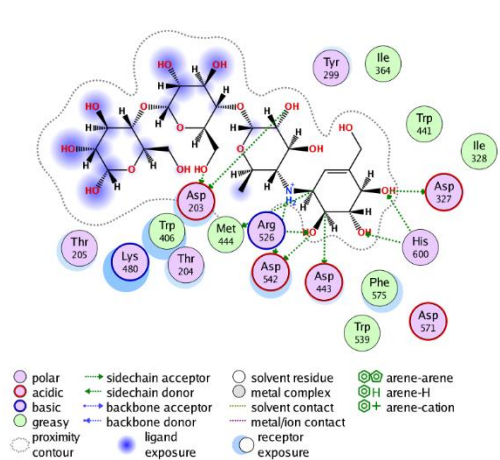
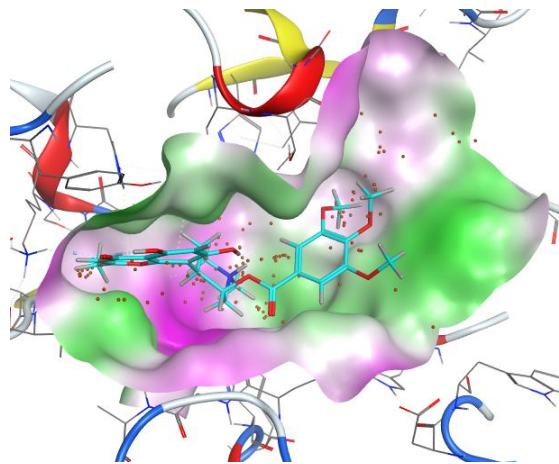
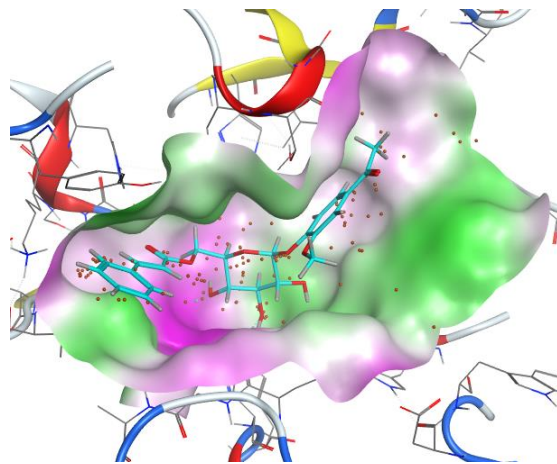


**Figure 16:** 2D interaction of the selected two ligands; NPC204580 and NPC137813 Acarbose with the receptors 3BAJ and 2QMJ

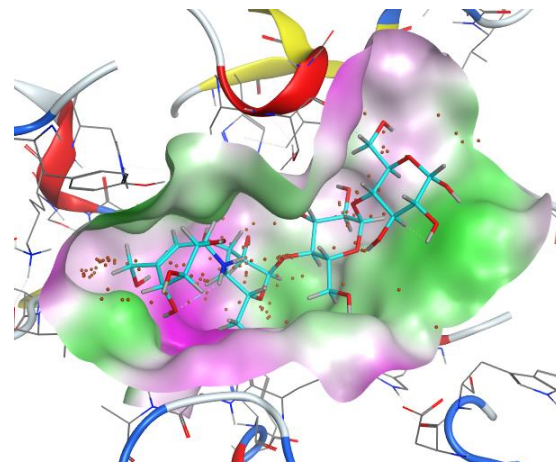
NPC204580 (3BAJ)



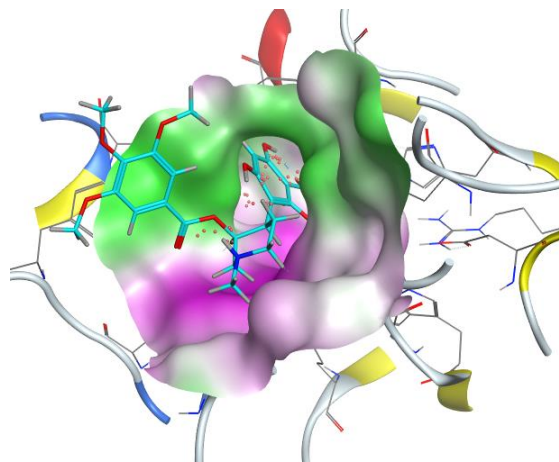
NPC137813 (3BAJ)



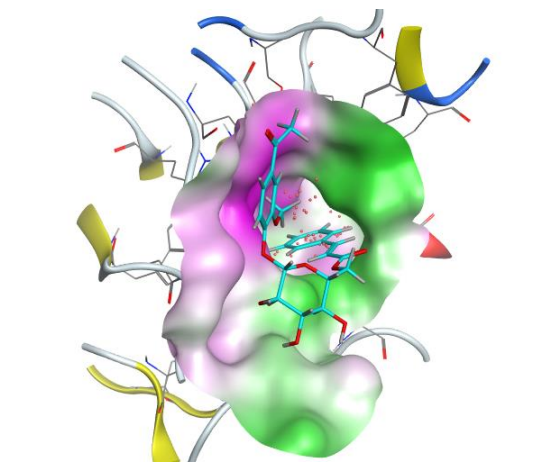
Acarbose(3BAJ)



NPC204580 (2QMJ)



NPC137813 (2QMJ)



Acarbose (2QMJ)

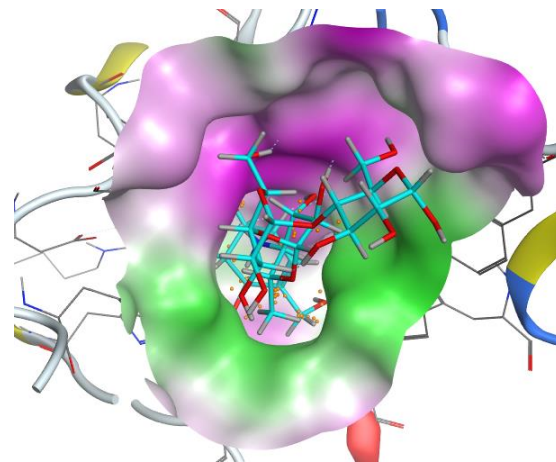


**Figure 17:** 3D docking conformation of the selected ligands; NPC204580 and NPC137813 and Acarbose in the binding site of  $\alpha$ -amylase (3BAJ) and  $\alpha$ -glucosidase (2QMJ). The molecular surface is colored green for the lipophilic regions and purple for the hydrophilic region of the receptor.

## 4.2 Pharmacokinetics properties of NPC204580 and NPC137813

During the arduous and resource-intensive endeavor of drug discovery and development, a multitude of molecular structures undergo comprehensive evaluation, encompassing diverse criteria. This evaluation aids in the selection of molecules to be synthesized, tested, and advanced, with the overarching objective of identifying compounds that exhibit the highest potential for therapeutic application in the treatment of various ailments (Daina et al., 2017). A powerful molecule needs to be concentrated sufficiently to reach its target in the body and remain there in bioactive form long enough for the anticipated biological activity to take place for it to be effective as a medication (Daina et al., 2017).

Bioavailability assessment of the final two proposed compounds was computed and evaluated using the Swiss ADME website (<http://www.swissadme.ch/>) accessed on (August 2, 2023) and the results are presented in Figures 18, 19 and Table 3. Gastrointestinal absorption and cerebral penetration of the selected molecules were predicted based on the BOILED-Egg plot (Figure 18), which illustrates the relationship between WLOGP and TPSA (Egan et al., 2000). The yolk (yellow region) representing the physicochemical area associated with highly probable blood-brain barrier (BBB) permeability, the white region represents the physicochemical space associated with highly probable human intestinal absorption (HIA), and the outer grey zone represents molecules with characteristics indicating anticipated low absorption and restricted brain penetration (Daina et al., 2017).

The two compounds are projected to have significant GI absorption, none of them have BBB permeation characteristics implying they are highly absorbable in the gastrointestinal tract (IG) (white region), but cannot cross the blood-brain barrier (BBB). Given that the selected molecules are substrates of P-glycoprotein (P-gp) (Table 3), it is anticipated we anticipate that they will be effluxed back into the gastrointestinal tract, hence localizing their activity within the intestinal lumen, while minimizing systemic absorption. Additionally, it has been reported that drug molecules demonstrating a greater negative Log  $K_p$  easily permeant through the skin (Potts & Guy, 1992). Therefore, the proposed compounds would justify having transdermal efficacy,

as evidenced by the skin permeability of -6.85 cm/s and -8.56 cm/s for NPC204580 and NPC137813 respectively.

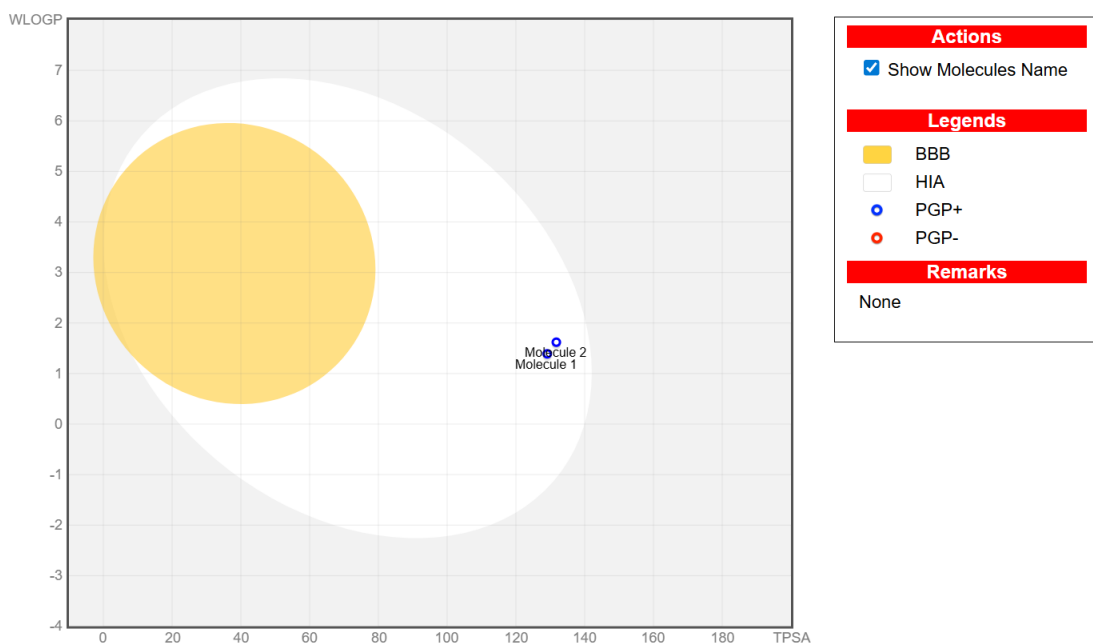


**Figure 18:** BOILED-Egg plot for proposed molecules Molecule\_1 (NPC204580) and Molecule\_2 (NPC137813).

The Bioavailability radar (Figure 19) predicted an ideal range of properties for the proposed molecules. The pink region is a representation of the ideal range of properties of the two molecules, including Polarity (TPSA between 20 and 130 Å), Lipophilicity (log P between -0.7 and +5), Size (MW between 150 and 500 g/mol), Flexibility (no more than 9 rotatable bonds), Saturation (proportion of carbon atoms exhibiting sp<sup>3</sup> hybridization no less than 0.25), and solubility, characterized by a logarithmic value of S (logS) not surpassing 6. This representation suggests that molecules falling within this pink region possess attributes that align with the features of a molecule to qualify as a therapeutic candidate. Therefore, the proposed molecules exhibited favorable bioavailability, indicating their potential effectiveness and suitability for further exploration.

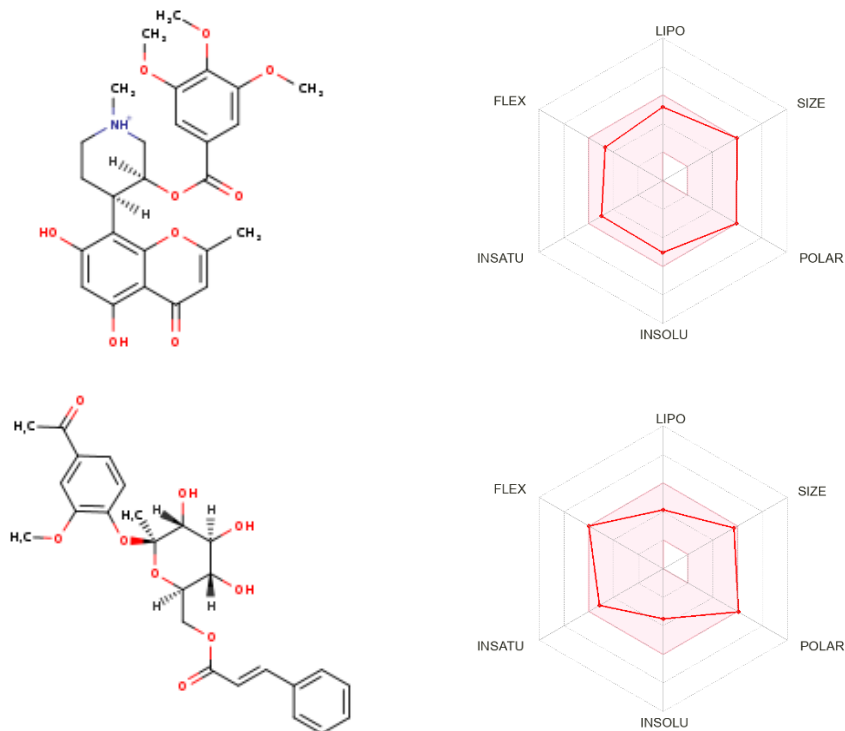


**Figure 19:** The Bioavailability Radar of the proposed ligands.

The metabolism and biotransformation of the drug are regulated by a number of cytochromes P450 isoenzymes, including CYP1A2, CYP2C19, CYP2C9, CYP2D6 and CYP3A4 (Ogu & Maxa, 2000). Therefore, comprehending the significance of the cytochrome P450 system in drug metabolism is essential for understanding drug interactions that may result in toxicities and reduced therapeutic efficacy. Therefore, it is crucial to know whether a molecule is a cytochrome P450 substrate inducer and inhibitor that can help prevent significant drug interactions from occurring. The two molecules were noted to be non-inhibitors of any of the isoenzymes: CYP1A2, CYP2C19, CYP2C9, CYP2D6, and CYP3A4 (Table 3) thus suitable drug candidates.

#### 4.3 Synthetic Accessibility (SA)

Based on the finding shown in Table 3, the two proposed molecules are considered synthetically feasible as their synthetic accessibility score range between 5.30 and 6.36 for NPC204580 and NPC137813 respectively. Synthetic accessibility (SA) is an important factor to take into account while selecting most promising lead molecules. According to Ertl and Schuffenhauer (2009), SA is evaluated by taking into account

factors related to size and complexity such as macrocycles, chiral centers, or spiro functions of a molecule. This leads to SA scores ranging from 1 (ease to synthesize) to 10 (difficult to synthesize) (Daina et al., 2017). Therefore, the discussed ADME properties further corroborated the good pharmacological attributes, predicted docking results about the two molecules.

**Table 3:** Pharmacological features of the proposed compounds

<b>Pharmacokinetics</b>	<b>NPC204580</b>	<b>NPC137813</b>
GI Absorption	High	High
BBB Permeant	No	No
P-gp substrate inhibitor	Yes	Yes
Cytochrome P450 (CYP) inhibitor	No	No
Log Kp (skin permeation)	-6.85 cm/s	-8.56 cm/s
Synthetic accessibility	5.03	6.36

#### **4.4 Molecular Dynamic Simulations**

Molecular dynamic simulation is an essential computational methodology employed in exploring the stability of macro and micro-molecules in a particular water-based environment. In this study, NPC137813 and NPC204580 proposed potential dual inhibitors of  $\alpha$ -amylase (3BAJ) and  $\alpha$ -glucosidase (2QMJ) receptors were considered for 100 ns molecular dynamic (MD) simulation. The MD simulation trajectories such as ligand RMSD, RMSF, and Generalized Born Surface Area (GBSA) were generated, analyzed and recorded as summarized in Figure 20 ,21 and Table 4.

##### **4.4.1 Ligand Root Mean Square Deviation (RMSD)**

The ligand RMSD and the protein backbone for each complex are shown over the course of simulation time, revealing a consistent deviation pattern exhibited by the two molecules throughout the simulation period (Figure 20). A low RMSD value indicates that the system is moderately stable, with relatively minimal deviation from the starting structure (Martínez, 2015). NPC204580 in complex with 3BAJ (Figure 20a) reached equilibrium at the start of the calculation at around ~5 ns with side chain residuals fluctuating from time to time. Throughout the simulation time, oscillation was around ~2.0 Å, however between 45 ns and 55 ns, there was a slight disparity as fluctuation

rose up to 2.9 Å. This suggest a transient deviation from equilibrium and could be attributed to conformational changes or fluctuation in the complex. While NPC137813 in complex with 3BAJ receptor (Figure 20b) reached equilibrium at 15 ns, after which the complex exhibited a stable oscillation at an average RMSD value of ~2.5 Å throughout the simulation period. This suggests a possible stable equilibrium of NPC137813 in complexed with 3BAJ protein. NPC204580 in complex with 2QMJ (Figure 20c) was stable until approximately 73 ns into the simulation after which fluctuations were observed and stabilized at 87 ns. This is indicative of a transient destabilization followed by re-stabilization of the complex. Conversely, NPC137813 in complex with 2QMJ (Figure 20d), exhibited initial fluctuation within the first 10 ns and attained equilibrium at ~11 ns that was maintained throughout the course of simulation time frame. This indicates that the ligand formed a stable complex with the receptor. Therefore, these findings enhance the docking results and dynamic behavior of NPC204580 and NPC137813 with the two receptors hence providing a valuable insight into their binding mechanism.

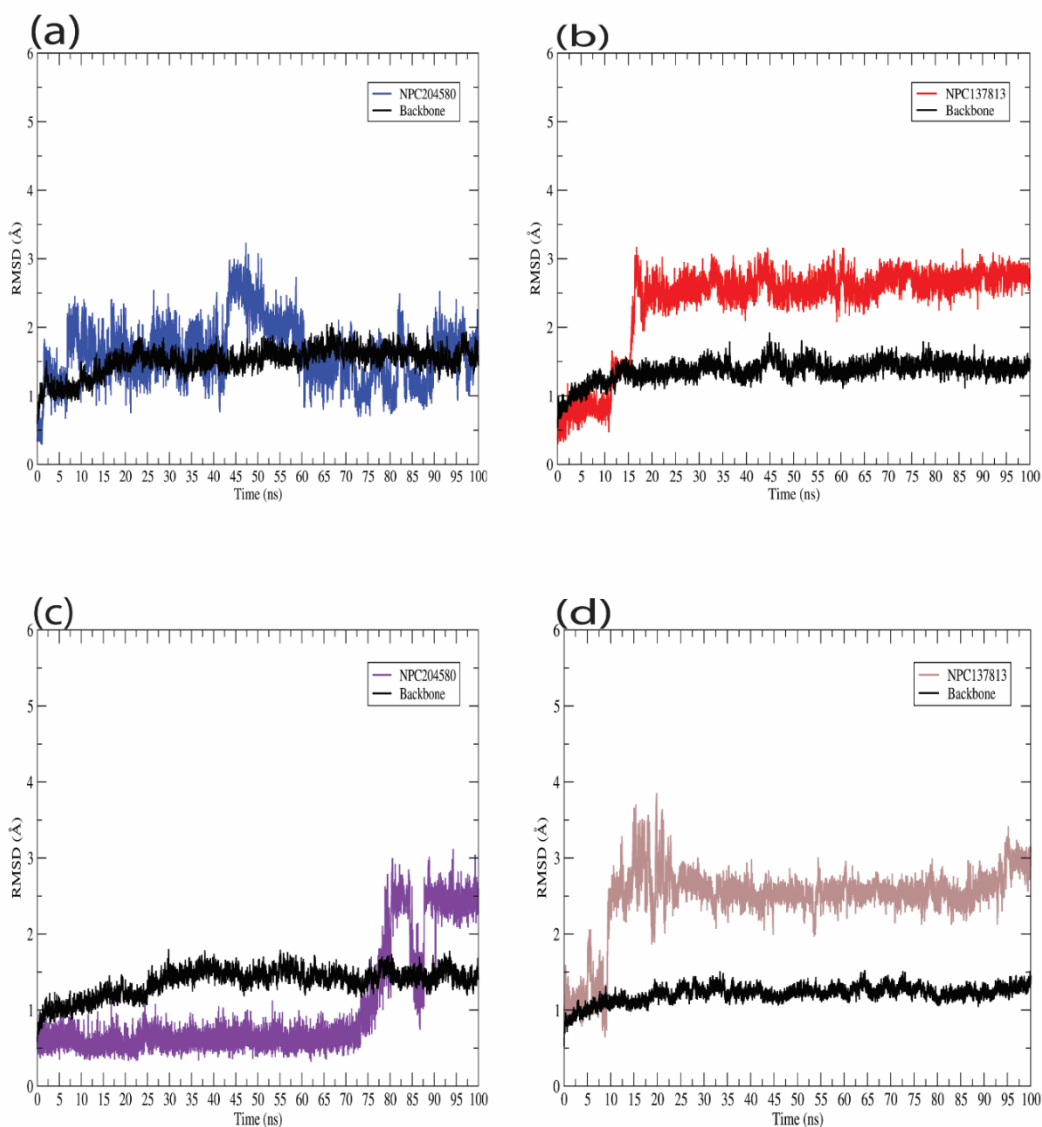


**Figure 20:** Graphical representation of the protein backbone RMSD (black) and ligand RMSD of the proposed molecules (a) NPC204580\_3BAJ, (b) NPC137813\_3BAJ, (c) NPC204580\_2QMJ and (d) NPC137813\_2QMJ.

#### 4.4.2 Root-Means-Square Fluctuation (RMSF)

The stability of the protein-ligand complex in its dynamic state is heavily influenced by the fluctuations occurring in the backbone of a particular amino acid residue. The amino acid residues with low RMSF value are relatively more rigid than those with higher RMSF values (Saddique et al., 2022). To assess the stability of each amino acid in the

two receptors, 3BAJ, and 2QMJ, when associated with the two proposed molecules, their RMSF value was computed (Figure 21). The protein's RMSF values, when complexed with the two molecules, exhibited comparable fluctuations during the whole duration of the simulation. The results revealed that in receptor 3BAJ (Figure 21a) only three amino acid residues exhibited a major fluctuation i.e. 240, 350 and 370 when bound with both NPC204580 and NPC137813, all the amino acid residues were below 10Å signifying that the protein-ligand complex was stable. Conversely, 2QMJ receptor in complex with NPC204580 and NPC137813 (Figure 21b) exhibited little fluctuation of its amino acid residues, except for four notable fluctuations at position 200, 340, 370, and 840. Among these residues, 840 exhibited a major fluctuation with a deviation of 42 Å, suggesting that the residue 840 experience a high degree of flexibility, possibly because of the residue being located on the flexible loop region of the binding site. However, the observed reduced fluctuations in the RMSF values provide clear evidence that the amino acids in both the 3BAJ and 2QMJ receptors effectively maintained their original conformational state throughout the duration of the molecular dynamics (MD) simulation. Furthermore, these amino acids effectively held the molecules, demonstrating a strong affinity and tight interaction.

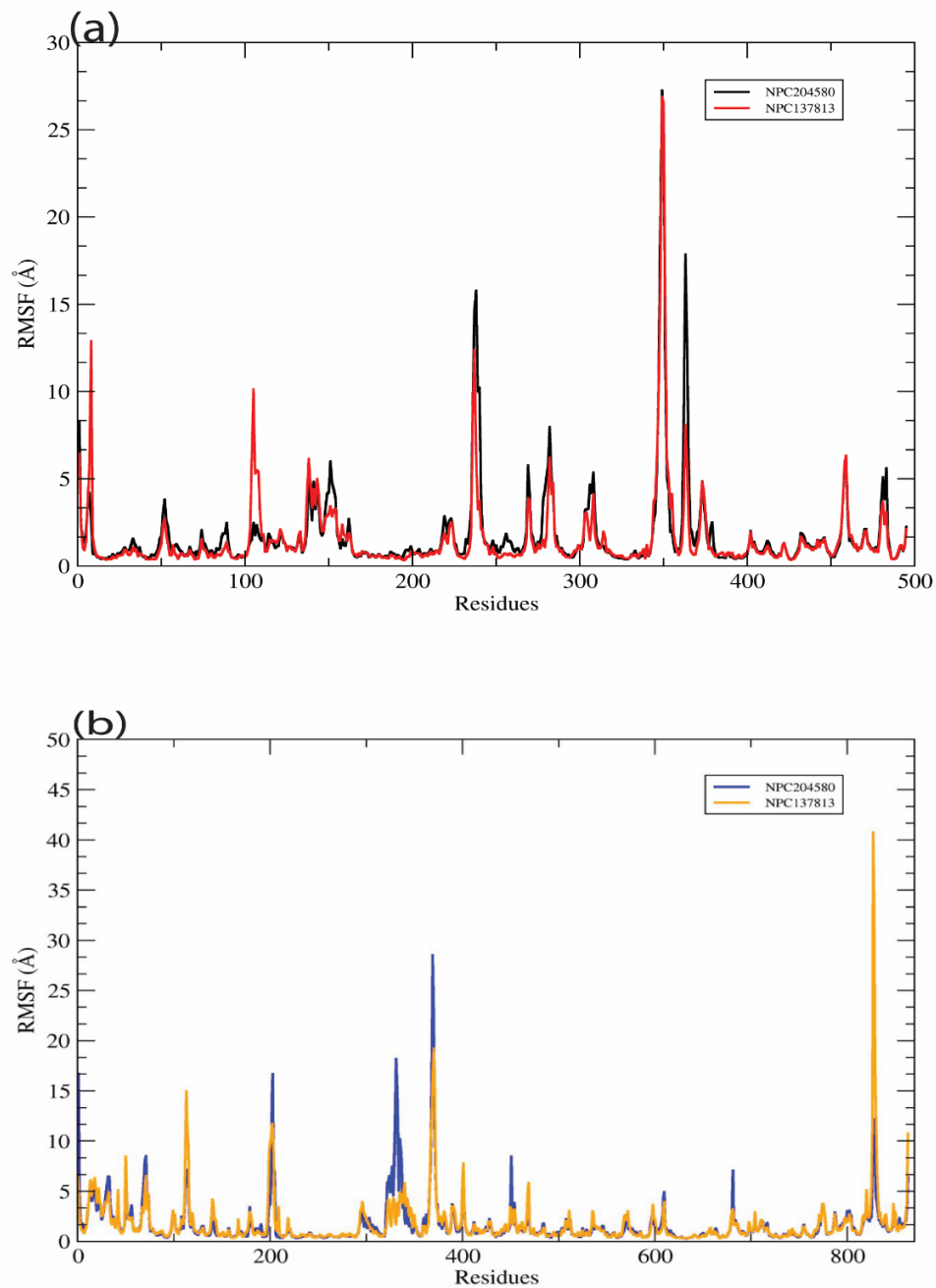


**Figure 21:** Graphical representation of the RMSF trajectories of individual amino acids of both the 3BAJ (a) and 2QMJ (b) receptors, in associated with the proposed ligands (a) 3BAJ (NPC204580-black, NPC137813-red) and (b) 2QMJ (NPC204580-blue, NPC137813-yellow).

#### 4.4.3 Molecular mechanism/ Generalized Born surface area (MM/GBSA)

The GBSA is a commonly used approach for calculating protein-ligand free energies due to its excellent mix of computation precision and effectiveness (Ahmed et al., 2022). In structure-based drug design, it is extensively used to determine end point binding free energy. MM/GBSA is much more precise and accurate as compared to most of the molecular docking (Rydberg et al., 2002). In this study, for  $\alpha$ -glucosidase and  $\alpha$ -amylase, the GBSA offered a valuable insight into the strength of binding between these enzymes and the proposed molecules. Both molecules NPC204580 and NPC137813 exhibited a negative GBSA value in both enzymes (Table 4), indicating favorable binding affinity. In particular, NPC137813 portrayed greater binding interaction with both enzyme than NPC204580, i.e.  $\Delta G_{\text{bind}}$  -32.82 kcal/mol with  $\alpha$ -amylase and  $\Delta G_{\text{bind}}$  -23.39 kcal/mol with  $\alpha$ -glucosidase as compared to NPC204580 which showed a much lower binding interaction, i.e.  $\Delta G_{\text{bind}}$  -23.63 kcal/mol with  $\alpha$ -amylase and  $\Delta G_{\text{bind}}$  -17.29 with  $\alpha$ -glucosidase. NPC137813's higher binding affinity for both enzyme complexes suggests that it may be a more potent inhibitor than NPC204580. However, the two molecules exhibiting good binding affinity to both enzymes could serve as promising therapeutic agents against P. hyperglycemia, pending *in-vivo* and *in-vitro* studies to validate computational finding.

**Table 4:** Binding free energy (GBSA) of NPC137813 and NPC204580 in the two receptors

Protein	Ligand	Binding affinity (kcal/mol)
$\alpha$ -Amylase	NPC204580	-23.63 $\pm$ 0.21
	NPC137813	-32.87 $\pm$ 0.19
$\alpha$ -Glucosidase	NPC204580	-17.29 $\pm$ 0.15
	NPC137813	-23.39 $\pm$ 0.15

## CHAPTER 5

### SUMMARY, CONCLUSION AND RECOMMENDATION

#### 5.1 Summary of the study

The objective of this study was to find a potentially effective dual inhibitor for  $\alpha$ -amylase and  $\alpha$ -glucosidase by utilizing the Natural Products Activity and Species Source Database (NPASS) molecules. Extensive and multi-tiered virtual screening techniques were employed to investigate a potential dual inhibitor of 3BAJ and 2QMJ receptors for the management of postprandial hyperglycemia. A total of 30,926 molecules from the Natural Products Activity and Species Source Database (NPASS) were subjected to an initial screening process, focusing on drug-like and pharmacokinetics properties following beyond Lipinski's rule of five principles (bRO5). Subsequently, Toxicity-based screening was employed, followed by molecular docking and molecular dynamic techniques. Ultimately, two potential drug candidate compounds NPC204580 (Chrotacumine C) and NPC137813 (1-O-(2-Methoxy-4-Acetylphenyl)-6-O-(E-Cinnamoyl)-Beta-D-Glucopyranoside) were identified possessing a notable propensity for binding to both 3BAJ and 2QMJ receptors. The binding interaction profile was elucidated by the analogous bond formation observed in the co-crystal ligand Acarbose.

#### 5.2 Conclusion

- (i) Following the structure activity virtual screening of the NPASS database, a total 2,228 molecules were successfully identified exhibiting favorable drug-like properties. These findings demonstrate the effectiveness of the employed virtual screening approach in selectivity enriching the dataset with structurally diverse, drug-like candidates suitable for further computational and experimental evaluation
- (ii) The consistency and stiffness of NPC204580 and NPC137814 with their associated receptors (3BAJ and 2QMJ) displayed by molecular docking and Molecular dynamic simulation, explains the stability of the ligand in the receptor's active site, further confirming their potential as inhibitors of  $\alpha$ -amylase and  $\alpha$ -glucosidase.

- (iii) The proposed molecules exhibit pharmacokinetics and pharmacodynamic profile that are deemed acceptable, suggesting that they can be readily delivered to the intended site of action.

### 5.3 Recommendation

- (i) Building on the successful identification of 2,228 drug-like molecules from the NPASS database, further computational optimization and experimental validation of the top-ranked candidates, particularly NPC204580 and NPC137813, are recommended to confirm their efficacy as  $\alpha$ -amylase and  $\alpha$ -glucosidase inhibitors.
- (ii) The molecular docking and molecular dynamics simulation results strongly suggest that NPC204580 and NPC137813 have the potential to act as lead compounds for the development of antidiabetic therapeutic agents targeting the regulation of postprandial hyperglycemia.
- (iii) Given their favorable pharmacokinetic and pharmacodynamic profiles, these molecules can serve as promising drug templates for the design of effective oral agents capable of reducing dietary carbohydrate digestion and absorption, thereby managing the post-meal rise in blood glucose levels.

### 5.4 Suggestions for further studies

The findings from this study, warrant further research to ascertain the safety profiles of the two compounds NPC204580 (Chrotacumine C) and NPC137813 (1-O-(2-Methoxy-4-Acetylphenyl)-6-O-(E-Cinnamoyl)-Beta-D-Glucopyranoside).

1. *In-Vitro* studies are crucial in validating the inhibitory effects of the identified molecules on the enzymatic activity of  $\alpha$ -amylase and  $\alpha$ -glucosidase receptors. Such experimental studies like enzyme kinetic assays could provide crucial information regarding the compound's specificity and selectivity towards the target enzymes, in addition to their potency and mode of action.
2. *In-Vivo* studies are essential to investigate the therapeutic potential of NPC204580 and NPC137813 in animal models. In-vivo experiments ought to evaluate compound's capacity to lower postprandial hyperglycemia, enhance glucose tolerance, and may be potentially mitigate diabetic complications.

## REFERENCES

- Abdullahi, M., Adeniji, S. E., Arthur, D. E., & Musa, S. (2020). Quantitative structure-activity relationship (QSAR) modelling study of some novel carboxamide series as new anti-tubercular agents. *Bulletin of the National Research Centre*, 44(1), 136. <https://doi.org/10.1186/s42269-020-00389-7>
- Ahmed, S., Ali, M. C., Ruma, R. A., Mahmud, S., Paul, G. K., Saleh, M. A., Alshahrani, M. M., Obaidullah, A. J., Biswas, S. K., Rahman, M. M., Rahman, M. M., & Islam, M. R. (2022). Molecular Docking and Dynamics Simulation of Natural Compounds from Betel Leaves (*Piper betle* L.) for Investigating the Potential Inhibition of Alpha-Amylase and Alpha-Glucosidase of Type 2 Diabetes. *Molecules*, 27(14), Article 14. <https://doi.org/10.3390/molecules27144526>
- Aminu, K. S., Uzairu, A., Umar, A. B., & Ibrahim, M. T. (2022). Salicylic acid derivatives as potential  $\alpha$ -glucosidase inhibitors: Drug design, molecular docking and pharmacokinetic studies. *Bulletin of the National Research Centre*, 46(1), 162. <https://doi.org/10.1186/s42269-022-00853-6>
- Anitha Gopal, B., & Muralikrishna, G. (2009). Porcine Pancreatic  $\alpha$ -Amylase and its Isoforms: Purification and Kinetic Studies. *International Journal of Food Properties*, 12(3), 571–586. <https://doi.org/10.1080/10942910801947755>
- Asmaa, M., Samira, S. Z., Aliaa, M., & Bassem, H. G. (2016). *The Relationship between Hypomagnesaemia and Glycemic Control in Children with Type 1 Diabetes Mellitus*. <https://doi.org/10.4172/2155-6156.1000693>
- Asmat, U., Abad, K., & Ismail, K. (2016). Diabetes mellitus and oxidative stress—A concise review. *Saudi Pharmaceutical Journal*, 24(5), 547–553. <https://doi.org/10.1016/j.jsps.2015.03.013>
- Ayers, M. (2012). ChemSpider: The Free Chemical Database. *Reference Reviews*, 26(7), 45–46. <https://doi.org/10.1108/09504121211271059>
- Bailey, C., & Day, C. (2004). Metformin: Its botanical background. *Practical Diabetes International*, 21(3), 115–117. <https://doi.org/10.1002/pdi.606>
- Balakumar, P., Maung-U, K., & Jagadeesh, G. (2016). Prevalence and prevention of cardiovascular disease and diabetes mellitus. *Pharmacological Research*, 113, 600–609. <https://doi.org/10.1016/j.phrs.2016.09.040>
- Bastos, R. S., de Lima, L. R., Neto, M. F. A., Maryam, Yousaf, N., Cruz, J. N., Campos, J. M., Kimani, N. M., Ramos, R. S., & Santos, C. B. R. (2023). Design and Identification of Inhibitors for the Spike-ACE2 Target of SARS-CoV-2. *International Journal of Molecular Sciences*, 24(10), Article 10. <https://doi.org/10.3390/ijms24108814>
- Bender, B. J., Gahbauer, S., Luttens, A., Lyu, J., Webb, C. M., Stein, R. M., Fink, E. A., Balius, T. E., Carlsson, J., Irwin, J. J., & Shoichet, B. K. (2021). A practical

- guide to large-scale docking. *Nature Protocols*, 16(10), Article 10. <https://doi.org/10.1038/s41596-021-00597-z>
- Brown, D. G., Wobst, H. J., Kapoor, A., Kenna, L. A., & Southall, N. (2021). Clinical development times for innovative drugs. *Nature Reviews Drug Discovery*, 21(11), 793–794. <https://doi.org/10.1038/d41573-021-00190-9>
- Chaudhury, A., Duvoor, C., Reddy Dendi, V. S., Kraleti, S., Chada, A., Ravilla, R., Marco, A., Shekhawat, N. S., Montales, M. T., Kuriakose, K., Sasapu, A., Beebe, A., Patil, N., Musham, C. K., Lohani, G. P., & Mirza, W. (2017). Clinical Review of Antidiabetic Drugs: Implications for Type 2 Diabetes Mellitus Management. *Frontiers in Endocrinology*, 8. <https://www.frontiersin.org/articles/10.3389/fendo.2017.00006>
- Cheenpracha, S., Jitnom, J., Komek, M., Ritthiwigrom, T., & Laphookhieo, S. (2016). Acetylcholinesterase inhibitory activity and molecular docking study of steroidal alkaloids from *Holarrhena pubescens* barks. *Steroids*, 108, 92–98. <https://doi.org/10.1016/j.steroids.2016.01.018>
- Daina, A., Michielin, O., & Zoete, V. (2017). SwissADME: A free web tool to evaluate pharmacokinetics, drug-likeness and medicinal chemistry friendliness of small molecules. *Scientific Reports*, 7(1), Article 1. <https://doi.org/10.1038/srep42717>
- Dixit, V. A., & Bharatam, P. V. (2013). SAR and Computer-Aided Drug Design Approaches in the Discovery of Peroxisome Proliferator-Activated Receptor  $\gamma$  Activators: A Perspective. *Journal of Computational Medicine*, 2013, 1–38. <https://doi.org/10.1155/2013/406049>
- Dutra, R. C., Campos, M. M., Santos, A. R. S., & Calixto, J. B. (2016). Medicinal plants in Brazil: Pharmacological studies, drug discovery, challenges and perspectives. *Pharmacological Research*, 112, 4–29. <https://doi.org/10.1016/j.phrs.2016.01.021>
- Egan, W. J., Merz, Kenneth M., & Baldwin, J. J. (2000). Prediction of Drug Absorption Using Multivariate Statistics. *Journal of Medicinal Chemistry*, 43(21), 3867–3877. <https://doi.org/10.1021/jm000292e>
- Elhag, I. Y. (2023). Chapter 12—Role of AI in ADME/Tox toward formulation optimization and delivery. In A. Philip, A. Shahiwala, M. Rashid, & Md. Faiyazuddin (Eds.), *A Handbook of Artificial Intelligence in Drug Delivery* (pp. 301–345). Academic Press. <https://doi.org/10.1016/B978-0-323-89925-3.00011-3>
- Ertl, P., & Schuffenhauer, A. (2009). Estimation of synthetic accessibility score of drug-like molecules based on molecular complexity and fragment contributions. *Journal of Cheminformatics*, 1(1), 8. <https://doi.org/10.1186/1758-2946-1-8>

- Fareed, M., Salam, N., Khoja, A., Mahmoud, M., & Ahamed, M. (2017). Life Style Related Risk Factors of Type 2 Diabetes Mellitus and Its Increased Prevalence in Saudi Arabia: A Brief Review. *International Journal of Medical Research & Health Sciences*, 6, 125–132. <https://www.indianjournals.com/ijor.aspx>
- Fujisawa, T., Ikegami, H., Inoue, K., Kawabata, Y., & Ogihara, T. (2005). Effect of two  $\alpha$ -glucosidase inhibitors, voglibose and acarbose, on postprandial hyperglycemia correlates with subjective abdominal symptoms. *Metabolism*, 54(3), 387–390. <https://doi.org/10.1016/j.metabol.2004.10.004>
- Funke, I., & Melzig, M. F. (2006). Plantas tradicionalmente utilizadas na terapia da diabetes: Fitomedicamentos como inibidores da atividade alfa-amilase. *Revista Brasileira de Farmacognosia*, 16, 1–5. <https://doi.org/10.1590/S0102-695X2006000100002>
- Gaitonde, V., Karmakar, P., & Trivedi, A. (2020). *Drug Discovery and Development: New Advances*. BoD – Books on Demand. <https://doi.org/10.5772/intechopen.77685>
- Ganesan, K., Rana, M. B. M., & Sultan, S. (2024). Oral Hypoglycemic Medications. In *StatPearls*. StatPearls Publishing. <http://www.ncbi.nlm.nih.gov/books/NBK482386/>
- Gaulton, A., Hersey, A., Nowotka, M., Bento, A. P., Chambers, J., Mendez, D., Mutowo, P., Atkinson, F., Bellis, L. J., Cibrián-Uhalte, E., Davies, M., Dedman, N., Karlsson, A., Magariños, M. P., Overington, J. P., Papadatos, G., Smit, I., & Leach, A. R. (2017). The ChEMBL database in 2017. *Nucleic Acids Research*, 45(D1), D945–D954. <https://doi.org/10.1093/nar/gkw1074>
- Glovaci, D., Fan, W., & Wong, N. D. (2019). Epidemiology of Diabetes Mellitus and Cardiovascular Disease. *Current Cardiology Reports*, 21(4), 21. <https://doi.org/10.1007/s11886-019-1107-y>
- Goyal, R., Jialal, I., & Castano, M. (2022). Diabetes Mellitus Type 2 (Nursing). In *StatPearls*. StatPearls Publishing. <http://www.ncbi.nlm.nih.gov/books/NBK568737>
- Honma, M. (2020). An assessment of mutagenicity of chemical substances by (quantitative) structure–activity relationship. *Genes and Environment*, 42(1), 23. <https://doi.org/10.1186/s41021-020-00163-1>
- Hua, J., Qi, J., & Yu, B.-Y. (2014). Iridoid and phenylpropanoid glycosides from *Scrophularia ningpoensis* Hemsl. And their  $\alpha$ -Glucosidase inhibitory activities. *Fitoterapia*, 93, 67–73. <https://doi.org/10.1016/j.fitote.2013.11.011>
- Huang, S.-Y., Grinter, S. Z., & Zou, X. (2010). Scoring functions and their evaluation methods for protein–ligand docking: Recent advances and future directions.

*Physical Chemistry Chemical Physics*, 12(40), 12899–12908.  
<https://doi.org/10.1039/C0CP00151A>

- Hui, H., Zhao, X., & Perfetti, R. (2005). Structure and function studies of glucagon-like peptide-1 (GLP-1): The designing of a novel pharmacological agent for the treatment of diabetes. *Diabetes/Metabolism Research and Reviews*, 21(4), 313–331. <https://doi.org/10.1002/dmrr.553>
- Ikeda, K., Takahashi, M., Nishida, M., Miyauchi, M., Kizu, H., Kameda, Y., Arisawa, M., Watson, A. A., Nash, R. J., Fleet, G. W. J., & Asano, N. (1999). Homonojirimycin analogues and their glucosides from *Lobelia sessilifolia* and *Adenophora* spp. (Campanulaceae). *Carbohydrate Research*, 323(1–4), 73–80. [https://doi.org/10.1016/S0008-6215\(99\)00246-3](https://doi.org/10.1016/S0008-6215(99)00246-3)
- Islam, M. A., Dudekula, D. B., Rallabandi, V. P. S., Srinivasan, S., Natarajan, S., Chung, H., & Park, J. (2022). Identification of Potential Cytochrome P450 3A5 Inhibitors: An Extensive Virtual Screening through Molecular Docking, Negative Image-Based Screening, Machine Learning and Molecular Dynamics Simulation Studies. *International Journal of Molecular Sciences*, 23(16), Article 16. <https://doi.org/10.3390/ijms23169374>
- Ismail, I. S., Nagakura, Y., Hirasawa, Y., Hosoya, T., Lazim, M. I. M., Lajis, N. H., Shiro, M., & Morita, H. (2009). Chrotacumines A–D, Chromone Alkaloids from *Dysoxylum acutangulum*. *Journal of Natural Products*, 72(10), 1879–1883. <https://doi.org/10.1021/np9003849>
- Itoh, H., Crotti, L., Aiba, T., Spazzolini, C., Denjoy, I., Fressart, V., Hayashi, K., Nakajima, T., Ohno, S., Makiyama, T., Wu, J., Hasegawa, K., Mastantuono, E., Dagradi, F., Pedrazzini, M., Yamagishi, M., Berthet, M., Murakami, Y., Shimizu, W., ... Horie, M. (2016). The genetics underlying acquired long QT syndrome: Impact for genetic screening. *European Heart Journal*, 37(18), 1456–1464. <https://doi.org/10.1093/eurheartj/ehv695>
- Jhong, C.-H., Riyaphan, J., Lin, S.-H., Chia, Y.-C., & Weng, C.-F. (2015). Screening alpha-glucosidase and alpha-amylase inhibitors from natural compounds by molecular docking in silico. *BioFactors*, 41(4), 242–251. <https://doi.org/10.1002/biof.1219>
- Kajaria, D., Ranjana, Tripathi, J., Tripathi, Y. B., & Tiwari, S. (2013). In-vitro  $\alpha$  amylase and glycosidase inhibitory effect of ethanolic extract of antiasthmatic drug—Shirishadi. *Journal of Advanced Pharmaceutical Technology & Research*, 4(4), 206–209. <https://doi.org/10.4103/2231-4040.121415>
- Kandra, L. (2003).  $\alpha$ -Amylases of medical and industrial importance. *Journal of Molecular Structure: THEOCHEM*, 666–667, 487–498. <https://doi.org/10.1016/j.theochem.2003.08.073>

- Kapetanovic, I. M. (2008). Computer-aided drug discovery and development (CADD): In silico-chemico-biological approach. *Chemico-Biological Interactions*, *171*(2), 165–176. <https://doi.org/10.1016/j.cbi.2006.12.006>
- Kibet, S., Kimani, N. M., Mwanza, S. S., Mudalungu, C. M., Santos, C. B. R., & Tanga, C. M. (2024). Unveiling the Potential of Ent-Kaurane Diterpenoids: Multifaceted Natural Products for Drug Discovery. *Pharmaceuticals*, *17*(4), Article 4. <https://doi.org/10.3390/ph17040510>
- Kim, S., Chen, J., Cheng, T., Gindulyte, A., He, J., He, S., Li, Q., Shoemaker, B. A., Thiessen, P. A., Yu, B., Zaslavsky, L., Zhang, J., & Bolton, E. E. (2023). PubChem 2023 update. *Nucleic Acids Research*, *51*(D1), D1373–D1380. <https://doi.org/10.1093/nar/gkac956>
- Kim, S.-D. (2013).  $\alpha$ -Glucosidase inhibitor from *Buthus martensi* Karsch. *Food Chemistry*, *136*(2), 297–300. <https://doi.org/10.1016/j.foodchem.2012.08.063>
- Kirchmair, J., Distinto, S., Roman Liedl, K., Markt, P., Maria Rollinger, J., Schuster, D., Maria Spitzer, G., & Wolber, G. (2011). Development of Anti-Viral Agents Using Molecular Modeling and Virtual Screening Techniques. *Infectious Disorders - Drug Targets Disorders*, *11*(1), 64–93. <https://doi.org/10.2174/187152611794407782>
- Kishimoto, I., & Ohashi, A. (2021). Impact of Lifestyle Behaviors on Postprandial Hyperglycemia during Continuous Glucose Monitoring in Adult Males with Overweight/Obesity but without Diabetes. *Nutrients*, *13*(9), Article 9. <https://doi.org/10.3390/nu13093092>
- Kitchen, D. B., Decornez, H., Furr, J. R., & Bajorath, J. (2004). Docking and scoring in virtual screening for drug discovery: Methods and applications. *Nature Reviews Drug Discovery*, *3*(11), Article 11. <https://doi.org/10.1038/nrd1549>
- Kontoyianni, M. (2017). Docking and Virtual Screening in Drug Discovery. In I. M. Lazar, M. Kontoyianni, & A. C. Lazar (Eds.), *Proteomics for Drug Discovery: Methods and Protocols* (pp. 255–266). Springer. [https://doi.org/10.1007/978-1-4939-7201-2\\_18](https://doi.org/10.1007/978-1-4939-7201-2_18)
- Krupanidhi, A. M., Kalleshappa, C. M., Chanchi, A. R., Dabadi, P., & Akshara, A. (2016). Antihyperlipidemic Activities of Isolated bio Compounds of *Aegle Marmelos*. *Undefined*. <https://www.semanticscholar.org/paper/Antihyperlipidemic-Activities-of-Isolated-bio-of-Krupanidhi-Kalleshappa/2e997d313af8ec2871a6e1e49f7df4e6b2d6692b>
- Kubínová, R., Pořízková, R., Navrátilová, A., Farsa, O., Hanáková, Z., Bačinská, A., Čížek, A., & Valentová, M. (2014). Antimicrobial and enzyme inhibitory activities of the constituents of *Plectranthus madagascariensis* (Pers.) Benth.

*Journal of Enzyme Inhibition and Medicinal Chemistry*, 29(5), 749–752.  
<https://doi.org/10.3109/14756366.2013.848204>

Kumar, A., Kini, S. G., & Rathi, E. (2021). A Recent Appraisal of Artificial Intelligence and In Silico ADMET Prediction in the Early Stages of Drug Discovery. *Mini Reviews in Medicinal Chemistry*, 21(18), 2788–2800.  
<https://doi.org/10.2174/1389557521666210401091147>

Kumar, S., Narwal, S., Kumar, V., & Prakash, O. (2011).  $\alpha$ -glucosidase inhibitors from plants: A natural approach to treat diabetes. *Pharmacognosy Reviews*, 5(9), 19–29. <https://doi.org/10.4103/0973-7847.79096>

Lavecchia, A., & Giovanni, C. (2013). Virtual Screening Strategies in Drug Discovery: A Critical Review. *Current Medicinal Chemistry*, 20(23), 2839–2860.  
<https://doi.org/10.2174/09298673113209990001>

Lee, S.-S., Lin, H.-C., & Chen, C.-K. (2008). Acylated flavonol monorhamnosides,  $\alpha$ -glucosidase inhibitors, from *Machilus philippinensis*. *Phytochemistry*, 69(12), 2347–2353. <https://doi.org/10.1016/j.phytochem.2008.06.006>

Li, X., Bai, Y., Jin, Z., & Svensson, B. (2022). Food-derived non-phenolic  $\alpha$ -amylase and  $\alpha$ -glucosidase inhibitors for controlling starch digestion rate and guiding diabetes-friendly recipes. *LWT*, 153, 112455.  
<https://doi.org/10.1016/j.lwt.2021.112455>

Lipinski, C. A. (2004). Lead- and drug-like compounds: The rule-of-five revolution. *Drug Discovery Today: Technologies*, 1(4), 337–341.  
<https://doi.org/10.1016/j.ddtec.2004.11.007>

Lipinski, C. A., Lombardo, F., Dominy, B. W., & Feeney, P. J. (2001). Experimental and computational approaches to estimate solubility and permeability in drug discovery and development settings. PII of original article: S0169-409X(96)00423-1. The article was originally published in *Advanced Drug Delivery Reviews* 23 (1997) 3–25.1. *Advanced Drug Delivery Reviews*, 46(1), 3–26. [https://doi.org/10.1016/S0169-409X\(00\)00129-0](https://doi.org/10.1016/S0169-409X(00)00129-0)

Liu, S., Alnammi, M., Ericksen, S. S., Voter, A. F., Ananiev, G. E., Keck, J. L., Hoffmann, F. M., Wildman, S. A., & Gitter, A. (2019). Practical Model Selection for Prospective Virtual Screening. *Journal of Chemical Information and Modeling*, 59(1), 282–293. <https://doi.org/10.1021/acs.jcim.8b00363>

Lo Piparo, E., Scheib, H., Frei, N., Williamson, G., Grigorov, M., & Chou, C. J. (2008). Flavonoids for Controlling Starch Digestion: Structural Requirements for Inhibiting Human  $\alpha$ -Amylase. *Journal of Medicinal Chemistry*, 51(12), 3555–3561. <https://doi.org/10.1021/jm800115x>

Lordan, S., Smyth, T. J., Soler-Vila, A., Stanton, C., & Ross, R. P. (2013). The  $\alpha$ -amylase and  $\alpha$ -glucosidase inhibitory effects of Irish seaweed extracts. *Food*

*Chemistry*, 141(3), 2170–2176.  
<https://doi.org/10.1016/j.foodchem.2013.04.123>

Maia, E. H. B., Assis, L. C., de Oliveira, T. A., da Silva, A. M., & Taranto, A. G. (2020). Structure-Based Virtual Screening: From Classical to Artificial Intelligence. *Frontiers in Chemistry*, 8. <https://www.frontiersin.org/articles/10.3389/fchem.2020.00343>

Martínez, L. (2015). Automatic Identification of Mobile and Rigid Substructures in Molecular Dynamics Simulations and Fractional Structural Fluctuation Analysis. *PLOS ONE*, 10(3), e0119264. <https://doi.org/10.1371/journal.pone.0119264>

Martinez-Gonzalez, A. I., Díaz-Sánchez, Á. G., de la Rosa, L. A., Bustos-Jaimes, I., & Alvarez-Parrilla, E. (2019). Inhibition of  $\alpha$ -amylase by flavonoids: Structure activity relationship (SAR). *Spectrochimica Acta Part A: Molecular and Biomolecular Spectroscopy*, 206, 437–447. <https://doi.org/10.1016/j.saa.2018.08.057>

Maurus, R., Begum, A., Williams, L. K., Fredriksen, J. R., Zhang, R., Withers, S. G., & Brayer, G. D. (2008). Alternative Catalytic Anions Differentially Modulate Human  $\alpha$ -Amylase Activity and Specificity. *Biochemistry*, 47(11), 3332–3344. <https://doi.org/10.1021/bi701652t>

McAnuff, M. A., Harding, W. W., Omoruyi, F. O., Jacobs, H., Morrison, E. Y., & Asemota, H. N. (2005). Hypoglycemic effects of steroidal saponins isolated from Jamaican bitter yam, *Dioscorea polygonoides*. *Food and Chemical Toxicology*, 43(11), 1667–1672. <https://doi.org/10.1016/j.fct.2005.05.008>

Meanwell, N. A. (2016). Improving Drug Design: An Update on Recent Applications of Efficiency Metrics, Strategies for Replacing Problematic Elements, and Compounds in Nontraditional Drug Space. *Chemical Research in Toxicology*, 29(4), 564–616. <https://doi.org/10.1021/acs.chemrestox.6b00043>

Minhas, S., Khan, F., Abbas, F., & Faiz, A. U. (2017). Phytochemical Screening and Determination of Antibacterial, Anti-Tumorigenic and DNA Protection Ability of Root Extracts of *Saussurea Lappa*. *Journal of Bioresource Management*, 4(4). <https://doi.org/10.35691/JBM.7102.0077>

Missoun, F., Fatma, B., nesrine ouda, A., & Djebli, N. (2018). *Antidiabetic bioactive compounds from plants*. <https://doi.org/10.26415/2572-004X-vol2iss1p199-214>

Mohiuddin, S. S., & Khattar, D. (2023). *Biochemistry, Ammonia*. In *StatPearls*. StatPearls Publishing. <http://www.ncbi.nlm.nih.gov/books/NBK541039/>

Murai, A., Iwamura, K., Takada, M., Ogawa, K., Usui, T., & Okumura, J. (2002). Control of postprandial hyperglycaemia by galactosyl maltobionolactone and its

- novel anti-amylase effect in mice. *Life Sciences*, 71(12), 1405–1415. [https://doi.org/10.1016/S0024-3205\(02\)01844-1](https://doi.org/10.1016/S0024-3205(02)01844-1)
- Nakano, T., Inoue, I., Seo, M., Takahashi, S., Komoda, T., & Katayama, S. (2009). Acarbose attenuates postprandial hyperlipidemia: Investigation in an intestinal absorptive cell model. *Metabolism - Clinical and Experimental*, 58(5), 583–585. <https://doi.org/10.1016/j.metabol.2009.02.003>
- Narayanaswamy, R. (2014). *Molecular docking analysis of natural compounds as Human neutrophil elastase (HNE) inhibitors*. [https://www.academia.edu/es/63457358/Molecular\\_docking\\_analysis\\_of\\_natural\\_compounds\\_as\\_Human\\_neutrophil\\_elastase\\_HNE\\_inhibitors](https://www.academia.edu/es/63457358/Molecular_docking_analysis_of_natural_compounds_as_Human_neutrophil_elastase_HNE_inhibitors)
- Narita, Y., & Inouye, K. (2015). *Inhibition of Porcine Pancreas  $\alpha$ -Amylase by Chlorogenic Acids from Green Coffee Beans and Cinnamic Acid Derivatives*. <https://doi.org/10.1016/B978-0-12-409517-5.00084-X>
- Neves Cruz, J., da Costa, K. S., de Carvalho, T. A. A., & de Alencar, N. A. N. (2020). Measuring the structural impact of mutations on cytochrome P450 21A2, the major steroid 21-hydroxylase related to congenital adrenal hyperplasia. *Journal of Biomolecular Structure and Dynamics*, 38(5), 1425–1434. <https://doi.org/10.1080/07391102.2019.1607560>
- Nguyen, P. T. V. (2015). *In silico drug discovery targeting Chikungunya virus*. *University of Wollongong Thesis Collection 1954-2016*. <https://ro.uow.edu.au/theses/4452>
- Ochieng, C. O., Nyongesa, D. W., Yamo, K. O., Onyango, J. O., Langat, M. K., & Manguro, L. A. O. (2020).  $\alpha$ -Amylase and  $\alpha$ -glucosidase inhibitors from *Zanthoxylum chalybeum* Engl. Root bark. *Fitoterapia*, 146, 104719. <https://doi.org/10.1016/j.fitote.2020.104719>
- Ogu, C. C., & Maxa, J. L. (2000). Drug interactions due to cytochrome P450. *Proceedings (Baylor University Medical Center)*, 13(4), 421–423. <https://doi.org/10.1080/08998280.2000.11927719>
- Palanisamy, S., Yien, E. L. H., Shi, L. W., Si, L. Y., Qi, S. H., Ling, L. S. C., Lun, T. W., & Chen, Y. N. (2018). Systematic Review of Efficacy and Safety of Newer Antidiabetic Drugs Approved from 2013 to 2017 in Controlling HbA1c in Diabetes Patients. *Pharmacy*, 6(3), Article 3. <https://doi.org/10.3390/pharmacy6030057>
- Pankaj Modi. (2007). Diabetes Beyond Insulin: Review of New Drugs for Treatment of Diabetes Mellitus. *Current Drug Discovery Technologies*, 4(1), 39–47. <https://doi.org/10.2174/157016307781115476>
- Parasuraman, S. (2011). Toxicological screening. *Journal of Pharmacology & Pharmacotherapeutics*, 2(2), 74–79. <https://doi.org/10.4103/0976-500X.81895>

- Pires, D. E. V., Blundell, T. L., & Ascher, D. B. (2015). pkCSM: Predicting Small-Molecule Pharmacokinetic and Toxicity Properties Using Graph-Based Signatures. *Journal of Medicinal Chemistry*, 58(9), 4066–4072. <https://doi.org/10.1021/acs.jmedchem.5b00104>
- Potts, R. O., & Guy, R. H. (1992). Predicting Skin Permeability. *Pharmaceutical Research*, 9(5), 663–669. <https://doi.org/10.1023/A:1015810312465>
- Prabhakar Reddy, P., Tiwari, A. K., Ranga Rao, R., Madhusudhana, K., Rama Subba Rao, V., Ali, A. Z., Suresh Babu, K., & Madhusudana Rao, J. (2009). New Labdane diterpenes as intestinal  $\alpha$ -glucosidase inhibitor from antihyperglycemic extract of *Hedychium spicatum* (Ham. Ex Smith) rhizomes. *Bioorganic & Medicinal Chemistry Letters*, 19(9), 2562–2565. <https://doi.org/10.1016/j.bmcl.2009.03.045>
- Prasathkumar, M., Anisha, S., Dhriya, C., Becky, R., & Sadhasivam, S. (2021). Therapeutic and pharmacological efficacy of selective Indian medicinal plants – A review. *Phytomedicine Plus*, 1(2), 100029. <https://doi.org/10.1016/j.phyplu.2021.100029>
- Ruiz-Tagle, B., Villalobos-Cid, M., Dorn, M., & Inostroza-Ponta, M. (2017). Evaluating the use of local search strategies for a memetic algorithm for the protein-ligand docking problem. *2017 36th International Conference of the Chilean Computer Science Society (SCCC)*, 1–12. <https://doi.org/10.1109/SCCC.2017.8405141>
- Rydberg, E. H., Li, C., Maurus, R., Overall, C. M., Brayer, G. D., & Withers, S. G. (2002). Mechanistic Analyses of Catalysis in Human Pancreatic  $\alpha$ -Amylase: Detailed Kinetic and Structural Studies of Mutants of Three Conserved Carboxylic Acids. *Biochemistry*, 41(13), 4492–4502. <https://doi.org/10.1021/bi011821z>
- Saddique, F. A., Ahmad, M., Ashfaq, U. A., Muddassar, M., Sultan, S., & Zaki, M. E. A. (2022). Identification of Cyclic Sulfonamides with an N-Arylacetamide Group as  $\alpha$ -Glucosidase and  $\alpha$ -Amylase Inhibitors: Biological Evaluation and Molecular Modeling. *Pharmaceuticals*, 15(1), Article 1. <https://doi.org/10.3390/ph15010106>
- Saddique, F. A., Zaib, S., Jalil, S., Aslam, S., Ahmad, M., Sultan, S., Naz, H., Iqbal, M., & Iqbal, J. (2018). Synthesis, monoamine oxidase inhibition activity and molecular docking studies of novel 4-hydroxy-N'-(benzylidene or 1-phenylethylidene)-2-H/methyl/benzyl-1,2-benzothiazine-3-carbohydrazide 1,1-dioxides. *European Journal of Medicinal Chemistry*, 143, 1373–1386. <https://doi.org/10.1016/j.ejmech.2017.10.036>
- Saeedi, P., Petersohn, I., Salpea, P., Malanda, B., Karuranga, S., Unwin, N., Colagiuri, S., Guariguata, L., Motala, A. A., Ogurtsova, K., Shaw, J. E., Bright, D., &

- Williams, R. (2019). Global and regional diabetes prevalence estimates for 2019 and projections for 2030 and 2045: Results from the International Diabetes Federation Diabetes Atlas, 9th edition. *Diabetes Research and Clinical Practice*, 157, 107843. <https://doi.org/10.1016/j.diabres.2019.107843>
- Sander, T., Freyss, J., von Korff, M., & Rufener, C. (2015). DataWarrior: An Open-Source Program For Chemistry Aware Data Visualization And Analysis. *Journal of Chemical Information and Modeling*, 55(2), 460–473. <https://doi.org/10.1021/ci500588j>
- Scapin, G. (2006). Structural Biology and Drug Discovery. *Current Pharmaceutical Design*, 12(17), 2087–2097. <https://doi.org/10.2174/13816120677585201>
- Shibano, M., Kakutani, K., Taniguchi, M., Yasuda, M., & Baba, K. (2008). Antioxidant constituents in the dayflower (*Commelina communis* L.) and their  $\alpha$ -glucosidase-inhibitory activity. *Journal of Natural Medicines*, 62(3), 349–353. <https://doi.org/10.1007/s11418-008-0244-1>
- Shultz, M. D. (2019). Two Decades under the Influence of the Rule of Five and the Changing Properties of Approved Oral Drugs. *Journal of Medicinal Chemistry*, 62(4), 1701–1714. <https://doi.org/10.1021/acs.jmedchem.8b00686>
- Silva, R. C., Freitas, H. F., Campos, J. M., Kimani, N. M., Silva, C. H. T. P., Borges, R. S., Pita, S. S. R., & Santos, C. B. R. (2021). Natural Products-Based Drug Design against SARS-CoV-2 Mpro 3CLpro. *International Journal of Molecular Sciences*, 22(21), Article 21. <https://doi.org/10.3390/ijms222111739>
- Sim, L., Quezada-Calvillo, R., Sterchi, E. E., Nichols, B. L., & Rose, D. R. (2008). Human Intestinal Maltase–Glucoamylase: Crystal Structure of the N-Terminal Catalytic Subunit and Basis of Inhibition and Substrate Specificity. *Journal of Molecular Biology*, 375(3), 782–792. <https://doi.org/10.1016/j.jmb.2007.10.069>
- Singh, B., Mal, G., Gautam, S. K., & Mukesh, M. (2019). Computer-Aided Drug Discovery. In B. Singh, G. Mal, S. K. Gautam, & M. Mukesh (Eds.), *Advances in Animal Biotechnology* (pp. 471–481). Springer International Publishing. [https://doi.org/10.1007/978-3-030-21309-1\\_44](https://doi.org/10.1007/978-3-030-21309-1_44)
- Siramshetty, V. B., Xu, X., & Shah, P. (2024). Artificial Intelligence in ADME Property Prediction. In M. Gore & U. B. Jagtap (Eds.), *Computational Drug Discovery and Design* (pp. 307–327). Springer US. [https://doi.org/10.1007/978-1-0716-3441-7\\_17](https://doi.org/10.1007/978-1-0716-3441-7_17)
- Sucharitha, P., Ramesh Reddy, K., Satyanarayana, S. V., & Garg, T. (2022). Chapter 15—Absorption, distribution, metabolism, excretion, and toxicity assessment of drugs using computational tools. In A. Parihar, R. Khan, A. Kumar, A. K. Kaushik, & H. Gohel (Eds.), *Computational Approaches for Novel Therapeutic and Diagnostic Designing to Mitigate SARS-CoV-2 Infection* (pp. 335–355). Academic Press. <https://doi.org/10.1016/B978-0-323-91172-6.00012-1>

- Sui, X., Zhang, Y., & Zhou, W. (2016). In vitro and in silico studies of the inhibition activity of anthocyanins against porcine pancreatic  $\alpha$ -amylase. *Journal of Functional Foods*, *21*, 50–57. <https://doi.org/10.1016/j.jff.2015.11.042>
- Sun, L., Chen, W., Meng, Y., Yang, X., Yuan, L., & Guo, Y. (2016). Interactions between polyphenols in thinned young apples and porcine pancreatic  $\alpha$ -amylase: Inhibition, detailed kinetics and fluorescence quenching. *Food Chemistry*, *208*, 51–60. <https://doi.org/10.1016/j.foodchem.2016.03.093>
- Suresh Babu, K., Tiwari, A. K., Srinivas, P. V., Ali, A. Z., China Raju, B., & Rao, J. M. (2004). Yeast and mammalian  $\alpha$ -glucosidase inhibitory constituents from Himalayan rhubarb *Rheum emodi* Wall.ex Meisson. *Bioorganic & Medicinal Chemistry Letters*, *14*(14), 3841–3845. <https://doi.org/10.1016/j.bmcl.2004.04.062>
- Tabopda, T. K., Ngoupayo, J., Awoussong, P. K., Mitaine-Offer, A.-C., Ali, M. S., Ngadjui, B. T., & Lacaille-Dubois, M.-A. (2008). Triprenylated Flavonoids from *Dorstenia psilurus* and Their  $\alpha$ -Glucosidase Inhibition Properties. *Journal of Natural Products*, *71*(12), 2068–2072. <https://doi.org/10.1021/np800509u>
- Tibbitts, J., Canter, D., Graff, R., Smith, A., & Khawli, L. A. (2015). Key factors influencing ADME properties of therapeutic proteins: A need for ADME characterization in drug discovery and development. *mAbs*, *8*(2), 229–245. <https://doi.org/10.1080/19420862.2015.1115937>
- Tiwari, A., & Singh, S. (2022). Chapter 13—Computational approaches in drug designing. In D. B. Singh & R. K. Pathak (Eds.), *Bioinformatics* (pp. 207–217). Academic Press. <https://doi.org/10.1016/B978-0-323-89775-4.00010-9>
- Tsopelas, F., Giaginis, C., & Tsantili-Kakoulidou, A. (2017). Lipophilicity and biomimetic properties to support drug discovery. *Expert Opinion on Drug Discovery*, *12*(9), 885–896. <https://doi.org/10.1080/17460441.2017.1344210>
- Tundis, R., Loizzo, M. R., & Menichini, F. (2010). Natural Products as  $\alpha$ -Amylase and  $\alpha$ -Glucosidase Inhibitors and their Hypoglycaemic Potential in the Treatment of Diabetes: An Update. *Mini-Reviews in Medicinal Chemistry*, *10*(4), 315–331. <https://doi.org/10.2174/138955710791331007>
- Turban, E., Pollard, C., & Wood, G. (2021). *Information Technology for Management: Driving Digital Transformation to Increase Local and Global Performance, Growth and Sustainability*. John Wiley & Sons.
- van de Laar, F. A., Lucassen, P. L., Akkermans, R. P., van de Lisdonk, E. H., Rutten, G. E., & van Weel, C. (2005). Alpha-glucosidase inhibitors for patients with type 2 diabetes: Results from a Cochrane systematic review and meta-analysis. *Diabetes Care*, *28*(1), 154–163. <https://doi.org/10.2337/diacare.28.1.154>

- Vázquez, J., López, M., Gibert, E., Herrero, E., & Luque, F. J. (2020). Merging Ligand-Based and Structure-Based Methods in Drug Discovery: An Overview of Combined Virtual Screening Approaches. *Molecules*, 25(20), 4723. <https://doi.org/10.3390/molecules25204723>
- Veber, D. F., Johnson, S. R., Cheng, H.-Y., Smith, B. R., Ward, K. W., & Kopple, K. D. (2002). Molecular Properties That Influence the Oral Bioavailability of Drug Candidates. *Journal of Medicinal Chemistry*, 45(12), 2615–2623. <https://doi.org/10.1021/jm020017n>
- Velmourougane, G. (2022, February 7). *Understanding Lipinski's Rule of 5 and the Role of LogP Value in Drug Design and Development*. Sai Life Sciences. <https://www.sailife.com/understanding-lipinskis-rule-of-5-and-the-role-of-logp-value-in-drug-design-and-development/>
- Wang, H., Zhao, W., Choomuenwai, V., Andrews, K. T., Quinn, R. J., & Feng, Y. (2013). Chemical investigation of an antimalarial Chinese medicinal herb *Picrorhiza scrophulariiflora*. *Bioorganic & Medicinal Chemistry Letters*, 23(21), 5915–5918. <https://doi.org/10.1016/j.bmcl.2013.08.077>
- Wang, J., Wang, W., Kollman, P. A., & Case, D. A. (2006). Automatic atom type and bond type perception in molecular mechanical calculations. *Journal of Molecular Graphics and Modelling*, 25(2), 247–260. <https://doi.org/10.1016/j.jmkgm.2005.12.005>
- Wang, N.-N., Huang, C., Dong, J., Yao, Z.-J., Zhu, M.-F., Deng, Z.-K., Lv, B., Lu, A.-P., Chen, A. F., & Cao, D.-S. (2017). Predicting human intestinal absorption with modified random forest approach: A comprehensive evaluation of molecular representation, unbalanced data, and applicability domain issues. *RSC Advances*, 7(31), 19007–19018. <https://doi.org/10.1039/C6RA28442F>
- Wansi, J. D., Wandji, J., Mbaze Meva'a, L., Kamdem Waffo, A. F., Ranjit, R., Khan, S. N., Asma, A., Iqbal, C. M., Lallemand, M.-C., Tillequin, F., & Fomum Tanee, Z. (2006).  $\alpha$ -Glucosidase Inhibitory and Antioxidant Acridone Alkaloids from the Stem Bark of *Oriciopsis glaberrima* ENGL. (Rutaceae). *Chemical and Pharmaceutical Bulletin*, 54(3), 292–296. <https://doi.org/10.1248/cpb.54.292>
- Wellsow, J., Grayer, R. J., Veitch, N. C., Kokubun, T., Lelli, R., Kite, G. C., & Simmonds, M. S. J. (2006). Insect-antifeedant and antibacterial activity of diterpenoids from species of *Plectranthus*. *Phytochemistry*, 67(16), 1818–1825. <https://doi.org/10.1016/j.phytochem.2006.02.018>
- Wen, X., Lv, C., Zhou, R., Wang, Y., Zhou, X., & Qin, S. (2024). The Molecular Mechanism Underlying the Therapeutic Effect of Dihydromyricetin on Type 2 Diabetes Mellitus Based on Network Pharmacology, Molecular Docking, and Transcriptomics. *Foods*, 13(2), Article 2. <https://doi.org/10.3390/foods13020344>

- Williams, A. J. (2008). Public chemical compound databases. *Current Opinion in Drug Discovery and Development*, 11(3), 393. <https://doi.org/10.1016/j.copdd.2008.05.003>
- World Health Organization. (2016). *Global report on diabetes*. World Health Organization. <https://apps.who.int/iris/handle/10665/204871>
- Xiao, J., Ni, X., Kai, G., & Chen, X. (2013). A review on structure-activity relationship of dietary polyphenols inhibiting  $\alpha$ -amylase. *Critical Reviews in Food Science and Nutrition*, 53(5), 497–506. <https://doi.org/10.1080/10408398.2010.548108>
- Xu, Y., Shrestha, N., Pr eat, V., & Beloqui, A. (2020). Overcoming the intestinal barrier: A look into targeting approaches for improved oral drug delivery systems. *Journal of Controlled Release*, 322, 486–508. <https://doi.org/10.1016/j.jconrel.2020.04.006>
- Yaribeygi, H., Sathyapalan, T., Atkin, S. L., & Sahebkar, A. (2020). Molecular Mechanisms Linking Oxidative Stress and Diabetes Mellitus. *Oxidative Medicine and Cellular Longevity*, 2020, e8609213. <https://doi.org/10.1155/2020/8609213>
- Yue, Y.-D., Zhang, Y.-T., Liu, Z.-X., Min, Q.-X., Wan, L.-S., Wang, Y.-L., Xiao, Z.-Q., & Chen, J.-C. (2014). Xanthone Glycosides from *Swertia bimaculata* with  $\alpha$ -Glucosidase Inhibitory Activity. *Planta Medica*, 80(06), 502–508. <https://doi.org/10.1055/s-0034-1368299>
- Zeng, X., Zhang, P., He, W., Qin, C., Chen, S., Tao, L., Wang, Y., Tan, Y., Gao, D., Wang, B., Chen, Z., Chen, W., Jiang, Y. Y., & Chen, Y. Z. (2018). NPASS: Natural product activity and species source database for natural product research, discovery and tool development. *Nucleic Acids Research*, 46(D1), D1217–D1222. <https://doi.org/10.1093/nar/gkx1026>
- Zhao, H., Yang, Y., Wang, S., Yang, X., Zhou, K., Xu, C., Zhang, X., Fan, J., Hou, D., Li, X., Lin, H., Tan, Y., Wang, S., Chu, X.-Y., Zhuoma, D., Zhang, F., Ju, D., Zeng, X., & Chen, Y. Z. (2023). NPASS database update 2023: Quantitative natural product activity and species source database for biomedical research. *Nucleic Acids Research*, 51(D1), D621–D628. <https://doi.org/10.1093/nar/gkac1069>
- Zhao, L., Ciallella, H. L., Aleksunes, L. M., & Zhu, H. (2020). Advancing computer-aided drug discovery (CADD) by big data and data-driven machine learning modeling. *Drug Discovery Today*, 25(9), 1624–1638. <https://doi.org/10.1016/j.drudis.2020.07.005>
- Zheng, L., Meng, J., Jiang, K., Lan, H., Wang, Z., Lin, M., Li, W., Guo, H., Wei, Y., & Mu, Y. (2022). Improving protein–ligand docking and screening accuracies by incorporating a scoring function correction term. *Briefings in Bioinformatics*, 23(3), bbac051. <https://doi.org/10.1093/bib/bbac051>

## APPENDICES

**Appendix1:** Docking score and the interactions of selected compounds and acarbose with the  $\alpha$ -amylase receptor (3BAJ) residues discovered during structure visualization

Compound ID	Binding residues		Interactions			Docking score	Rmsd
	ligand	Receptor	Type of interaction	Distance	E(kcal/mol)		
NPC204580	C 18	OD1 ASP 300	H-donor	3.25	-1.5	-14.4621	1.8020
	C 21	OE1 GLU 233	H-donor	3.64	-0.6		
	O 37	NZ LYS 200	H-acceptor	3.50	-1.1		
	N 19	OD1 ASP 197	Ionic	3.60	-1.5		
	6-ring	CE1 HIS 201	pi-H	3.48	-0.9		
NPC137813	O 34	OD1 ASP 300	H-donor	2.83	-4.2	-12.5790	1.7879
	O 35	OD1 ASP 197	H-donor	2.75	-4.2		
	O 34	NE2 HIS 299	H-acceptor	2.97	-1.5		
	O 35	NH2 ARG 195	H-acceptor	3.11	-0.4		
NPC76084	O 33	OD1 ASP 197	H-donor	2.89	-3.1	-11.5494	1.9626
	O 37	OE1 GLU 233	H-donor	2.72	-3.3		
	O 33	NE2 HIS 299	H-acceptor	3.37	-1.2		
NPC27750	O 6	NH2 ARG 195	H-acceptor	3.45	-1.1	-10.1729	1.9334
	O 7	NH2 ARG 195	H-acceptor	2.99	-2.3		
	O 7	NE2 HIS 299	H-acceptor	2.98	-5.1		
	O 22	NE2 HIS 305	H-acceptor	2.92	-3.2		
Acarbose	O 17	OE1 GLN 63	H-donor	2.97	-1.1	-12.9946	1.6148
	C 34	6-ring TRP 59	H-pi	4.13	-0.6		

**Appendix 2:** Docking score and the interactions of selected top four compounds and acarbose with the  $\alpha$ -glucosidase receptor upon visualization.

Compound ID	Binding residues		Interactions			Docking score	Rmsd
	ligand	Receptor	Type of interaction	Distance	E(kcal/mol)		
NPC25750	O 7	NE2 HIS 600	H-acceptor	3.33	-2.3	-9.0762	1.1439
NPC137813	O 33	OG1 THR 205	H-acceptor	3.12	-0.6	-8.7610	1.8797
	O 37	NH2 ARG 202	H-acceptor	3.42	-1.6		
	6-ring	CA THR 204	Pi-H	4.30	-0.9		
NPC76084	O 33	NH2 ARG 202	H-acceptor	3.06	-0.7	-8.5586	1.9705
NPC204580	C 16	SD MET 444	H-donor	4.36	-0.7	-8.4181	1.7932
	C 21	OD2 ASP 542	H-donor	3.17	-0.8		
	N 19	OD1 ASP 203	Ionic	3.63	-1.4		
	N 19	OD2 ASP 542	Ionic	3.88	-0.8		
	C 34	6-ring PHE575	H-pi	4.19	-0.6		
Acarbose	O 6	OD2 ASP 203	H-donor	3.14	-1.6	-8.2153	1.2913
	O 10	OD1 ASP 542	H-donor	2.58	-3.0		
	O 13	OD2 ASP 327	H-donor	2.83	-3.8		
	C 28	SD MET444	H-donor	4.03	-1.2		
	C 31	OD2 ASP 443	H-donor	2.98	-0.9		
	O 10	NH1 ARG 526	H-acceptor	2.99	-2.8		
	O 13	NE2 HIS 600	H-acceptor	3.20	-0.9		
	N 19	OD1 ASP 542	Ionic	2.80	-5.9		

**Appendix 3:** Top ten docked poses of the selected molecules; NPC137813, NPC204580, and the reference molecules Acarbose in 3BAJ and 2QMJ receptors.

<b>Top ten poses of NPC137813 with <math>\alpha</math>-glucosidase docking scores</b>									
mol	rseq	mseq	S	rmsd_refine	E_conf	E_place	E_score1	E_refine	E_score2
NPC137813	1	2	-8.76103	1.88837	85.29571	-83.3143	-9.99738	-36.6662	-9.2534
NPC137813	1	2	-8.75338	2.335788	85.44517	-77.0259	-11.2897	-36.0383	-9.19404
NPC137813	1	2	-8.75286	2.307614	81.04989	-79.7755	-9.9185	-32.9176	-8.82857
NPC137813	1	2	-8.65404	1.879722	80.33741	-56.6988	-11.4196	-34.169	-8.76103
NPC137813	1	2	-8.6334	2.032482	81.6442	-47.1956	-9.97571	-37.6139	-8.75338
NPC137813	1	2	-8.57736	1.422926	87.25224	-73.1741	-10.1413	-28.6268	-8.57736
NPC137813	1	2	-8.48899	2.347135	81.07302	-68.2018	-10.3797	-36.5783	-8.48899
NPC137813	1	2	-8.47267	1.840335	86.29304	-52.6786	-9.93029	-34.4236	-8.47267
NPC137813	1	2	-8.4563	0.858618	77.3781	-61.8478	-10.586	-30.1771	-8.4563
NPC137813	1	2	-7.97356	3.661563	80.2841	-72.1777	-10.9016	-36.5147	-7.97356
<b>Top ten poses of NPC204580 with <math>\alpha</math>-glucosidase docking scores</b>									
mol	rseq	mseq	S	rmsd_refine	E_conf	E_place	E_score1	E_refine	E_score2
NPC204580	1	1	-8.41812	1.81453	37.66348	-74.4597	-12.6435	-30.7556	-9.53172
NPC204580	1	1	-8.33172	1.414635	46.23306	-72.5077	-11.7797	-27.0719	-9.46326
NPC204580	1	1	-8.26326	2.281953	51.31535	-95.1984	-12.7989	-26.1012	-9.34617
NPC204580	1	1	-8.14617	1.64102	51.29466	-30.0781	-12.3616	-26.0921	-9.3434
NPC204580	1	1	-7.91415	2.313433	48.75798	-59.6185	-11.7639	-21.648	-9.00827
NPC204580	1	1	-7.90918	2.344837	33.95421	-51.8933	-13.8899	-26.6873	-8.9918
NPC204580	1	1	-7.8434	1.68587	48.60243	-47.6315	-11.436	-18.739	-8.95654
NPC204580	1	1	-7.55654	1.830331	37.8803	-40.4604	-11.6829	-27.0826	-8.89724
NPC204580	1	1	-7.00827	1.793209	46.58095	-58.2082	-11.7229	-15.3986	-8.41812
NPC204580	1	1	-6.99724	1.450214	51.88573	-57.3436	-12.235	-6.6618	-7.91415

**Top ten poses of Acarbose (reference) with  $\alpha$ -glucosidase docking scores**

mol	rseq	mseq	S	rmsd_refine	E_conf	E_place	E_score1	E_refine	E_score2
Acarbose	1	1	-8.21532	1.291318	212.3576	-120.893	-18.6244	-51.7974	-8.21532
Acarbose	1	1	-8.20762	1.899994	209.3934	-72.1205	-7.54501	-51.1153	-8.20762
Acarbose	1	1	-8.09206	2.439259	203.5718	-53.2627	-7.76199	-49.3812	-8.09206
Acarbose	1	1	-7.85153	1.972781	208.2269	-11.193	-12.9505	-50.7465	-7.85153
Acarbose	1	1	-7.61379	2.078672	202.6323	-51.2126	-10.1361	-40.9282	-7.61379
Acarbose	1	1	-6.68334	3.878601	209.0457	-22.5269	-7.34448	-30.6757	-6.68334
Acarbose	1	1	-6.53984	3.653367	211.0734	-18.6017	-8.35201	-24.7315	-6.53984
Acarbose	1	1	-6.43713	3.176234	202.4566	-15.052	-7.37009	-30.7312	-6.43713
Acarbose	1	1	-6.26708	2.066111	201.5151	-31.8053	-10.4304	-26.3252	-6.26708
Acarbose	1	1	-6.18494	1.642416	195.9855	-37.8749	-9.1099	-34.1819	-6.18494

**Top ten poses of NPC137813 with  $\alpha$ -amylase docking scores**

mol	rseq	mseq	S	rmsd_refine	E_conf	E_place	E_score1	E_refine	E_score2
NPC137813	1	2	-12.579	1.787946	82.39311	-109.39	-9.45829	-46.6145	-12.579
NPC137813	1	2	-12.4238	2.800655	83.07259	-78.0329	-11.381	-48.1373	-12.0238
NPC137813	1	2	-12.3167	2.212599	80.9527	-73.6801	-9.92959	-43.9197	-12.0167
NPC137813	1	2	-12.2597	2.020088	80.90101	-81.0404	-10.0047	-47.8929	-11.8597
NPC137813	1	2	-12.1003	2.068335	81.28394	-57.3591	-9.42862	-41.4155	-11.6003
NPC137813	1	2	-11.9654	1.796654	79.8654	-96.8604	-11.8691	-38.8472	-11.4654
NPC137813	1	2	-11.7918	1.808322	76.39182	-51.2327	-10.1116	-42.3986	-11.3918
NPC137813	1	2	-11.6813	1.276934	78.07275	-73.426	-11.099	-37.4805	-11.3813
NPC137813	1	2	-11.571	2.674014	79.4208	-60.1333	-9.64488	-32.5571	-11.271
NPC137813	1	2	-11.2295	1.821809	83.52885	-72.2422	-11.3819	-37.622	-11.2295

**Top ten poses of NPC204580 with  $\alpha$ -amylase docking scores**

mol	rseq	mseq	S	rmsd_refine	E_conf	E_place	E_score1	E_refine	E_score2
NPC204580	1	1	-14.4621	1.802011	35.44961	-77.4254	-11.2925	-51.3837	-14.4621
NPC204580	1	1	-14.4618	1.764134	35.45652	-85.0054	-11.6847	-51.3917	-14.4618
NPC204580	1	1	-14.4515	1.555651	37.22322	-51.1362	-12.6259	-52.3352	-14.4515

NPC204580	1	1	-13.8753	1.501828	41.37893	-65.137	-12.082	-41.9747	-13.8753
NPC204580	1	1	-13.5826	1.381291	35.50892	-62.686	-12.1202	-47.2696	-13.5826
NPC204580	1	1	-13.4791	1.311957	31.43153	-70.639	-10.9814	-43.5377	-13.4791
NPC204580	1	1	-13.1947	2.065751	37.44419	-70.5433	-12.8651	-46.7403	-13.1947
NPC204580	1	1	-13.0065	2.262682	34.99592	-70.1336	-11.516	-45.7864	-13.0065
NPC204580	1	1	-12.6875	2.242865	37.04658	-72.9694	-10.949	-45.9202	-12.6875
NPC204580	1	1	-12.4081	1.318545	37.40218	-75.272	-11.4409	-34.5008	-12.4081
<b>Top ten poses of Acarbose (reference) with <math>\alpha</math>-amylase docking scores</b>									
mol	rseq	mseq	S	rmsd_refine	E_conf	E_place	E_score1	E_refine	E_score2
Acarbose	1	1	-12.9946	1.614768	215.7984	-96.1983	-12.287	-32.0879	-12.9946
Acarbose	1	1	-12.939	2.287654	207.5058	-58.3788	-12.4294	-38.9517	-12.939
Acarbose	1	1	-12.8094	1.62795	202.8693	-78.2057	-12.5704	-56.5978	-12.8094
Acarbose	1	1	-12.7258	2.19905	210.229	-63.6874	-13.7739	-42.27	-12.7258
Acarbose	1	1	-12.6237	1.378166	199.1647	-97.7129	-13.3631	-49.572	-12.6237
Acarbose	1	1	-12.5692	2.531663	200.1203	-86.9518	-13.1016	-56.4331	-12.5692
Acarbose	1	1	-12.3928	2.056788	197.6421	-84.6215	-12.4115	-49.4384	-12.3928
Acarbose	1	1	-12.2175	1.401791	202.1732	-101.743	-16.0715	-47.6254	-12.2175
Acarbose	1	1	-12.2072	0.771867	204.1883	-96.3818	-14.8308	-47.1893	-12.2072
	1	1	-12.0608	2.252975	201.2899	-94.0029	-12.5127	-44.6178	-12.0608

#### Appendix 4: Articles published

- i) **Ndarawit, W.**, Ochieng, C. O., Angwenyi, D., Cruz, J. N., Santos, C. B., & Kimani, N. M. (2024). Discovery of  $\alpha$ -amylase and  $\alpha$ -glucosidase dual inhibitors from NPASS database for management of Type 2 Diabetes Mellitus: A chemoinformatic approach. *Plos one*, 19(11), e0313758.
- ii) Ojuka, P., Ochieng, C. O., **Ndarawit, W.**, Nyongesa, D. W., Mukavi, J., Nyabuga Nyariki, J., ... & Kimani, N. M. (2025). Alkaloids Isolated from *Vepris glandulosa* with Antidiabetic Properties: An In Vitro and In Silico Analysis. *Chemistry & Biodiversity*, 22(3), e202401515.
- iii) Wekesa, E. N., Ojuka, P., Ochieng, C. O., **Ndarawit, W.**, Kituyi, S. N., Omosa, L. K., ... & Kimani, N. M. (2025). Antidiabetic Activity of Compounds Isolated From *Zanthoxylum mildbraedii*: An In Vitro  $\alpha$ -Amylase Inhibition and In Silico Analysis. *Chemistry & Biodiversity*, e01439.
- iv) Bodun, D. S., Ibrahim, I. O., Bashiru, M., Abolade, R. O., **Ndarawit, W. K.**, Owolade, A. J. J., ... & Ajani, O. O. (2025). De novo design and bioactivity prediction of mitotic kinesin Eg5 inhibitors using MPNN and LSTM-based transfer learning. *Computers in Biology and Medicine*, 195, 110672.
- v) Osunnaya, S. A., **Ndarawit, W. K.**, Aderibigbe, I., Omolopo, I. A., Aribisala, P. O., Oluwasegun, E. A., ... & Bodun, D. S. (2025). Identification and Exploration of Novel FGFR-1 Inhibitors in The Lotus Database for Cholangiocarcinoma (CCA) Treatment. *Aspects of Molecular Medicine*, 100085.